

Design and Construction of a Continuous Solar Absorption Refrigeration Unit

A thesis submitted to the University of Khartoum in fulfillment
of the requirement for the degree of Ph.D.
in Mechanical Engineering

By

Manahil Zaki A/Wahab Ali
B.Sc. (1993) University of Khartoum
M.Sc. (1999) University of Khartoum

Supervisor: Dr. M. A/Bagi Siraj
Co-Supervisor: Dr. Kamal Nasr ElDin Abdalla
Faculty of Engineering/Mechanical
Engineering Department

Acknowledgements

I wish to express my gratitude to all the people that encouraged and supported me during this project.

In the first place, I wish to thank my supervisor, Dr. M. A/Bagi Siraj and my co-supervisor, Dr. Kamal Nasar Aldin for their support. I am grateful to the Department of Mechanical Engineering , Mechanical Workshop at U.K and Energy Research Institute for their provision of facilities with which the work was accomplished.

Abstract

The main objective of this thesis is to design and construct a continuous solar absorption refrigeration machine. A solar heated ammonia-water refrigeration machine with 0.111kw cooling capacity was designed and built. It consists of five heat exchangers (generator, condenser, evaporator, absorber and solution heat exchanger), two pumps, two throttle valves, two cooling water tanks and solar collectors with storage tanks (two evacuated and two flat plate collectors). The refrigeration unit was set up on roof of the north building of Faculty of Engineering, Khartoum University. A series of experiments were carried out to evaluate the performance of the heat exchangers and the solar collector fields. Then the absorption machine was tested to validate the design procedure and to evaluate the impact of the system components on the overall performance of the refrigerating system. It was found that reduction of heat losses, increase of streams flow rates, increase of delivery temperature of the evacuated collector field and further optimization of the system components are necessary for better system performance.

الخلاصة

كان الهدف الرئيسي لهذا البحث هو تطوير المعرفة والخبرة العملية لتصميم وتنفيذ وحدة تبريد شمسي امتصاصي مستمر. لقد تم تصميم وتنفيذ وحدة تبريد تعمل بالطاقة الشمسية وتستخدم مخلوط الأمونيا والماء كسائل تبريد، وتبلغ قدرة الوحدة 0.111 كيلو واط. تحتوي الوحدة على خمس مبادلات حرارية (المولد، المكثف، المبخر، المبادل الحراري للسائل والماص)، مضختين، صمامي خنق، خزان ماء للتبريد ومجمعات شمسية. تم تصنيع وتركيب الوحدة بكلية الهندسة - جامعة الخرطوم. لقد أجريت سلسلة من التجارب العملية على المبادلات الحرارية والمجمعات الشمسية وتمت مقارنة النتائج العملية بالتصميم النظري. وقد تبين أن هناك حاجة لرفع درجة حرارة الماء بواسطة مجمعات شمسية ذات كفاءة أعلى وخفض فقدان الطاقة الحرارية وتقييم قدرة الجهاز تحت ظروف تشغيل مختلفة وذلك لتحديد عوامل التشغيل المثالي من أجل أداء أفضل.

Table of Contents

1	INTRODUCTION	1
1.1	Background	1
1.2	Objective and Approach	3
1.3	Structure of This Thesis	3
2	LITERATURE REVIEW	4
2.1	The Basic Principles of Refrigeration	4
2.2	Solar Cooling Technologies	6
2.2.1	Solar Collection Technologies:	7
2.2.1.1	Solar (Photovoltaic) Cell:	7
2.2.1.2	Solar Thermal	11
2.2.2	Cooling Technologies	16
2.2.2.1	Photovoltaic Operated Refrigeration Cycle (Solar Electric)	17
2.2.2.2	Solar Mechanical Refrigeration	17
2.2.2.3	Solar Absorption Refrigeration	18
2.2.2.4	Comparison of Solar Cooling Technologies	19
2.3	The Absorption Cooling Process	20
2.3.1	The Components of the absorption cooling Process	21
2.3.1.1	The Condenser	21
2.3.1.2	The Evaporator	22
2.3.1.3	The Generator	22
2.3.1.4	The Absorber	23
2.3.1.5	The Solution Heat Exchanger	23
2.3.2	Physical Principals of the Absorption Process	23
2.3.2.1	Vapor Pressure Curve of Material Pairs	23
2.3.2.2	Ideal Performance Figures	25
2.3.2.3	Real Performance Figures	26
2.3.2.4	Mass and Energy Balances[14]	26
2.4	The Solar Energy Collection	29
2.4.1	Thermal Analysis of Flat Plate Collector[1]	29
2.4.2	Performance Prediction of Solar System[1]	31
3	SYSTEM CONFIGURATION AND DESIGN APPROACH	33
3.1	Configuration of the Refrigerator	33
3.1.1	Description of the System and Physical Layout of Components	33
3.1.2	Design and Operation Strategy	35
3.2	Design Approach	40
3.2.1	Pre-Design Condition	40
3.2.1.1	Cooling Capacity	40
3.2.1.2	The Temperature Limits of The processes	40
3.2.1.3	The System Operating Pressures and Solution Concentrations	41
3.2.2	Energy Balances	43
3.2.2.1	Enthalpies at State Points	43
3.2.2.2	Heating and Cooling Loads	45
3.3	Sizing of Heat Exchangers	46
3.3.1	Generator Design	50
3.3.2	Condenser Design	57

3.3.3	Evaporator Design	67
3.3.5	Absorber Design	76
3.4	Sizing and Performance Prediction of Solar Collectors	81
3.4.1	Solar Collectors Sizing	81
3.4.2	Performance Prediction of Solar Collectors	85
3.4.2.1	Long Term Performance of Evacuated Tube Collector	87
4	CONSTRUCTION AND PERFORMANCE TESTING	93
4.1	Construction and Assembly	93
4.2	Materials and Methods	95
4.2.1	Description of Experimental Set Up	95
4.2.1.1	Overall Description of Experimental Unit	95
4.2.1.2	Measuring Instruments	98
4.2.1.3	Detailed Description of the Test Components	98
4.2.2	Test Procedure and Result	104
4.2.2.1	Initial Observed Operation of the System Components	104
4.2.2.2	Test Procedure of Experimental Unit and Result	105
4.3	Analysis of Result	114
4.3.1	Shell and Tube Heat Exchanger	114
4.3.1.1	Energy Gain and Loss between Cold and Hot Streams	114
4.3.1.2	Temperature Ranges	115
4.3.1.3	Flow Rates	115
4.3.1.4	Heat Transfer Coefficient	116
4.3.2	Double Tube Heat Exchanger	116
4.3.2.1	Energy Gain and Loss between Cold and Hot Streams	117
4.3.2.2	Temperature Ranges	118
4.3.2.3	Flow Rates	118
4.3.2.4	Heat Transfer Coefficient	118
4.3.3	Flat Plate Collector Field	118
4.3.3.1	Efficiency Test of Flat Plate Collector	119
4.3.3.2	Variation of Storage Tank Temperature with Ambient Conditions	119
4.3.4	Evacuated Collector Field	120
4.3.4.1	Effect of Constant Load Withdrawal On Storage Tank Temperature Variation.	120
4.3.4.2	Variation of Storage Tank Temperature under Different Weather Conditions	120
5	CONCLUSION AND RECOMMENDATION	122
5.1	General Conclusion and Recommendation	122
5.2	Further Work	122
	References	123
	Appendix	124

Chapter 1

1. Introduction

1.1 Background

As the world concerns more and more on global climate changes and depleting energy resources, solar cooling technology receives increasing interests from the public as an environment-friendly and sustainable alternative. The coincidence of solar intensity and cooling demand has long been inspiring people to invent a machine that cools when the sun shines[16]. It motivated the first solar cooling machine of the history dating back to as early as 1878 when the French mathematician Augustin Mouchot demonstrated his solar engine with the absorption cooling machine of Edmond Carré to produce ice at the World Exhibition in Paris[22]. But as energy prices went down with diversifying energy sources and developing transportation technologies, the idea of using solar energy became less attractive. It was not until the 1970s that solar cooling received great interests again from the public, when the world suffered from the oil crisis that had been initiated by Arab members of OPEC for political motivations. The world realized that they could no longer depend on cheap oil prices and began to look for alternatives. Industries tried to reduce energy consumptions by improving energy efficiency on one hand and diversifying energy sources on the other. There were many projects for development or demonstration of solar cooling technologies and solar cooling continued to be an important issue in the 1980s [16]

Solar cooling and refrigeration is technically possible for a wide variety of applications. There are two quite different major applications. The first is the cooling of buildings of all types, ranging from individual houses to large public buildings such as hospitals. The second is refrigeration for food preservation with a second application in the storage of vaccines for medical purposes- a vital need and an attractive option in many of the developing countries particularly in remote regions with no access to electricity supply.

Of the several refrigeration system alternatives which might be considered for solar cooling applications, the absorption system stands out as one most promising at the present state. Absorption cooling is the first and oldest form of air conditioning and refrigeration. The principle of absorption refrigeration was first demonstrated by Faraday as early as 1825. An absorption refrigerator or air conditioner does not use an electric compressor to mechanically pressurize the refrigerant. Instead, heat is supplied to the system and the cooling effect is produced directly with no significant

amount of rotating machinery. The absorption device uses a heat source, such as natural gas or a larger solar collector, to evaporate the already pressurized refrigerant from an absorbent/refrigerant mixture.

Unlike electric or gas powered air conditioners, solar-powered refrigerators and air conditioning are not widely acceptable. The popularity of these conventional air conditioners and refrigerators has been attributed to low cost, compactness, and the universal availability of electricity and gas. Now that oil, coal and natural gas have risen to the present price levels, solar thermal driven or assisted absorption cooling machines are gaining increasing importance due to the continually growing operating cost of conventional units. Solar-powered machines combine the advantage of low cost operation, widespread energy availability, and unlimited energy supply. However, no cost-competitive system for widespread application exists. As already stated, two main reasons that solar powered refrigeration and air conditioning are not in widespread use today are high initial cost and large equipment size. Much of the high cost and bulky equipment is due to the fact that most of the refrigerators and air conditioners built to date have been custom made for case of testing rather than compactness. With additional research, a more compact and inexpensive refrigerators and air conditioner will be produced. A major obstacle in achieving reliable cost-effective solar thermal absorption coolers is the problem of adapting individual components of the system to operate at the normal working temperatures for solar collectors, between 82 to 121°C. Specially designed units for use with a wide range of temperatures and in a variety of climates need to be developed.

There are currently much stronger economic and political drives to promote solar cooling technology in the market. However, making a competitive solar cooling machine for the market still remains a challenge to the academic and industrial communities. The common goals of present day research activities on solar assisted cooling are to find, for each different application of cooling, an optimum combination of collector and cooling system that matches the special cooling demands and also the constraints of the available solar radiation in the best way, with only marginal need for fossil fuels.

1.2 Objective and Approach

In this thesis, a prototype of a continuous absorption refrigeration machine (0.111kW) with water-cooled condenser and absorber has been developed. Its input energy is hot water between 83 to 100°C. The working fluid is ammonia solution with ammonia as refrigerant and water as absorber. The driving heat for the absorption refrigerator comes from the solar heat production system, which uses water as a heat transfer fluid and includes the evacuated collectors and the hot water storage tanks. The main target of the design has been to keep the driving heat as low as possible so that to guarantee effective operation of the system using evacuated collectors with maximum temperature below 100 °C. This unit has been conceived as an experimental laboratory test device with removable components to facilitate modifications with respect to the initial design.

1.3 Structure of This Thesis

This thesis is intended to provide detailed information on the design, construction, and performance potential of 0.111kw solar-driven ammonia/water continuous absorption machine.

Chapter two of this thesis, introduces the basic concepts and principles of refrigeration, reviews and compares the solar cooling technologies that can provide refrigeration and air conditioning. In addition to reviewing the potential technologies, it presents the principles and operating characteristics of the most viable technology. The third chapter deals with the design and construction of the cooling machine. Chapter four concentrates on the testing and performance of the unit. Finally, chapter 5 gives overall conclusions and recommendations regarding the research activities reported in this thesis. The recommendations given are focusing on what has been missing or was insufficient in the course of the research hoping for a follow-up research in the future.

Chapter 2

2. Literature Review

The first aim of this chapter is to introduce the basic concepts and principles of refrigeration and to give an overview of the state-of-the-art of the different technologies that are available to deliver refrigeration from solar energy. The second aim is to compare the potential of these different technologies in delivering competitive sustainable solutions. Finally, the basics of absorption refrigeration and solar collectors are illustrated.

2.1 The Basic Principles of Refrigeration

A refrigeration machine consumes energy to transfer heat from a source at a low temperature, to a sink at a higher temperature. The heat extracted from the low temperature source is the useful cooling. The basic principles of a refrigerating machine working between two temperatures are illustrated by figure 2.1. Heat \dot{Q}_0 collected at a lower temperature level T_0 is lifted and ejected at a higher temperature level T_1 . To accomplish this lift \dot{W}_i power is needed, during the process this power is degraded to heat and ejected together with collected heat at temperature level T_1 (see Eqn. 2.1.1)

$$\dot{Q}_1 = \dot{Q}_0 + \dot{W}_i \text{-----(2.1.1)}$$

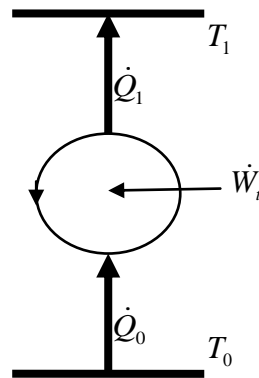


Fig. 2.1 Refrigeration Machine Working Between Two Temperatures[17]

To achieve any cooling in a refrigeration machine, a refrigerant (working substance): a gas, vapor or a vapor/liquid combination has to be circulated through a cycle in a refrigeration system. The refrigeration cycle involves movement of refrigerant through a system, to ultimately provide either comfort cooling, beverage cooling, to preserve food over a period of time, and to control humidity in a "refrigerated space". The refrigeration cycle repeats as many times as necessary in a system until the desired temperature is achieved.

Refrigeration is firmly rooted in two basic principles known as the first law and second law of thermodynamics. The first law states that energy neither created nor destroyed. If energy disappears in one form, it must reappear in another. The second law states that no system can receive energy at low temperature and reject it at higher temperature without receiving work from the surroundings.

A key figure to characterize the energy performance of a refrigeration machine is the Coefficient of Performance, COP. In refrigeration systems the Coefficient of Performance C.O.P is a term used to compare the performance of different units. The C.O.P is defined as the ratio of the refrigerant effect, or heat removed in the evaporator, to the energy input to a system.

$$\text{COP} = \frac{\text{Heat Energy Removed from Evaporator}}{\text{Energy Supplied From External Source}}$$

The Ideal Refrigerating Cycle

The ideal refrigeration process is given by the so-called Carnot refrigeration cycle. The Carnot cycle is a cycle composed of the totally reversible processes of isentropic compression and expansion and isothermal heat addition and rejection, so it is the most efficient refrigeration cycle. The thermal efficiency of a Carnot cycle depends only on the temperatures in kelvins of the two reservoirs in which heat transfer takes place. Figure 2.2 is a T-s diagram of a Carnot cycle refrigerating system.

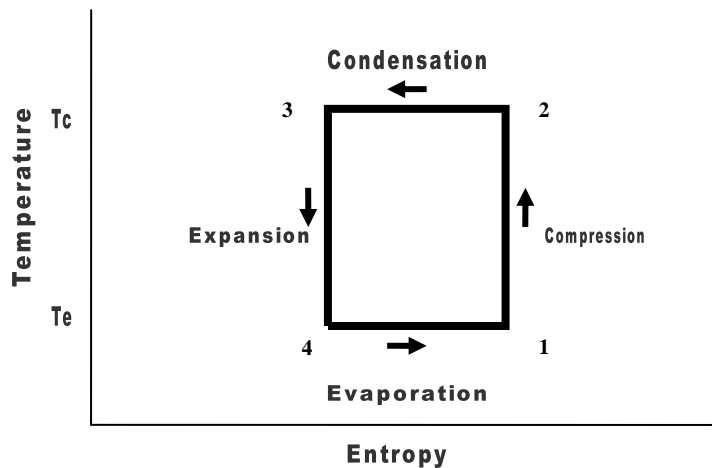


Fig. 2.2 Ideal Reversed Carnot Cycle

This Carnot cycle is composed of four reversible processes:

1. An isothermal process 4-1 in which heat is extracted at constant temperature T_e per lb (kg) of working substance
2. An isentropic compression process 1-2
3. An isothermal process 2-3 in which heat is rejected at constant temperature T_c per lb (kg) of working substance
4. An isentropic expansion process 3-4

The Carnot refrigeration cycle shows the highest coefficient of performance COP between the two temperature limits. The Coefficient of Performance of Carnot refrigeration cycle is given by:

$$COP = \frac{T_L}{T_H - T_L} \quad \text{-----(2.2.2)}$$

where T_L is the lowest cycle temperature and T_H the highest.

In an actual refrigeration cycle reversibility does not exist and therefore there will be losses, which means that this cycle is ideal and cannot be achieved in a real machine, but it gives a yardstick for comparison of real refrigeration machines and processes. Any real refrigeration machine would have a COP less than COP Carnot.

2.2 Solar Cooling Technologies

From a sustainability perspective, directly using solar as a primary energy source is attractive because of its universal availability, low environmental impact, and low or no ongoing fuel cost. But there are many problems associated with its use. The main problem is that it is a dilute source of energy. Even in the hottest regions on earth, the solar radiation flux available rarely exceeds 1kW/m^2 , which is a low value for

technological utilization. Consequently, large collection areas are required in many applications and this results in excessive costs.

A second problem associated with the use of solar energy is that its availability varies widely with time. The variation in availability occurs daily because of the day-night cycle and also seasonally because of the earth's orbit around the sun. In addition, variations occur at a specific location because of local weather conditions. Consequently, the energy collected when the sun is shining must be stored for use during periods when it is available. The need of storage also adds significantly to the cost of any system. Thus, the real challenge in utilizing solar energy as an energy alternative is of an economic nature. One has to strive for the development of cheaper methods of collection and storage so that the large initial investments required at present in most applications are reduced.

In principle, there are many different ways to convert solar energy into cooling or air-conditioning processes; an overview is given in Fig. 2.3 which describes the cooling technologies capable of utilizing solar radiation as an energy source.

A main distinction can be made between thermally and electrically operated systems. Among the thermally driven processes, thermo-mechanical processes and processes based on heat transformation can be distinguished. The latter are all based on reversible thermo-chemical reactions with relatively low binding energies.

There are two main concepts that can be combined with each other for cooling with solar energy:

(A) Solar collection technology

(B) Technologies for cold production

2.2.1 Solar Collection Technologies:

Utilization of solar energy requires solar collectors. There are two general types:

1- Solar cells which can be used to produce electricity.

2- Solar thermal collector which can be utilized to generate heat.

2.2.1.1 Solar (Photovoltaic) Cell:

A solar cell or photovoltaic cell is a device that converts solar radiation energy directly into electrical energy.

The solar cell consists of a disc or surface with two thin layer of differently doped *semiconductor* material, often silicon, forming a junction in between (see Fig.2.4). Metal stripes runs along the front of the surface and along the back is a metal plate. When solar

radiation hits the top of the upper layer, the disc is polarized. The upper layer becomes negatively charged and the lower layer becomes positively charged [17]. If the metal stripes and plate are connected in a closed circuit, an electrical current will flow through the circuit. Thus electrical power is accessible. The voltage obtained from a single disc is rather low, in the range of 0.5 V. To obtain higher voltage, several discs are connected in series. To increase the current rows of serially connected solar cells can be connected in parallel. Thus solar cell panels, also called *modules*, are constructed. The cells are encapsulated in a transparent material (often plastic and low-iron glass) to protect them from the environment (but not to heat insulate them). Several solar cell panels can be combined into a solar cell *array*. This is illustrated in (Fig. 2.5). Commonly the output voltage from solar cell panels seems to be in the range of 12-24 V. In this study solar cells will be referred to only as a source of electric current, hence readers are referred to text books dealing with fundamentals of photovoltaic technology.

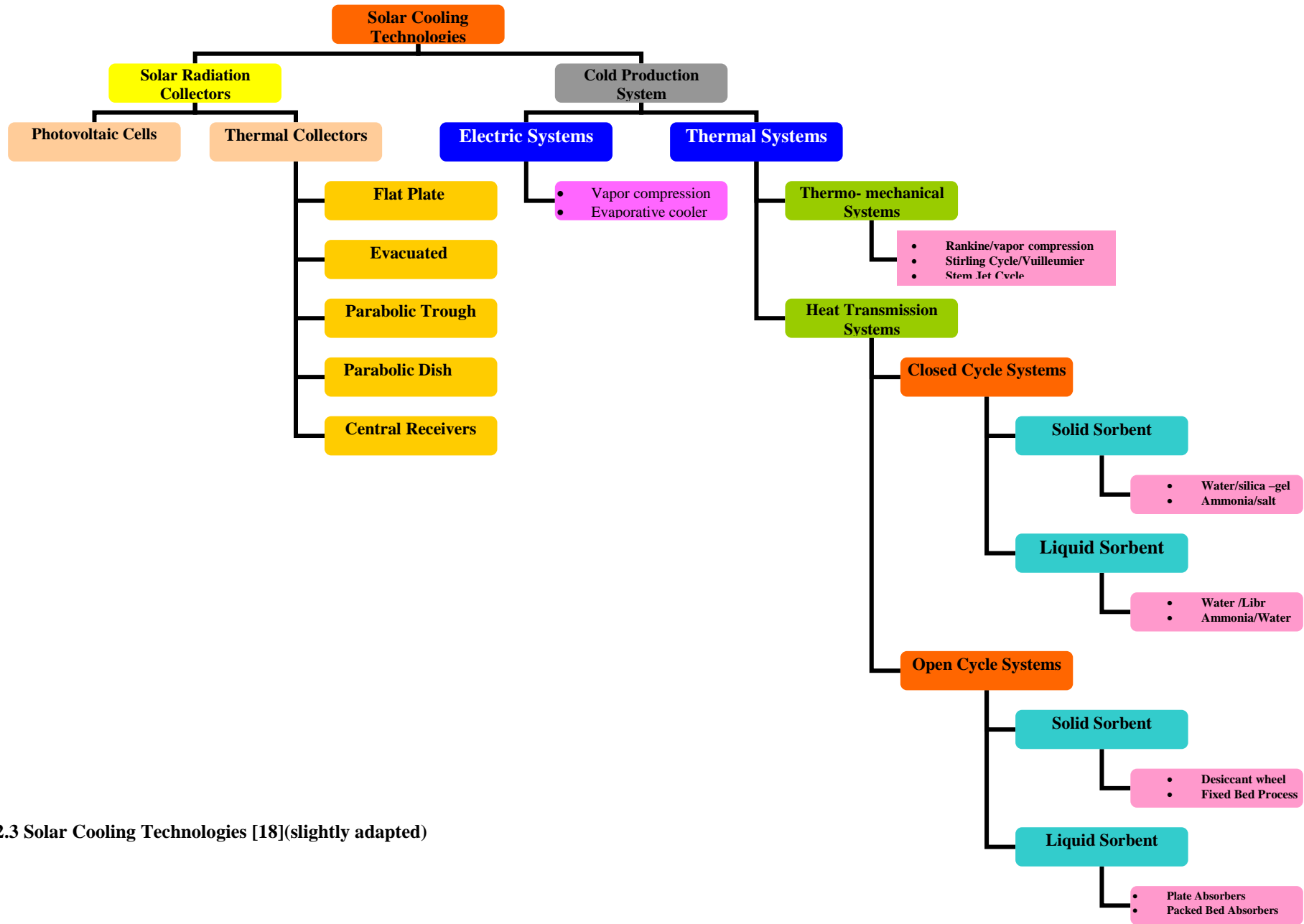


Fig. 2.3 Solar Cooling Technologies [18](slightly adapted)

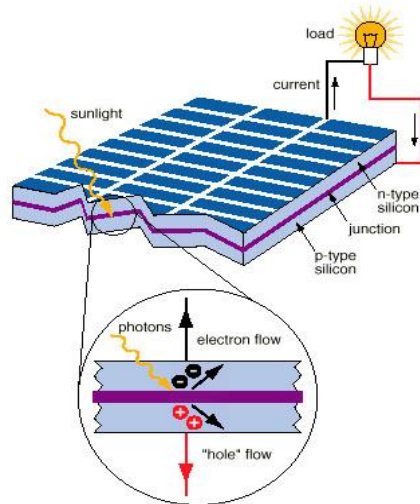


Fig. 2.4 Principles of a silicon photovoltaic cell [17]

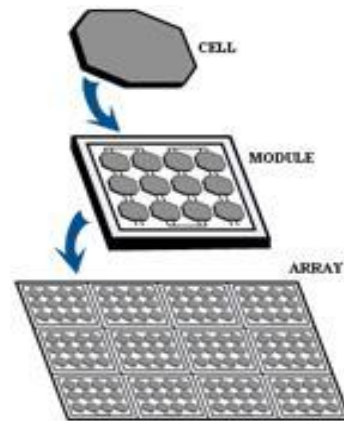


Fig. 2.5 Solar cell, module and array [17]

2.2.1.2 Solar Thermal

(i) Basic Principles

The basic principle of solar thermal collection is that when solar radiation strikes a surface, part of it is absorbed, thereby increasing the temperature of the surface. The central component in each solar collector is the absorber. Here, the absorbed solar radiation is transformed into heat; part of this heat is transferred to the heat transfer fluid and another part is lost to the environment.

The useful energy output, Q_u , per unit time of collector of area, A_c , is the difference between the absorbed solar radiation, S , and the thermal loss, U_L , and is given by:

$$Q_u = A_c [S - U_L (T_{pm} - T_a)]$$

Where T_{pm} is plate mean temperature and T_a is ambient temperature

(ii) Classification of Solar Thermal Collectors

Based on the techniques employed in heat collection and losses reduction solar thermal collectors may be classified according (a) their collecting characteristics, (b) operating temperature ranges (c) the way in which they are mounted, and (d) the type of transfer fluid they employ. Table 2.1 lists the relevant solar collector technologies.

(a) Collecting characteristics:

1) **A non –concentrating collector** is one in which the absorbing surface for solar radiation is essentially flat with no means for concentrating the incoming solar radiation. The technologies considered relevant are:

- i. Flat plate collectors: consist of an absorbing surface with passages for heat transfer fluid enclosed in an insulated casing with a transparent cover.

ii. Evacuated tubular collectors: consist of an absorbing surface mounted in a vacuum to eliminate convection heat loss.

2) A **concentrating or focusing collector** is one which usually contains reflectors or employs other optical means to concentrate the energy falling on the aperture to a heat exchanger of surface area smaller than the aperture.

The technologies considered relevant are:

i. Dish type concentrating collectors.

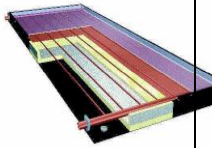

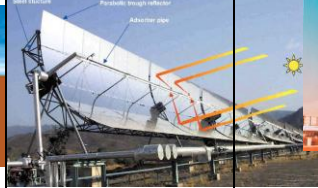

ii. Linear concentrating collectors (parabolic trough)

(b) Operating Temperature Range [17]: A division can be made between high temperature collectors with a temperature range above 150 °C, medium temperature collectors with a temperature range of 30-150 °C, and low temperature collectors with a temperature range below 30°C.

(c) Mounting. A collector can be mounted to remain stationary, be adjustable so as tilt angle (measured from the horizontal and equivalent to latitude) to follow the change in solar declination or be designed to track the sun. Tracking is done by employing either an equatorial mounting or an azimuth mounting, for the purpose of increasing the absorption of the daily solar radiation. The operation of the tracking mechanism can be either manual or automatic.

(d) Types of fluid. A collector will usually use either a liquid or a gas as the transfer fluid. The most common liquids are water or a water- ethylene glycol solution. The most common gas is air.

Table 2.1 Solar Collectors Types [17]

Type of Collector	Flat Plate Collectors	Evacuated Collectors	Parabolic trough collectors	Parabolic dish collectors
Concentration Ration	1	1	15-45	100-1000
Typical Working Temperature°C	30-80	50-200	80-300	100-500
Diagrams				

(iii) Types of Solar Thermal Collectors

a) Non –concentrating Collectors

1) Flat Plate Collectors

The main components of the flat plate collector are (see Fig. 2.6) :

- The absorber plate which absorbs solar radiation into heat and then transfer it fluids passing through flow passages attached to the absorber plate. (*Note: for highly efficient flat plate collector, the absorber is coated with a selective material to reduce radiative heat losses*)
- The Cover plate which is made of glass or various plastic transparent materials. It reduces the convective and radiative heat losses to the outside air. Insulation at the back and sides of the collector reduces heat losses.
- Enclosure- a box to hold collector components together and protect them from the weather.

(*Note: low temperature flat plate collectors do not have covers, enclosure, or insulation*).

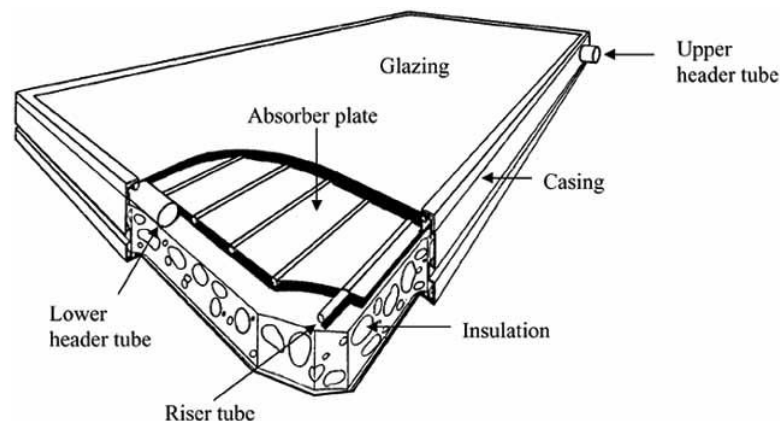


Fig. 2.6 Flat Plate Collector [17]

2) Vacuum Tube Collector

In vacuum collectors the absorbers are separated thermally from their surroundings by a transparent cover. In addition to the reduction in radiation exchange, convective heat transport is reduced by a very good vacuum of approximately 10^{-3} to 10^{-2} Pa. The result is heat transfer coefficient of values of around $1\text{W/m}^2\text{K}$. A range of different vacuum tube geometries is available on the market (see Fig. 2.7). The absorber is either a standard finned tube design within an evacuated glass tube or coated directly on the inner surface of a double glass tube, with the heat transferred to liquid circulating in separate tubes on the inside of the double glass. This technology results in better collector performance at higher temperatures (see Fig. 2.8)

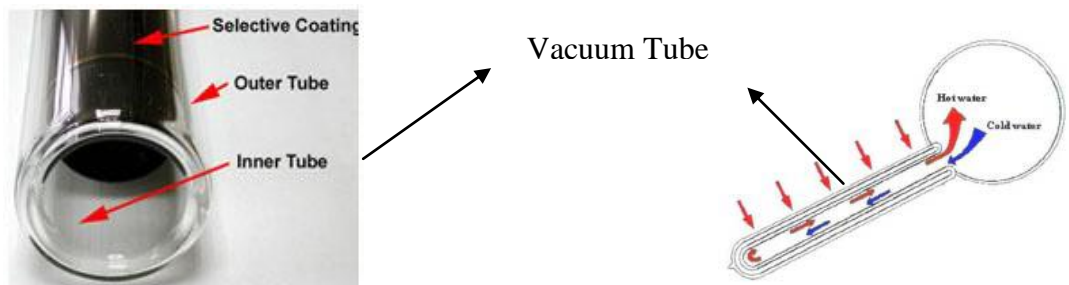
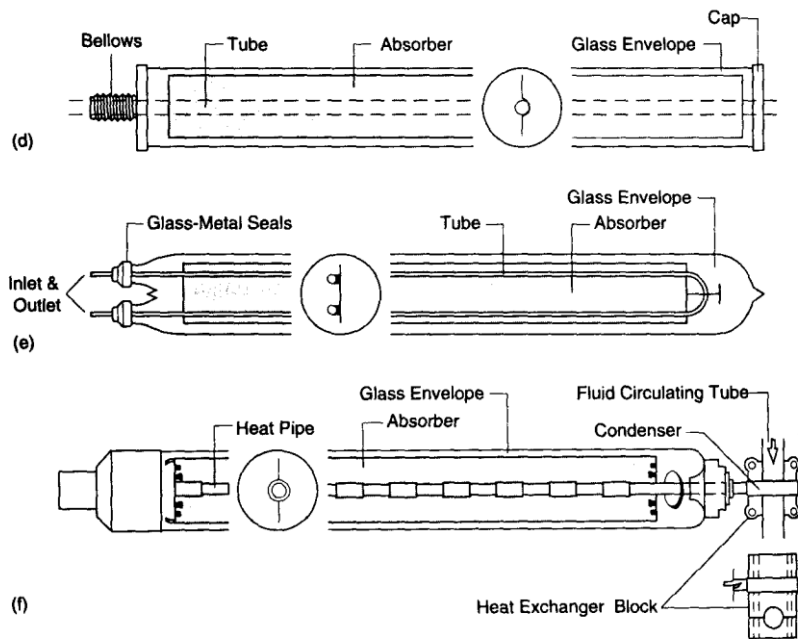


Fig.2.7 Different Vacuum Tube Geometries [1,23]

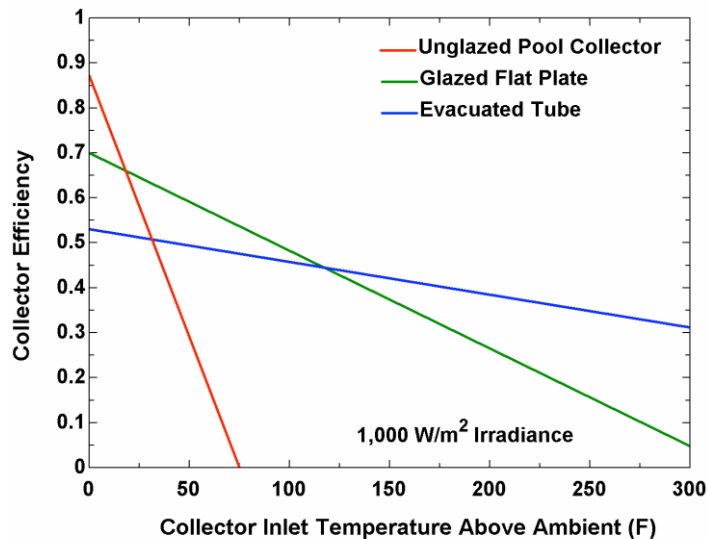


Fig. 2.8 Performance Comparing of Solar Collectors

b) Concentrating Collectors

Solar concentrator is a device which concentrates the solar energy incident over a large surface onto a smaller surface. The concentration is achieved by use of suitable

reflecting or refracting elements which results in an increased flux density on the absorber surface as compared to that existing on the concentrator aperture. In order to get a maximum concentration, an arrangement for tracking the sun's virtual motion is required. An accurate focusing device is also required. Thus, a solar concentrator consists of:

- The receiver: is that element of the system where the radiation is absorbed and converted to some other energy form; it includes the absorber, its associated covers, and insulation.
- The concentrator: or optical system, is the part of the collector that directs radiation onto the receiver.
- A tracking arrangement.

1) Classification of Concentrating Collectors

Solar concentrators may be classified as (i) tracking type and(ii) non-tracking type. Tracking may be continuous or intermittent and may be one-axis or two axes. As the sun may be moving either the focusing part or the receiver or both; concentrators may be classified accordingly. Further, the system may have distributed receiver or central receiver.

The concentrators may also be classified on the basis of optical components. They may(i) reflecting or refracting type,(ii) imaging or non-imaging type, and (iii) line focusing or point focusing type.

2) Types of Concentrating Collectors(*Note: only relevant types will be considered*)

.i **Parabolic Trough Concentrator**(*one-axis tracking*)

A parabolic trough concentrator is a conventional optical imaging device used as a solar concentrator. It consists of a parabolic reflector and a metal tube receiver at its focal plane. The receiver of a parabolic trough is linear. Usually, a tube is placed along the focal line to form an external surface receiver as shown in (Fig 2.9). The size of the tube, and therefore the concentration ratio, is determined by the size of the reflected sun image and the manufacturing tolerances of the trough. The surface of the receiver is typically plated with selective coating that has a high absorbance for solar radiation but a low remittance for thermal radiation loss. A glass cover tube is usually placed around the receiver tube to reduce the convective heat loss from the receiver, thereby further reducing the heat loss coefficient.

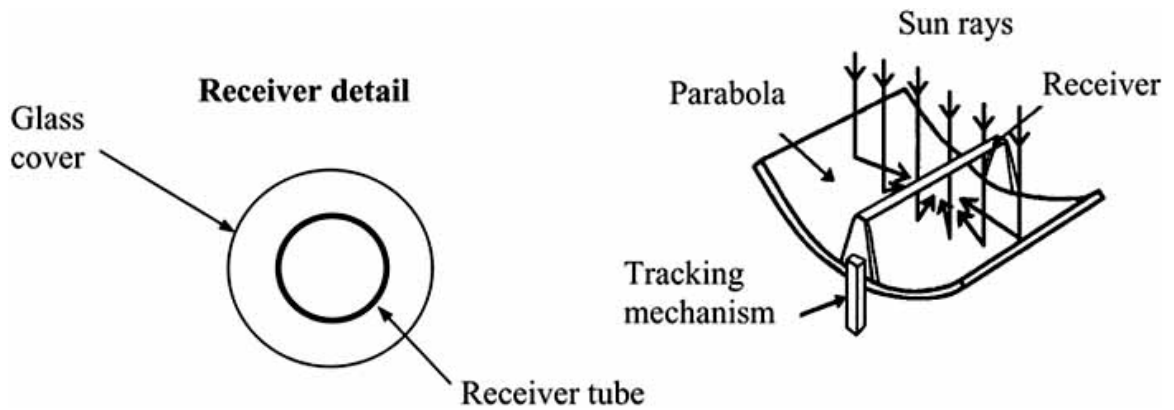


Fig. 2.9 Parabolic Dish Solar Collector [17]

.ii **Parabolic dish concentrator** (*Two-axis tracking*)

A parabolic dish reflector, shown schematically in Fig. 2.10, is a point-focus collector that tracks the sun in two axes, concentrating solar energy onto a receiver located at the focal point of the dish. The dish structure must track fully the sun to reflect the beam into the thermal receiver. The receiver absorbs the radiant solar energy, converting it into thermal energy in a circulating fluid. The thermal energy can then either be converted into electricity using an engine-generator coupled directly to the receiver, or it can be transported through pipes to a central power-conversion system.

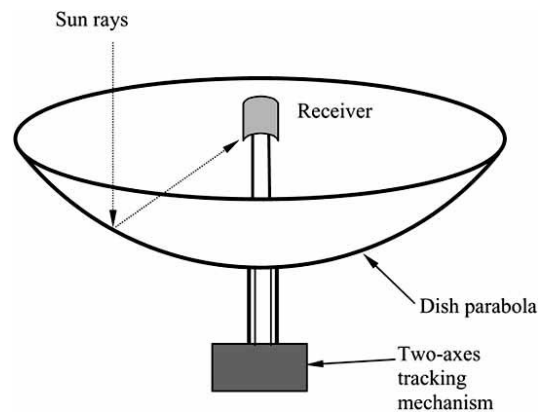


Fig. 2.10 Parabolic Dish Collector

2.2.2 Cooling Technologies

Solar energy can be used as a primary energy input to different kinds of cooling systems. For example, electricity generated by PV can be used to drive a vapour compression system. Solar thermal collectors can be used to run a sorption cooling system or a thermo-mechanical cooling system.

In this section, three approaches will be reviewed and their operating characteristics will be highlighted.

The cooling technologies considered relative are:

- 1) Solar Electric
- 2) Solar Mechanical
- 3) Solar Absorption

2.2.2.1 Photovoltaic Operated Refrigeration Cycle (Solar Electric)

A solar electric cooling system consists mainly of photovoltaic panels and an electrical cooling device. In concept, the operation of a PV-powered solar refrigeration cycle is simple. Solar photovoltaic panels produce dc electrical power that can be used to operate a dc motor, which is coupled to the compressor of a vapor compression refrigeration system (see Fig. 2.11).

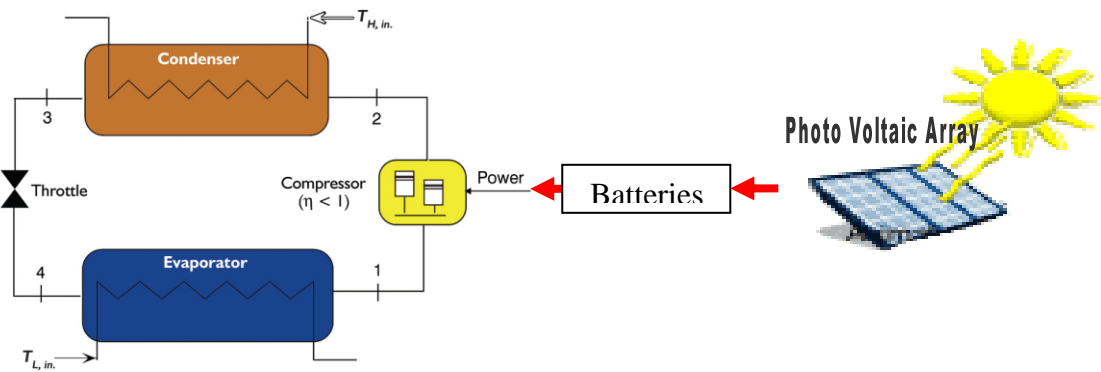


Fig. 2.11 Photovoltaic Operated Refrigeration Cycle[21]

Firstly, the systems should be equipped with some means to cope with the varying electricity production rate with time, e.g. electric battery, mixed use of solar- and grid electricity or a variable-capacity compressor and so on.

Secondly, the price of a solar electric panel should be further decreased to compete with other solar cooling technologies.

2.2.2.2 Solar Mechanical Refrigeration

Solar mechanical refrigeration uses a conventional vapor compression system driven by mechanical power that is produced with a solar-driven heat power cycle. The heat power cycle usually considered for this application is a Rankine cycle in which a fluid is vaporized at an elevated pressure by heat exchange with a fluid heated by solar collectors. A storage tank can be included to provide some high temperature thermal storage.

The vapor flows through a turbine or piston expander to produce mechanical power, as shown in figure 2.12. The fluid exiting the expander is condensed and pumped back to the boiler pressure where it is again vaporized. The efficiency of the Rankine cycle increases with increasing temperature of the vaporized fluid entering the expander. High temperatures can be obtained from concentrating solar collectors that track the sun's position in one or two dimensions. Tracking systems add cost, weight and complexity to the system.

Solar mechanical systems are competitive only at higher temperatures for which tracking solar collectors are required. Because of its economy-of-scale, this option would only be applicable for large refrigeration systems (e.g., 1,000 tons or 3,517 kW)

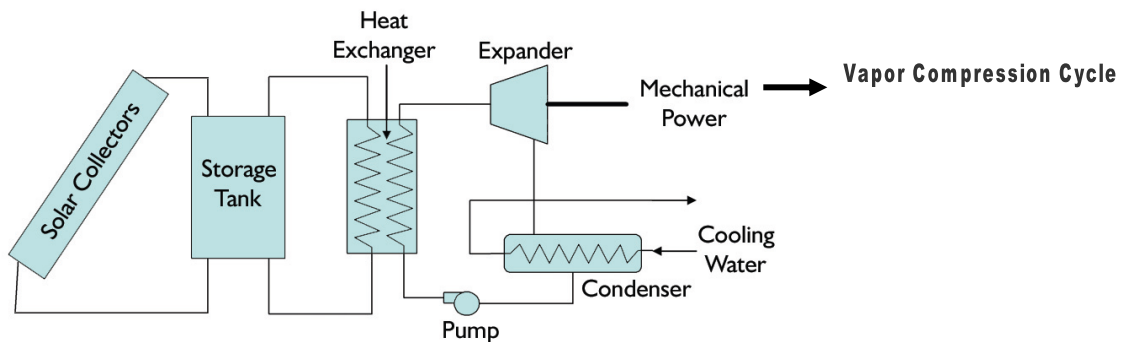


Fig. 2.12 Solar Mechanical Refrigeration [21]

2.2.2.3 Solar Absorption Refrigeration

An absorption cooling system is considered as a “heat driven” system. It has a unique capability of transforming thermal energy directly into cooling power. The working fluid for the system is a solution containing a refrigerant and an absorbent which have strong chemical affinity for each other. To examine the operation of such a system, consider the generator in figure 2.13. Heat is transferred to the solution of refrigerant and absorbent contained in the generator and as result, refrigerant is vaporized from mixture, leaving a solution having a low refrigerant concentration behind. The liberated vapor is free to flow to the condenser where heat is removed from it to bring about its liquefaction. The generator and the condenser comprise the high pressure section of the system. Liquid refrigerant which is accumulated in the condenser is available for expansion from this high pressure portion of the system into the low pressure evaporator, wherein vaporization of refrigerant takes place and the cooling effect is achieved. Once the refrigerant has been vaporized, the evaporator and has removed heat from cold storage or space being cooled it is discharged to the

absorber, which is weak in refrigerant concentration. Since this combination reaction is exothermic, heat must be removed from the absorber to maintain its temperature at a sufficiently low value to assure the desired high chemical affinity between the refrigerant and the solution. The resulting absorber solution which is rich in refrigerant is collected in the bottom of the absorber and pumped back into the generator to maintain the generator solution level and concentration. It is the pump shown in Figure 2.13 that maintains the desired pressure difference in the system.

The requirement to circulate refrigerant –weak solution continuously from the high temperature generator to the low temperature absorber and refrigerant-strong solution in the opposite direction necessitates the installation of the generator-absorber solution heat exchanger shown. The solution heat exchanger is a simple counter –flow heat exchanger which minimizes the heat loss associated with the fluid transfer between these two components. Without this exchanger, the heat load on the collector and the heat rejection load associated with the absorber would both be increased with consequent reduction in the coefficient of performance of the system. The absorption refrigeration system includes five heat exchangers and a pump together with the necessary piping and controls (see Fig.2.13).

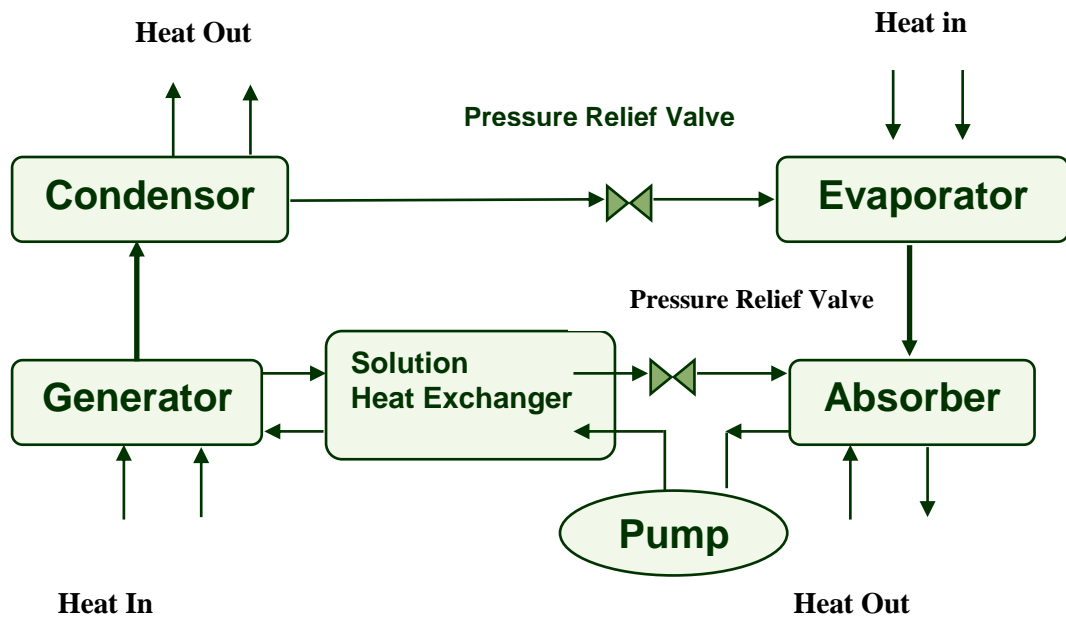


Fig. 2.13 Absorption Refrigeration Cycle

2.2.2.4 Comparison of Solar Cooling Technologies

The current commercial status of different solar cooling technologies may be quickly viewed in a comparison of the initial costs of various cooling systems. From the review of three previously mentioned solar cooling technologies (see Table 2.2), it

was concluded that solar electric and thermo mechanical technologies are currently not competitive with solar thermal absorption technology in terms of initial cost. Absorption cooling is found to be the most cost-effective for solar cooling applications and it is a promising technology and can play a vital role to reduce GHG emission. It was also concluded that the direction of future R&D would better be focused on low temperature-driven cooling system. It is because initial cost can be lowered significantly, if cheaper solar collectors are used.

Table 2.2 Comparison of Solar Refrigeration Systems[2]

Comparison of Solar Refrigeration Systems			
Cold Production System	Electric System	Thermo mechanical	Sorption Systems
• Solar Energy Collection System	Photovoltaic Panels	Concentrating Collectors	Non-Concentrating Collectors
• Refrigeration Cycle	Vapor Compression	Vapor Compression/ Rankine	Absorption
• Minimum Driving Temperature	inapplicable	Above 200 °C	80-150°C
• Price per W or kW	€1,667/Kw(<i>cost of solar panels alone</i>)	€7.71/Watt(<i>not including the price of the heat engine</i>)	€500-800/KW
• C.O.P	0.25-0.3(<i>due to low solar cell efficiency</i>)	0.3-0.4	0.6-0.7

2.3 The Absorption Cooling Process

The simplest absorption cycle, single effect cycle, have five main components, namely generator, absorber, condenser, evaporator and a solution heat exchanger. In order to clarify the principle, figure 2.14 will be discussed briefly. A binary mixture (refrigerant/absorbent) circulates between generator and absorber. At point (1) mixture with high concentration of refrigerant (strong) enters the generator. When heat Q_G supplied on the high temperature level T_G , refrigerant is driven out of this mixture and it becomes weak (point 2). The escaping refrigerant vapour (point 5) flows to the condenser (point 6) where it condensates at temperature T_c (point 7), provided that the vapour pressure at the condenser is lower than at the generator. Condensation heat Q_c must be removed. This liquid refrigerant is throttled to low pressure (point 8) and fed to evaporator. If heat Q_E is supplied, the liquid evaporates at temperature T_E (point 9). The vapour flows to the absorber, provided that the vapour pressure at the absorber is lower than at the evaporator. In the absorber, weak mixture that has left the generator and has been throttled to low pressure, enters (point 3). This weak mixture absorbs the vapour and absorption heat Q_A must be rejected. The

strong mixture is pumped back to the generator (point 1), which completes the cycle. The work done by the pump (W_p) is small compared to the heat flows. In the considered system, Q_E will be provided by the storage room.

Through the representation of the components in the Pressure-Temperature-concentration diagram (P-T-x diagram with the concentration of the solution, x , as parameter) the individual process steps can be reconstructed (see Fig 2.15). On the high pressure side, with pressure P_h , are the condenser and generator, on the low pressure side, with pressure level P_L , are the evaporator and absorber. In the evaporator and condenser the refrigerant concentration is 100 %, which corresponds to a concentration of solution of $x = 1.0$. The lowest refrigerant concentration in the solution is produced in the generator (concentration lines on the right of the P-T-x diagram)

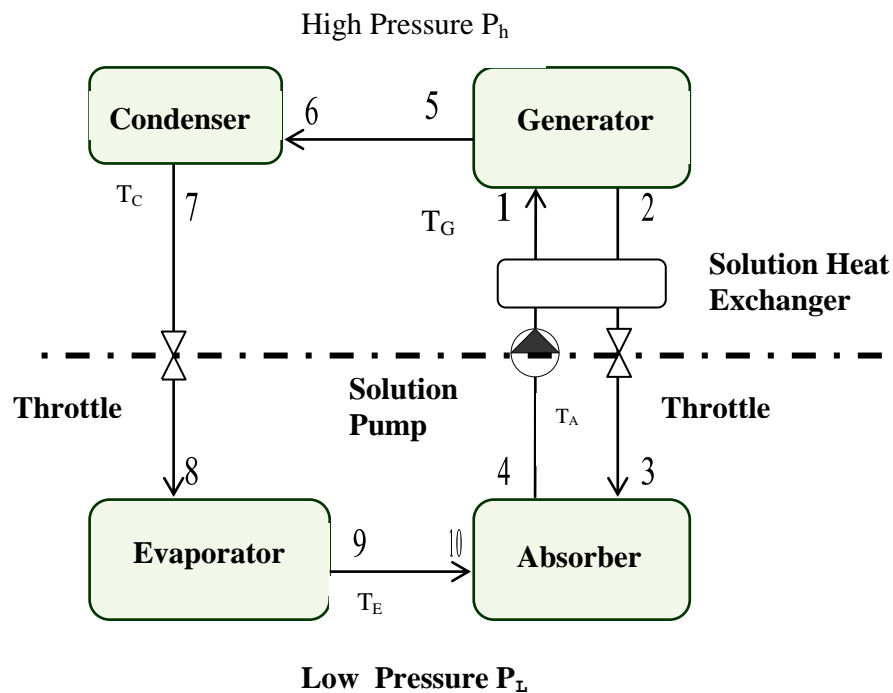


Fig. 2.14 Absorption Cycle (state Points)

2.3.1 The Components of the Absorption Cooling Process

2.3.1.1 The Condenser

The condenser is the device that transfers heat from the refrigeration system to a medium which can absorb and move it to a final disposal point. Heat release takes place either by air or a liquid circuit. It is in the condenser that superheated, high pressure refrigerant vapor is cooled to its boiling (condensing) point by rejecting

sensible heat. The additional rejection of latent heat causes the vapor to condense into the liquid state.

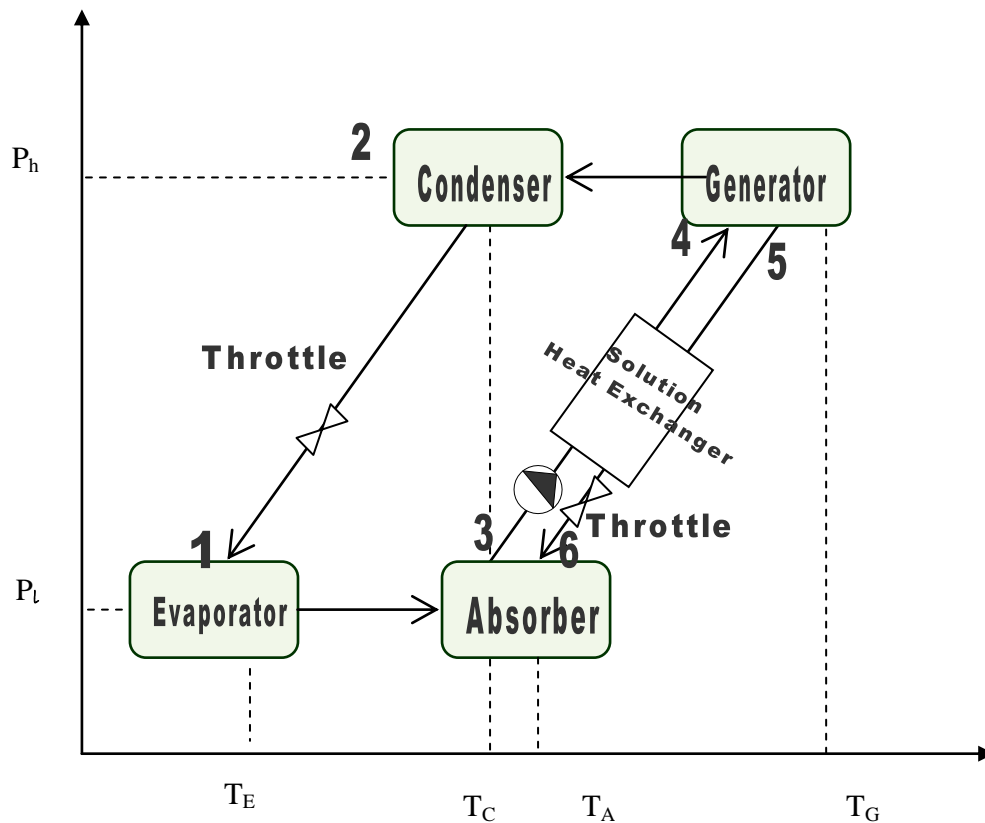


Fig. 2.15 Absorption Cycle on the P-T-X Diagram[2]

2.3.1.2 The Evaporator

The evaporator is that part of the refrigeration system in which the refrigerant boils and, in doing so, absorbs heat. Heat uptake takes place either by air or a liquid circuit. Before the condensed refrigerant enters the evaporator, the pressure must be reduced to the low evaporator pressure. This is usually done by a throttle valve. The purpose of the evaporator is to receive low-pressure, low temperature fluid from the throttle valve and to bring it in close thermal contact with the load and leaves the evaporator as a dry gas.

2.3.1.3 The Generator

The rich (strong) solution (rich in refrigerant) contained in the generator is heated by conventional heat sources like gas, other fossil sources, or by solar thermal energy using collectors. The rise in temperature of the rich solution raises the vapor pressure such that the vapor pressure in the condenser equals the saturation pressure in the

generator. The refrigerant, expelled in the vapor form goes to the condenser , and the weak solution returns through a throttle valve to the absorber.

2.3.1.4 The Absorber

The refrigerant-poor solution flows back into the absorber from the generator. The refrigerant vapor produced in the evaporator is absorbed there as function of the absorber temperature and solvent concentration. The evaporator and absorber are at the same refrigerant pressure level. The refrigerant poor solution in the absorber must constantly take up the refrigerant produced in the evaporator, since otherwise the evaporator pressure would rise. Through refrigerant absorption the concentration of refrigerant vapor in the solution rises. The concentration modification between the rich and the poor solution ξ_r and ξ_p is called the degassing width.

2.3.1.5 The Solution Heat Exchanger

The requirement to circulate refrigerant weak solution continuously from the high temperature generator to the low temperature absorber and refrigerant-strong solution in the opposite direction necessitates the installation of the solution heat exchanger shown in Fig 2.14. The installation of this counter flow heat exchanger minimizes the heat loss associated with the fluid transfer between these two components. Without it, the heat load on the collector and the heat rejection load associated with the absorber would both be increased with consequent reduction in the coefficient of performance of the system. This exchange of heat may bring the rich solution close to the boiling point or even higher.

2.3.2 Physical Principals of the Absorption Process

2.3.2.1 Vapor Pressure Curve of Material Pairs

In thermal equilibrium, a saturation vapor pressure arises over a pure liquid, depending solely on the temperature. As a function of the evaporation enthalpy of the pure working material, an exponential rise of the saturation vapor pressure, P, with the negative reciprocal value of the temperature $-\frac{1}{T}$ results [2] . For pure ammonia, this results in an approximation solution with logarithmic function(see Eqn. 2.3.2.1.1):

$$\log_{10} p = a - \frac{b}{T} \text{-----(2.3.2.1.1)}$$

Indicated by the coefficients $a= 10.018$ and $b= 1204.3$ for pressures up to $25 \times 10^5 Pa$ (T in Kelvin). According to the equation 2.3.2.1.1 (Chaperon's equation) if a curve is plotted between logarithm of vapor pressure and reciprocal of the absolute temperature, then the lines of constant concentration will be practically straight lines (see Fig.2.16). According to the pressure-temperature-concentration diagram (P-T-X diagram), a fixed relation exists between temperature, pressures and concentrations of the absorbent-refrigerant pair in the absorption cooling process.

The low pressure level P_e of the cooler is determined by the saturation vapor pressure at the desired evaporator temperature T_e . The temperature level of the condenser T_c determines the high pressure level P_h in the absorption cooler.

The maximum concentration of solution at which absorption can still occur is determined by the absorber temperature T_a . The generator temperature T_g on the high pressure side determines the minimum solution concentration and so determines the degassing width, i.e. the concentration difference, between the strong solution in the absorber and the weak solution in the generator. As shown in the diagram, the concentration of solution varies in 10% steps from 0.1 to 1 (pure ammonia corresponds to $x = 1$, left curve).

As illustrated above, the performance of an absorption cooler like the one shown schematically in Figure 2.14 is determined by the temperatures of the various components. The condenser and absorber temperatures are determined primarily by the available heat rejection temperature. The evaporator temperature must be sufficient to produce the desired cooling effect in the space being cooled. With these three temperature prescribed, the generator temperature and hence heat source temperature necessary to effect proper system operation are fixed by thermodynamic consideration. The maximum generator temperature results when refrigerant vapor has already been expelled from the solution, i.e. at the end of the expulsion process.

As shown in figure 2.15 & 2.16, the process runs via the evaporator(status point 1), condenser(2), the absorption of the refrigerant in the solution (3), the entry of the rich solution into the generator (4), the weak solution at the end of the expulsion process(5) and the weak solution cooled by the solution heat exchanger before re-entry into the absorber(6). The refrigerant vapor in the generator is then in equilibrium with the refrigerant-weak solution leaving the generator.

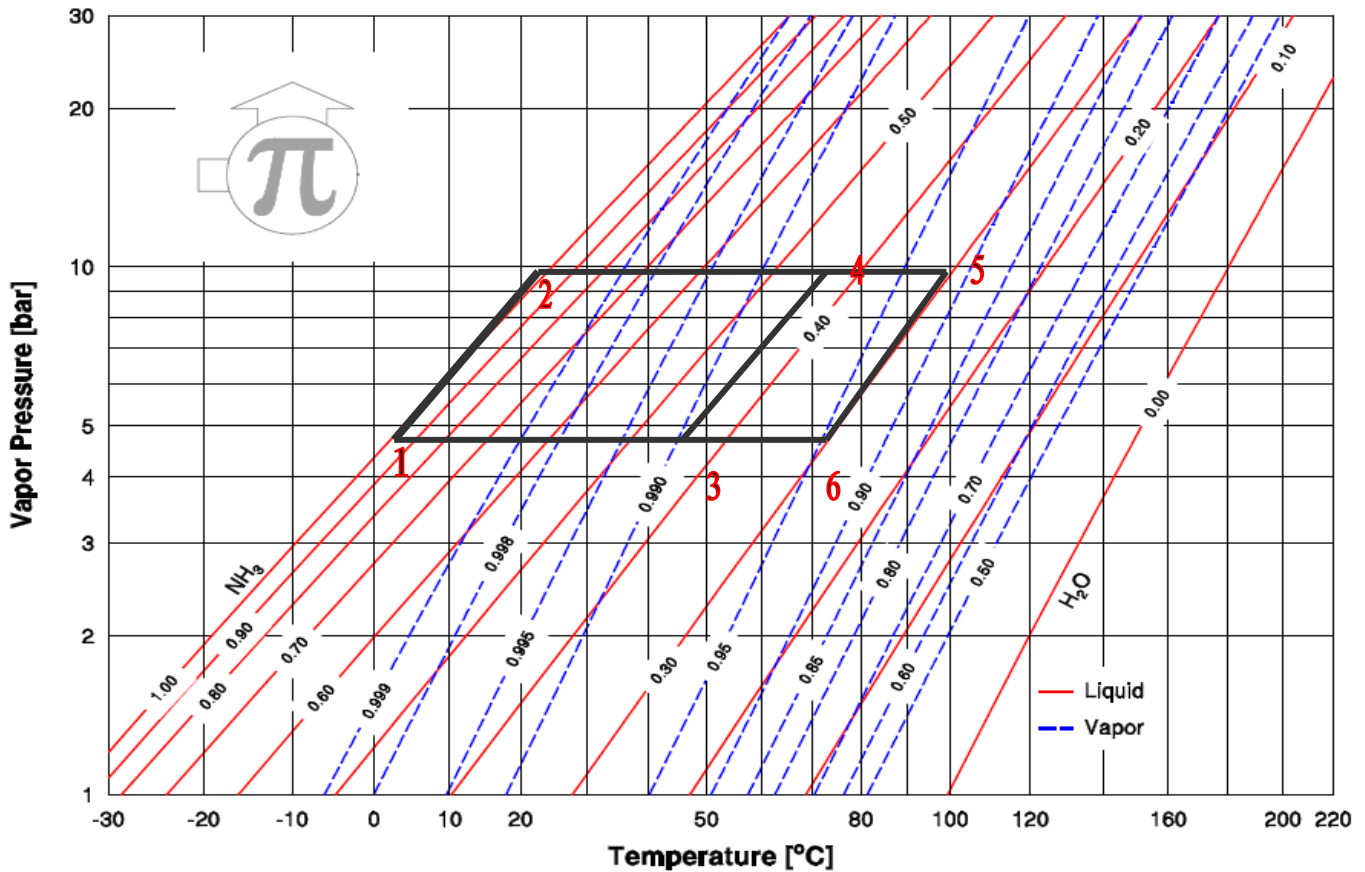


Fig. 2.16 Vapor Pressure Curve of Ammonia-Water Solution in the log -1/T Diagram

2.3.2.2 Ideal Performance Figures

In an ideal absorption process the cyclic process of the refrigerant is regarded as loss-free and thermodynamically reversible. Based on the principle of conservation of energy, the heat taken up in the evaporator and in the generator must equal the delivered heat in the condenser and absorber (see Eqn. 2.3.2.2.1).

$$Q_E + Q_G = Q_A + Q_c \text{ ----- (2.3.2.2.1)}$$

Since an ideal process runs reversibly, the entropy must remain constant according to the second law of thermodynamics. The reduced entropy in the condenser corresponds to the entropy increase in the evaporator, and the entropy decrease in the absorber corresponds to the entropy increase in the generator. If instead of the energy balance a power balance is set up and the power is related to the circulating refrigerant mass flow, the result is

$$\frac{\dot{Q}_e / \dot{m}_v}{T_e} = \frac{\dot{Q}_c / \dot{m}_v}{T_c} \text{ ----- (2.3.2.2.2)}$$

$$\frac{\dot{Q}_a / \dot{m}_v}{T_a} = \frac{\dot{Q}_g / \dot{m}_v}{T_g} \text{ ----- (2.3.2.2.3)}$$

The coefficient of performance (COP) of an absorption cooler is defined by the relation of the power taken up in the evaporator to the supplied power in the generator, and can by reformulation the above equations be represented as a temperature relation.

$$COP = \frac{\dot{Q}_E}{\dot{Q}_G} = \frac{T_G - T_a}{T_G} \times \frac{T_E}{T_C - T_E} \text{----- (2.3.2.2.4)}$$

The COP of an absorption cooler is thus the product of a right-circulating Carnot thermal engine between the temperatures of the generator and the absorber and a left-circulating Carnot cooling machine between the temperatures of the evaporator and the condenser.

Good COPs result if the condenser and absorber temperature can be kept low, since on the one hand the temperature lifting capacity of the thermal machine rises between the absorber and generator, and on the other hand the temperature difference between the evaporator and condenser for an efficient cooler cyclic process remains small.

2.3.2.3 Real Performance Figures

In an ideal absorption cooling process, COP over 1.0 can readily occur. In a cooler, however, irreversible processes occur during absorption of the refrigerant in the solution. The real COPs depend furthermore on whether the freed amounts of heat in the absorber, condenser can be recovered and supplied to the process again.

2.3.2.4 Mass and Energy Balances[14]

(i) Generator

At the generator, 3 mass flows occur and heat is supplied externally (see Fig.2.17) . Rich(strong) *solution is supplied to a generator at the flow rate \dot{m}_r , concentration x_r and Temperature T_7 . Poor(weak)* solution leaves the generator at flow rate \dot{m}_p , concentration x_p and T_8 . Superheated vapor leaves for condenser with flow rate \dot{m}_v Temperature T_1 , pressure P_H . Heating medium enters the generator at \dot{m}_w and Temperature T_{11} .

$$Q_G = \dot{m}_8 h_8 + \dot{m}_1 h_1 - \dot{m}_7 h_7 \text{----- (2.3.2.4.1)}$$

$$x_p \dot{m}_p + \dot{m}_v = x_r \dot{m}_r \text{----- (2.3.2.4.2)}$$

* rich and poor solution are strong and weak solutions respectively.

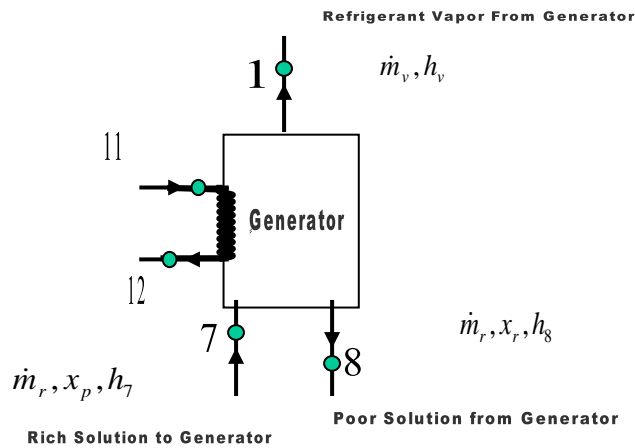


Fig. 2.17 Mass Flows at the Generator

(ii) Absorber

Poor solution is supplied to absorber at a rate of \dot{m}_p , concentration of x_p , temperature of T_{10} . Rich solution leaves the absorber at flow rate \dot{m}_r , concentration x_r , and temperature T_5 . Saturated vapor from the evaporator enters at flow rate \dot{m}_v . Coolant enters the absorber at temperature T_{13} (see Fig. 2.18).

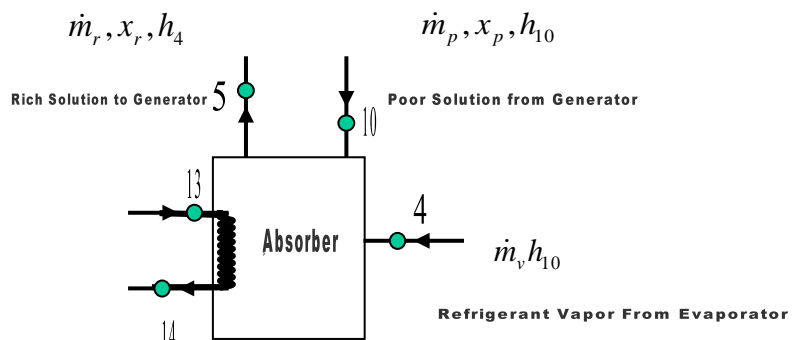


Fig. 2.18 Mass Flows at the Absorber

$$Q_A = \dot{m}_{10}h_{10} + \dot{m}_4h_4 - \dot{m}_5h_5 \text{-----(2.3.2.4.3)}$$

(iii) Condenser

The vapor condenses in a condenser with at the rate of \dot{m}_v and at a temperature T_2 . Coolant at temperature T_{15} (see Fig. 2.19).

$$\dot{m}_1 = \dot{m}_2 \text{-----(2.3.2.4.4)}$$

$$Q_c = \dot{m}_2h_2 - \dot{m}_1h_1 \text{-----(2.3.2.4.5)}$$

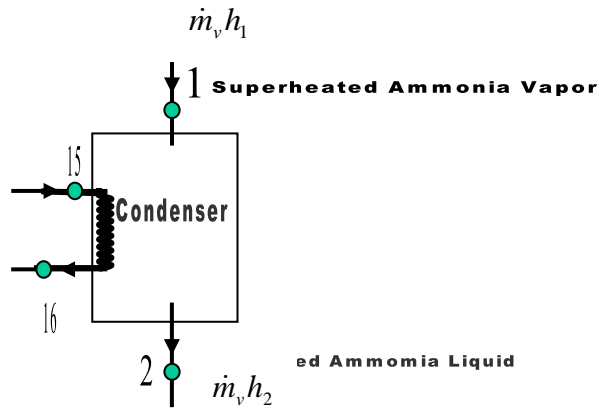


Fig. 2.19 Mass Flows at the Condenser

(iv) **Evaporator**

The magnitude of the heat transfer and fluid flow rates within the system are determined by the power level of the evaporator. Refrigerant evaporates under pressure P_L , flow rate \dot{m}_v . Chilled water enters the evaporator at T_{17} (see Fig. 2.20)

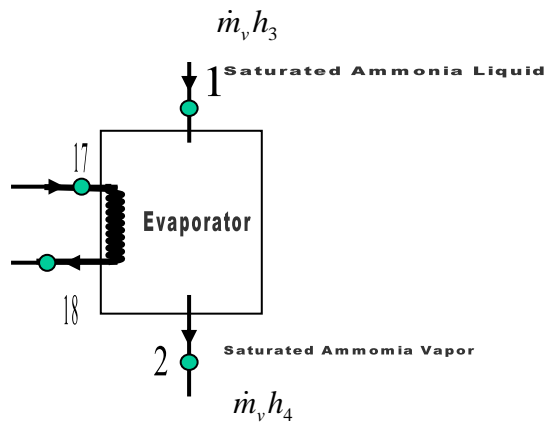


Fig. 2.20 Mass Flows at the Evaporator

$$\dot{m}_3 = \dot{m}_4 \text{-----(2.3.2.4.6)}$$

$$Q_E = \dot{m}_4 h_4 - \dot{m}_3 h_3 \text{-----(2.3.2.4.7)}$$

(v) **Solution Heat Exchanger**

Rich solution at the flow rate of \dot{m}_r is heated from T_6 to T_7 and poor solution at \dot{m}_p is cooled down from T_8 to T_9 (see Fig. 2.21).

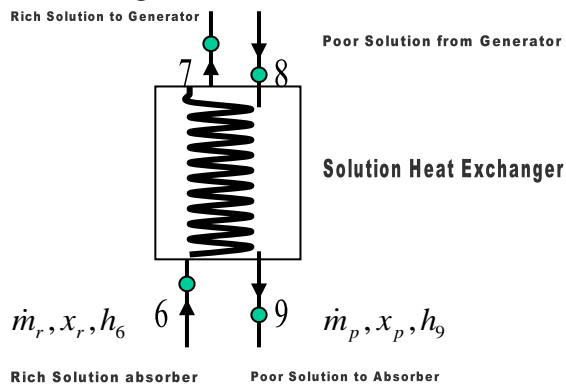


Fig. 2.21 Mass Flows at the Solution Heat Exchanger

$$\dot{m}_r(T_7 - T_6) = \dot{m}_p(T_9 - T_8) \text{-----}(2.3.2.4.8)$$

$$\dot{m}_5 x_5 + \dot{m}_1 x_1 = \dot{m}_2 x_2 + \dot{m}_6 x_6 \text{-----}(2.3.2.4.9)$$

2.4 The Solar Energy Collection

The driving heat for the absorption refrigeration system comes from the solar heat production sub-system, which includes the collectors and storage tanks.

2.4.1 Thermal Analysis of Flat Plate Collector[1]

The important parts of a typical liquid heating flat-plate solar collector are shown in Fig.2.22. In steady state, the performance of a solar collector is described by an energy balance that indicates the distribution of incident solar radiation into useful energy gain, thermal losses, and optical losses. The solar radiation absorbed by a collector per unit area of absorber, S , is equal to the difference between the incident radiation I_t and the optical losses (average-absorptance-transmittance ratio $(\tau\alpha)_{av}$) as defined by:.

$$S = (\tau\alpha)_{av} I_t \text{-----}(2.4.1.1)$$

The thermal energy lost from the collector to the surrounding by conduction, convection, and infrared radiation can be represented as the product of heat transfer coefficient U_L times the difference between the mean absorber plate temperature T_{pm} and the ambient temperature.

The useful energy output of a collector area, A_c , is the difference between the absorbed solar radiation and the thermal loss:

$$Q_u = A_c [S - U_L (T_{pm} - T_a)] \text{-----}(2.4.1.2)$$

Where $U_L = U_s$ (side-losses) + U_b (bottom-losses) + U_t (top Losses)

The temperature on the absorber sheet metal T_{pm} is, however, a complicated function of the distance from the heat-removing fluid tubes and the flow length, so an average value can only be determined very laboriously from a measured temperature distribution. What is measurable, however, is the fluid inlet temperature into the collector or the mean fluid temperature, which at not too low flow rates is given by arithmetical average value between entry and exit temperatures. Above all the representation of the available energy as a function of the fluid inlet temperature is very useful for system simulations, since the fluid inlet temperature is given by

storage return temperature. To be able to determine analytically the available energy at a given fluid inlet temperature or mean fluid temperature, the temperature distribution on the absorber sheet metal must first be calculated as the solution of a thermal conduction problem(See Fig. 2.22). Subsequently the local fluid temperature is calculated by heat transfer to the fluid.

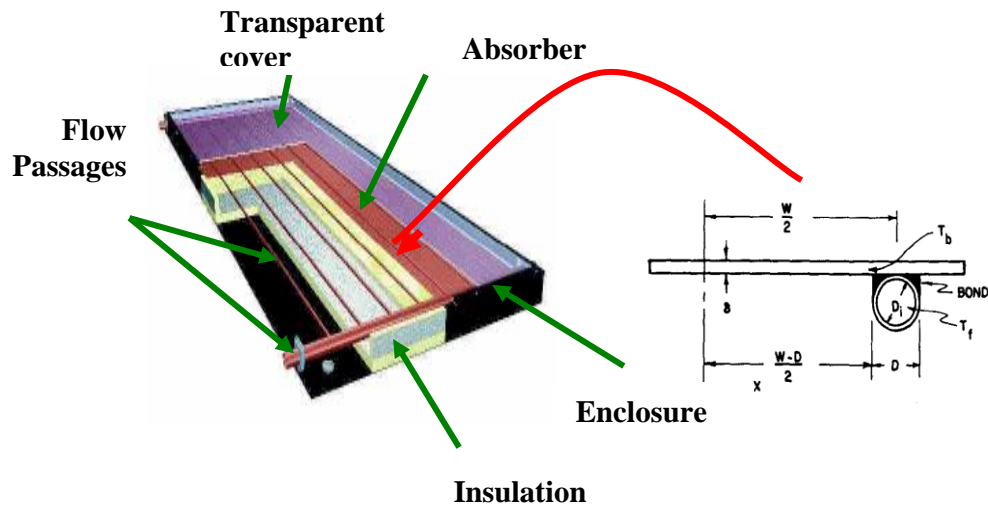


Fig. 2.22 Flat plate Collector[1]

At a given mass flow, the entire rise in temperature and available energy can then be calculated by an integration over the flow length, and represented as a function of the fluid inlet temperature as shown by the following equation:

$$Q_u = A_c F_r [S - U_L (T_i - T_a)] \text{-----}(2.4.1.3)$$

Where F_r is the collector heat removal factor and is defined as the ratio of the actual useful energy gain to the useful energy gain if the entire collector were at the fluid inlet temperature T_i , and can be expressed as

$$F_r = [\dot{m} C_f / (A_c U_L)] [1 - \exp(-A_c U_L F' / (\dot{m} C_f))] \text{-----}(2.4.1.4)$$

Where F' is the collector efficiency factor and is defined as the ratio of actual heat collection rate to the useful heat collection rate when the collector absorbing plate T_p is at the local fluid temperature T_f can be written as:

$$F' = \frac{1}{U_L W \left\{ \frac{1}{U_L [D + (W - D) F]} + \frac{1}{C_B} + \frac{1}{\Pi D_i h_f} \right\}} \text{-----}(2.4.1.5)$$

Where F is the fin efficiency factor and is given by equation:

$$F = \frac{\tanh m(W - D)/2}{m(W - D)/2} \text{-----} \quad (2.4.1.6)$$

Where $m = \sqrt{U_L / k\delta}$

Where k is the plate thermal conductivity, δ is the plate thickness, D_i is the inside tube diameter and h_{fi} is the heat transfer coefficient between the fluid and the tube wall. The bond conductance C_b can be estimated from knowledge of the bond thermal conductivity k_b , the average bond thickness γ , and the bond width b . On a per unit length basis

$$C_b = \frac{k_b b}{\gamma}$$

2.4.2 Performance Prediction of Solar System[1]

The solar system can be considered to consist of solar collectors with a fully mixed sensible heat storage units supplying a load at a fixed flow rate at a constant temperature. Thus, the energy provided from the collectors to the storage and then to the process load depends on the storage tank temperature. The energy balance equation for the whole system during sunshine hours can be written as:

$$(m_s C_s) \frac{dT_s}{dt} + A_c F_r U (T_m - T_a) + (UA)_s (T_s - T_a) + \dot{m}_l C_l (T_s - T_{l,r}) = (\alpha\tau) F_r I(t) A_c \text{----} (2.4.2.1)$$

Rate of heat stored	Rate of heat lost from collector	Rate of heat lost from Storage	Energy to load	Rate of solar radiation absorber by collector
---------------------------	--	--------------------------------------	-------------------	--

Where m_s is the mass of stored water, C_s is the specific heat capacity T_s is the storage temperature A_c is the collector area F_r heat removal factor U collector loss coefficient T_a ambient temperature $(UA)_s$ is the loss coefficient-area product \dot{m}_l rate of water flow to the load C_l is the specific heat capacity $T_{l,r}$ return load temperature $(\alpha\tau)$ absorptivity-transmittivity product, I solar radiation intensity.

By integrating the above equation an expression for the change in storage tank temperature for a certain time period can be obtained.

$$T_s^+ = T_{si} + \frac{\Delta t}{2(m_s C_s)} F_r A_c [(\alpha\tau) I(t) - U(T_m - T_a)] + (UA)_s (T_s - T_a) + \dot{m}_l C_l (T_s - T_{l,r}) \text{-----} (2.4.2.2)$$

Thus, the elevation in storage tank temperature during a given time increment can be calculated if the following parameters were determined:

- The collector parameters
- The storage size and loss coefficient
- The energy to load
- The meteorological data

Note that since the storage is generally only discharged down to the return load temperature, the minimum tank temperature should be the load return temperature $T_{l,r}$

Chapter 3

3. System Configuration and Design Approach

The purpose of this analysis is to present a step by step detailed design procedure of a continuous solar absorption refrigeration system using aqua-ammonia as a working fluid and operates under fixed set of conditions. This analysis includes refrigerant and solution flow rates, heating and cooling requirements, solution concentrations, pressures and temperatures, heat exchangers dimensions and collectors areas.

3.1 Configuration of the Refrigerator

3.1.1 Description of the System and Physical Layout of Components

The designed cooling capacity of the refrigerator is 0.111 kW(nominal capacity is 0.1kW+11% efficiency losses) evaporator temperatures of +5°C with indirect heating through commercial vacuum tube collectors. Its input energy is hot water below 100°C. It has five heat exchangers (generator, condenser, evaporator, absorber, and a solution heat exchanger). The generator is heated by hot water provided by a solar vacuum collector. The condenser and the absorber are water cooled. The evaporator provides the cold storage. The solution heat exchanger makes possible the exchange of heat between the low and high temperature ammonia solution. Finally two flat plate solar collectors are inserted between the solution heat exchanger and absorber, which works as a pre-heater to raise the cold rich solution temperature to an intermediate level. The basic components of the system are shown schematically in Figure 3.1(adapted from reference) and the types of components are presented in table 3.1.

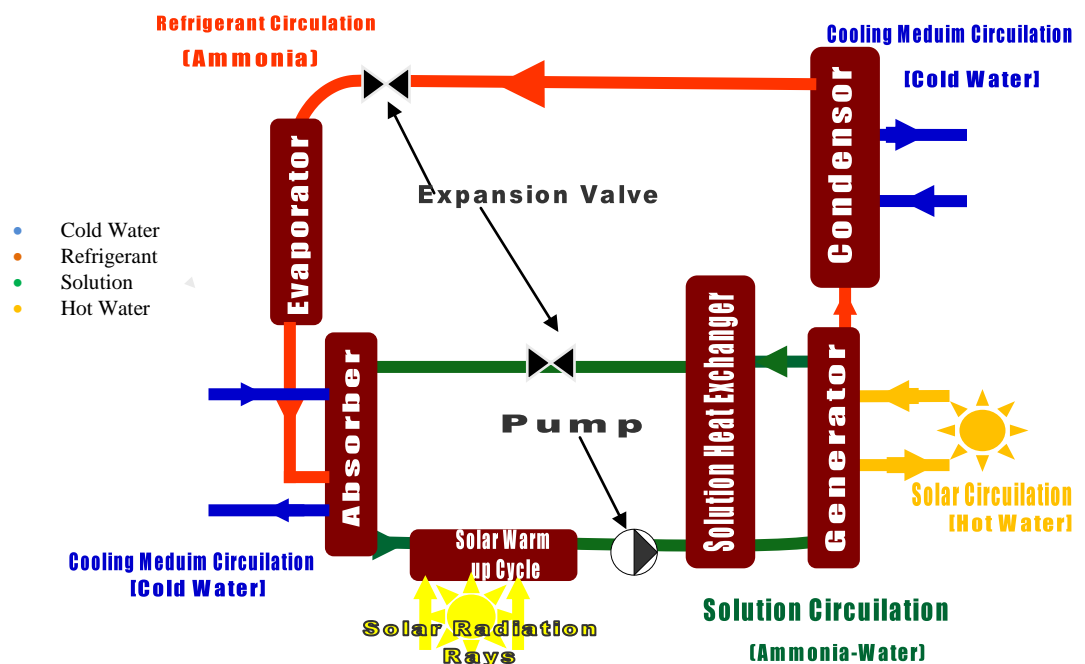
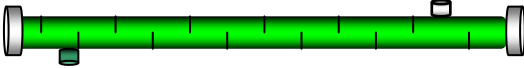
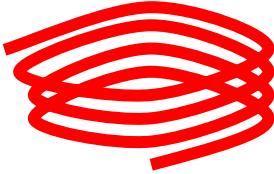
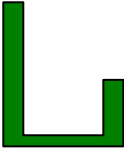
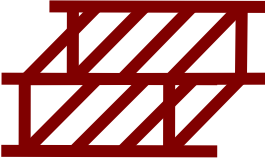
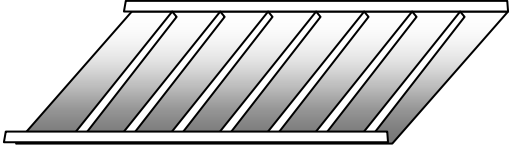




Fig.3.1 Absorption Refrigeration Cycle[20]

Table 3.1 Types of Components of the Refrigeration System





<u>No</u>	<u>Name</u>	<u>Type</u>	<u>Schematic Diagram</u>
1	<u>Generator</u>	<u>Shell and Tube</u>	
2	<u>Condenser</u>	<u>Coil</u> <u>(in Stagnant Water)</u>	
4	<u>Evaporator</u>	<u>Coil</u> <u>(in Stagnant Water)</u>	
5	<u>Absorber</u>	<u>Header- Riser</u> <u>(in Stagnant Water)</u>	
6	<u>Solar Warm up Cycle</u> <u>(Flat Plate Collector)</u>	<u>Header - Riser</u>	
8	<u>Solution Heat Exchanger</u>	<u>Double Tube</u>	
9	<u>Solar Heating Cycle</u> <u>(Evacuated Collector)</u>	<u>Dewar Flask</u>	

3.1.2 Design and Operation Strategy

The physical layout of the prototype and the proposed operation scheme are illustrated in figure 3.2 and table 3.2 respectively. The Methodology employed in designing this refrigeration unit is presented in Figure 3.3. Main decisions during the design process of the refrigerating system comprise the following measures:

- The design of this system requires six effective solar hours to generate the refrigerant needed by the refrigerator to work twenty four hours daily. A liquid ammonia storage tank is installed in the system to store the refrigerant sufficient for twenty four hour operation.
- To achieve a continuous and thereby effective refrigerant generation process even under variable solar irradiation, a minimum hot water storage tank volume is required. The solar collectors system are equipped with storage tanks.
- The driving heat for the sorption refrigerator comes from the solar collectors system. The cycle is started after the minimum driving temperature is reached. The solar collectors system will be in the preheating phase during the early morning hours.
- The primary-circuit pump of the solar system, i.e., the pump which moves the fluid from the evacuated solar collector to the generator and the secondary pump which moves the rich ammonia solution to the generator are switched on when minimum driving temperature is reached.
- The solution heat exchanger makes possible the exchange of heat between the low and high temperature ammonia solution, and it raises the strong ammonia solution temperature to the designed generation temperature.
- The solar warm up cycle, which consists of two flat plate collectors with different storage capacities, work alternatively as a pre-heater, i.e. raising the rich ammonia solution temperature during the early morning hours to an intermediate level while solution heat exchanger raises it to the final temperature level that is actually required by the generator. The solar collector, with the minimum capacity and the higher storage temperature, supplies the system with the warm rich ammonia solution during the first hour of operation.

- The physical layout of the components allows the flow of the working fluid by gravity, and not by pressure gradient from the condenser and the absorber.
- The arrangement of the components in the prototype is determined by the common pressure level of the generator and condenser on the one hand, and the evaporator and the absorber on the other hand. The generator and condenser are located in the upper part of the prototype, while the evaporator and absorber are located in the lower part. This arrangement allows flow of working fluid by gravity from the upper to the lower components of the system .

1	Evacuated Collector
2	Flat Plate collector
3	Hot Water Tank
4	Cold Water Tank
5	Liquid Ammonia Reservoir
6	Generator
7	Condenser
8	Solution Heat Exchanger
9	Absorber
10	Evaporator
	Hot Water Circulation
	Refrigerant Circulation
	Strong Ammonia Solution Circulation
	Weak Ammonia Solution Circulation

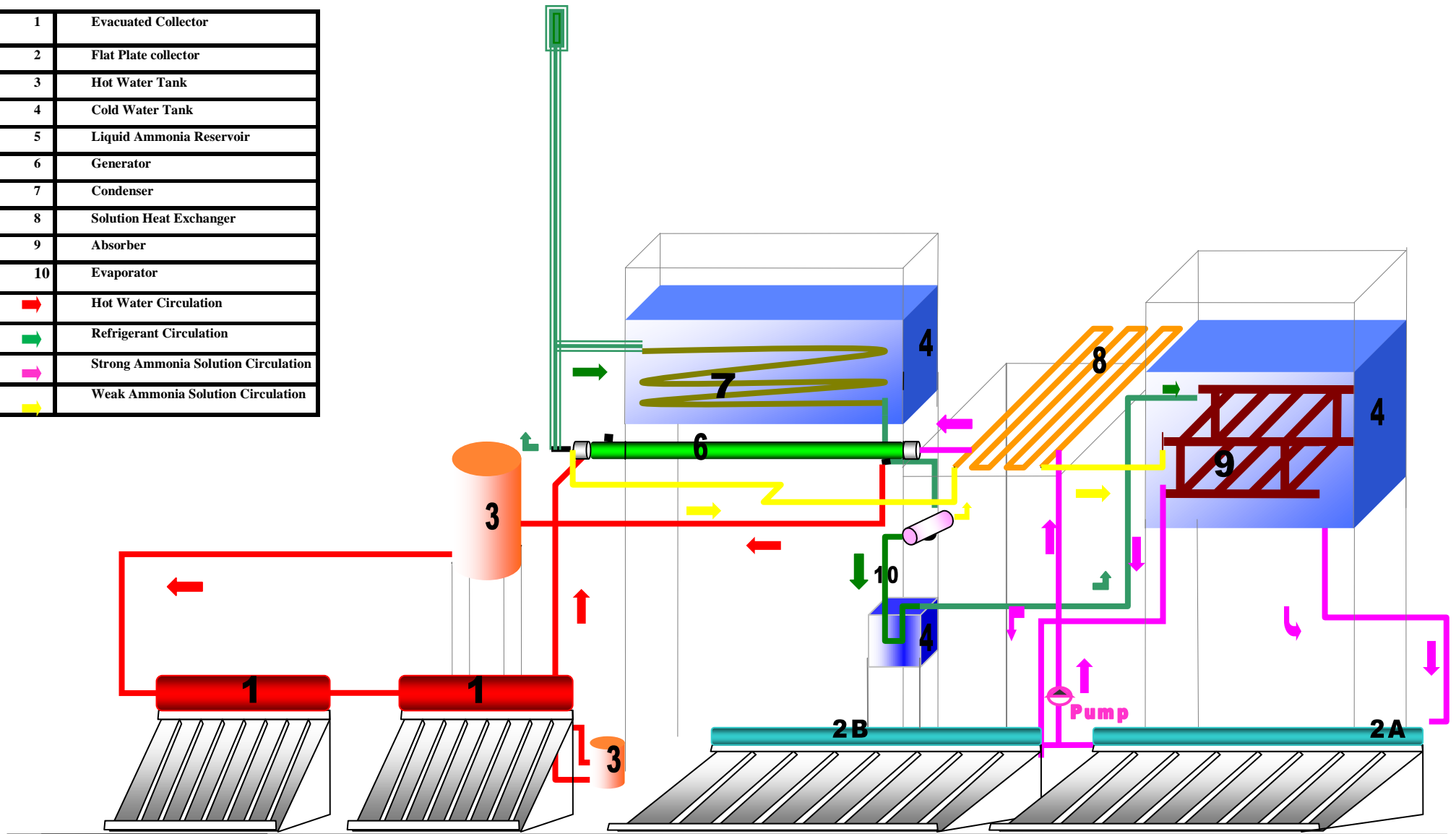


Fig. 3.2 Physical Layout of the Solar Absorption Refrigeration Prototype

Table 3.2 Operation Scheme of the Refrigeration System

No	Components <i>(refer to Fig. 3.2)</i>	Quantity of Circulating Fluids during operation *	1-6am	7 am	8 am	9 am	10 am	11 am	12	1 pm	2 pm	3 pm	4 pm	5 pm	6 pm	7-12 pm	
The Solar Collector System	Solar Warm up Cycle (Flat Plate Collector 2A)	15 kg of strong ammonia Solution during first hour of operation	-	-	-	-	-	-	+	-	-	-	-	-	-	-	
	Solar Warm up Cycle (Flat Plate collector 2B)	65 kg of strong ammonia solution during next 5 hours of operation	-	-	-	-	-	-	-	+	+	+	+	+	-	-	
	Evacuated Collector (Component 1A)	35.7 kg /hr of hot water during 3 hours of Operation	-	-	-	-	-	-	+	+	+	+	+	+	+	-	
	Evacuated Collector (Component 1B)		-	-	-	-	-	-	+	+	+	+	+	+	+	+	-
	Hot Water Pump		-	-	-	-	-	-	+	+	+	+	+	+	+	+	-
The cold production system	Generator	71 kg of strong ammonia Solution during 6 hours of operation	-	-	-	-	-	-	+	+	+	+	+	+	+	+	-
	Condenser	9.16 kg of ammonia vapor during 6 hours of operation	-	-	-	-	-	-	+	+	+	+	+	+	+	+	-
	Evaporator	9.16 kg of ammonia liquid during 24 hours of operation	+	+	+	+	+	+	+	+	+	+	+	+	+	+	+
	Absorber	61kg of weak ammonia Solution during next 5 hours of operation+9.16 kg of ammonia vapor during 24 hours of operation	+	+	+	+	+	+	+	+	+	+	+	+	+	+	+
	Double Tube Heat Exchanger		-	-	-	-	-	-	+	+	+	+	+	+	+	+	-
	Ammonia Solution ◊ Pump		-	-	-	-	-	-	+	+	+	+	+	+	+	+	-

**Note: refer to section 3.3 for quantities of circulating fluids*

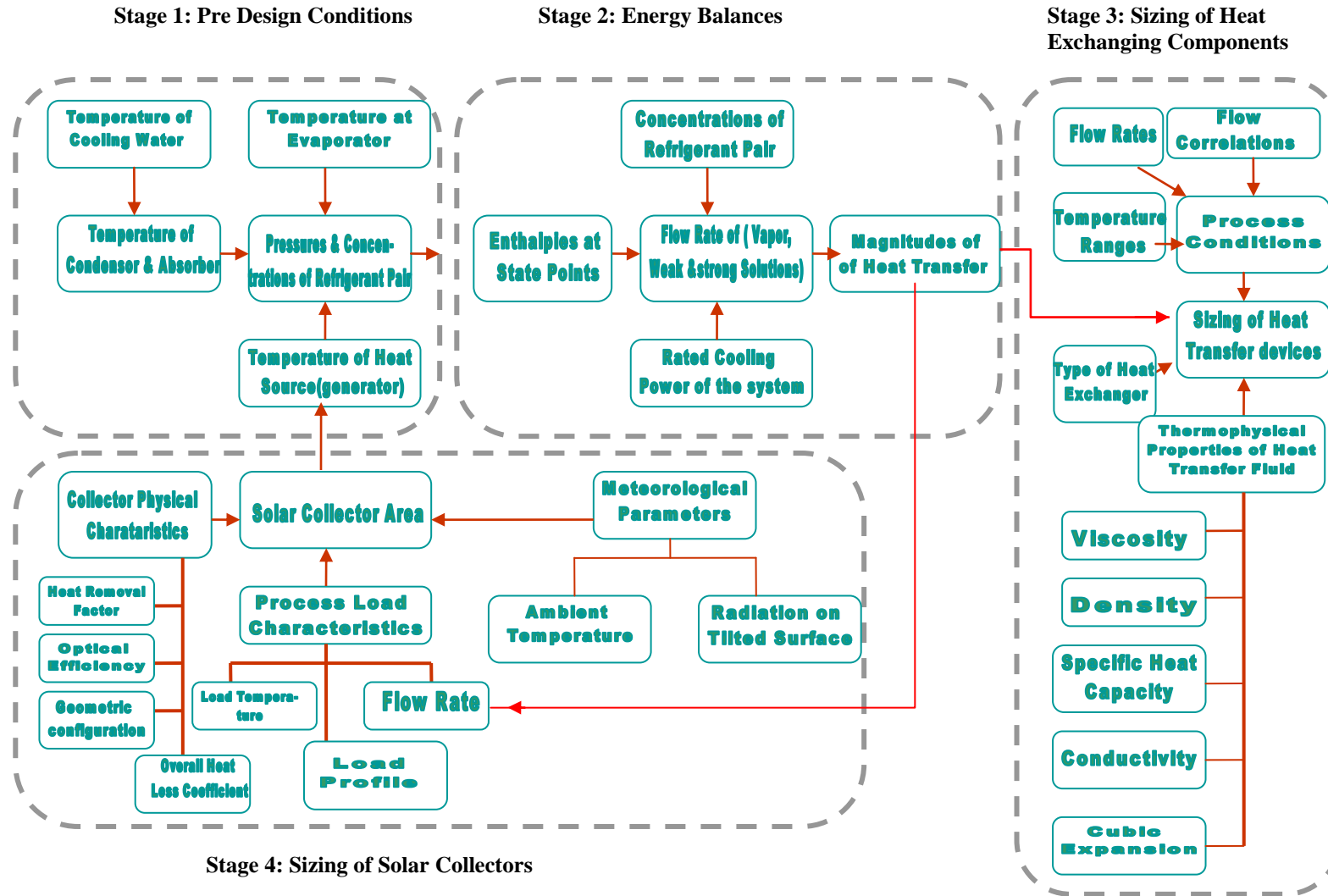


Fig. 3.3 Design Methodology

3.2 Design Approach

Design activities undertaken during the development of the refrigerator system as illustrated by Figure 3.4 are subdivided into four main stages as follows;

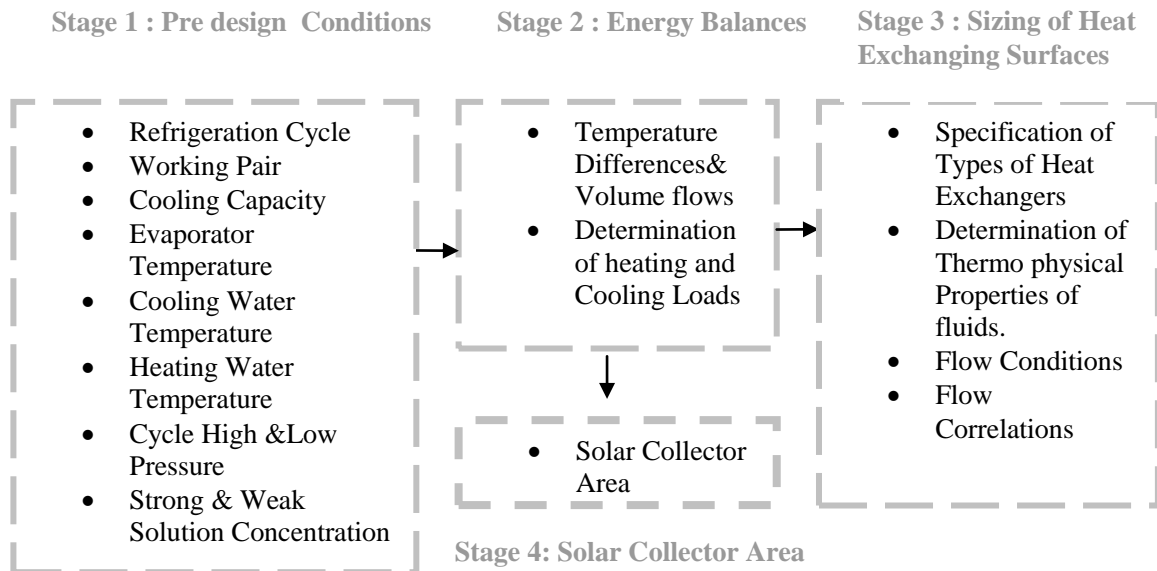


Fig. 3.4 Design Stages

3.2.1 Pre-Design Condition

3.2.1.1 Cooling Capacity

The designed cooling capacity of the system is chosen to be 0.111Kw.

3.2.1.2 The Temperature Limits of The processes

According to the second law of thermodynamics, it is necessary to assume operating temperatures for the generator, evaporator and condenser before establishing properties at the state points of the system cycle. The operating temperatures are chosen as follows:-

- 1- The temperature of the condenser and absorber may be selected if the temperature of the available cooling water is known. According to the temperature expected in Sudan, the cooling water will have a temperature T_{cw} of 25 to 35°C.
- 2- The designed evaporator temperature is 5 ° C.
- 3- The generator temperature is selected on the basis of the available hot water temperature. If flat plate collectors are to be used, the maximum hot water that can be attained is 100° C.

This gives the process limits:

Minimum and Maximum Generator Temperature T_g are 73 and 83 °C respectively.

Minimum and Maximum Absorber Temperature T_a are 38 and 46° C respectively.

Condenser Temperature T_c is 38 °C

Evaporator Temperature T_e is 5 °C

3.2.1.3 The System Operating Pressures and Solution Concentrations

The influence of the limiting temperature on the system pressures and concentration can be shown clearly on the equilibrium diagram for aqua ammonia (P-T-X), see Fig. 3.5

According to the diagram,

T_c determines the high pressure P_c

T_g and P_c determine the poor solution concentration X_p , so

X_p is determined by T_c and T_g

T_e determines the low pressure P_e

T_a and P_e determine X_r , so

The rich solution concentration X_r is determined by T_e and T_a

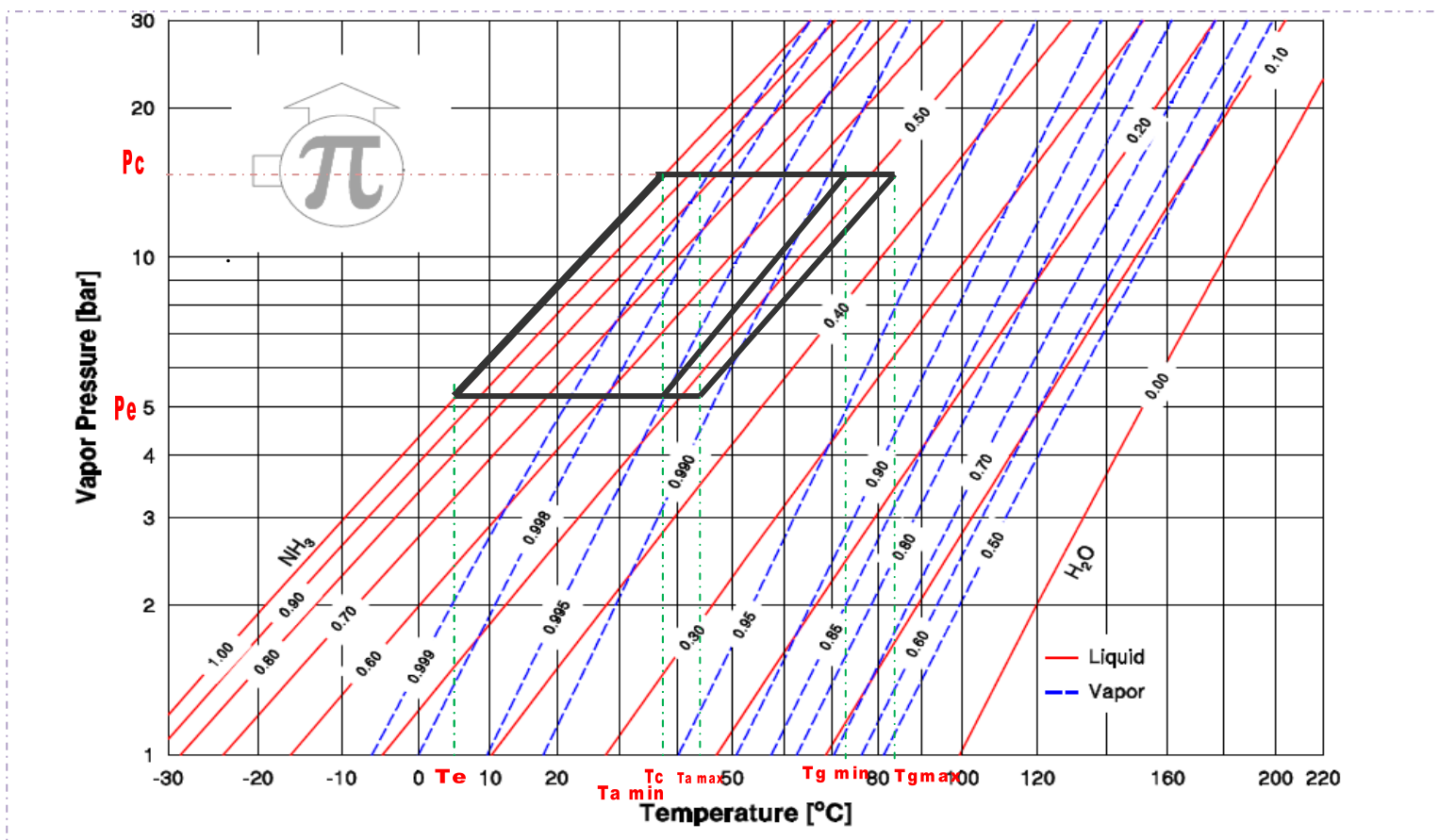


Fig. 3.5 P-T-X Diagram

The major pre-design parameters with their corresponding values and ranges are listed in table 3.3. The values or ranges of these parameters are determined by conventional design practice.

Table 3.3 Pre-design Conditions

	Parameter	Standard value	Range	Remark
1	Cooling Capacity	0.111KW		required cooling power of the cycle
2	Evaporator Temperature	5°C		required design temperature
3	Condenser Temperature	38°C		Assuming cooling water is available for a heat sink at 35°C and allowing temperature differential of 3 degrees,
4	Absorption Temperature		38-46°C	Assuming cooling water is available for a heat sink at 35°C and allowing temperature differential of 3 degrees,
5	Generator Temperature		73-83°C	Determined by the collector temperature
6	Cycle High Pressure	15.5bar		P-T-X diagram*
7	Cycle Low Pressure	5.5bar		P-T-X diagram
8	Ammonia Solution Concentration		46%-54%	P-T-X diagram
9	Mass of pure Refrigerant Circulated	9kg		Determined by power level of the cycle
10	Mass of Rich Solution Circulated	71kg		The amount of solution need to be circulated to generate the required refrigerant
11	Mass of Poor Solution Circulated	62kg		The amount of solution need to be circulated to generate the required refrigerant.

* Note P-T-X diagram is an abbreviation of Pressure- Temperature-Concentration Diagram

3.2.2 Energy Balances

3.2.2.1 Enthalpies at State Points

The quantities of heat transferred to and from the solution during the different processes can be found from the enthalpies of solution and vapor (see Table 3.4). In this analysis of the absorption refrigerator, it is necessary to make several assumptions, so referring to Figure 3.6

- 1- The fluids at points 2, 4, 5, and 8 can be assumed to be under equilibrium conditions.
- 2- The enthalpies at points 6 and 5 are assumed to be equal. Also, the temperature rise through pump is neglected.
- 3- It is assumed that there are no pressure drops through the connecting lines and heat exchangers.

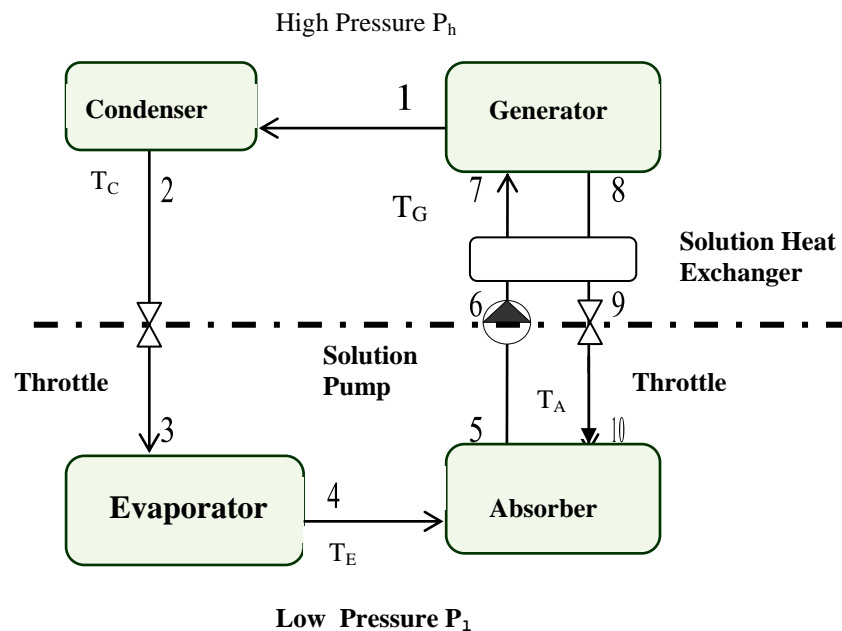
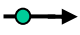
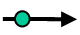
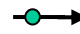
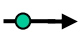
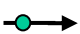


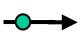
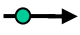
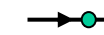


Fig. 3.6 State Points at Absorption Cycle Schematic Diagram

Note that the numbers in the above diagram refer to the following state points:

- 1- ammonia vapour out of the generator
- 2- ammonia liquid out of the condenser
- 3- ammonia vapour/liquid going to the evaporator
- 4- ammonia vapour out of the evaporator
- 5- strong ammonia solution out of the absorber (rich in ammonia weak in water)
- 7- strong ammonia solution into the generator after passing through the solution heat exchanger.
- 8- Weak ammonia solution out of the generator (weak in ammonia rich in water)
- 10- ammonia solution into the absorber after passing solution heat exchanger (weak in ammonia rich in water)

Table 3.4 Enthalpies at State Points

State Point	Components	Flow Direction	Temperature (°C)	Pressure (bar)	Ammonia Solution Conc.	Enthalpy (kJ/Kg)	Equilibrium Status
1	Generator		73-83	14.5	x	1533.99 (See eqn. 3.2.2.1.2)	Superheated Ammonia Vapor
2	Condenser		38	14.5	x	346.736 (from tables)	Saturated Ammonia Liquid
3	Throttle Valve						
4	Evaporator		5	5.5	x	1384.11 (from tables)	Saturated Ammonia Vapor
5	Absorber		38-46	5.5	0.54	23 See eqn. (3.2.2.1.1)	Strong Ammonia Solution
6	Solution Heat Exchanger		59	14.5	x	67.48 See eqn. (3.2.2.1.1)	Strong Ammonia Solution
7	Generator		73	14.5	0.54	221.69 See eqn (3.2.2.1.3).	Strong Ammonia Solution
8	Generator		83	14.5	0.46	221.933 See eqn (3.2.2.1.1)	Weak Ammonia Solution
9	Solution Heat Exchanger		66	14.5	x	304 See eqn. (3.2.2.1.4)	Weak Ammonia Solution
10	Absorber		66	14.5	0.46	142.44 See eqn. (3.2.2.1.1)	Weak Ammonia Solution

The enthalpy of an aqua-ammonia solution [15] at an ammonia concentration x and temperature T (° F) is:

$$h_{(x,T)} = -33.5 - 334x + 414x^2 + (1.03 - 0.401x + 0.435x^2)T - (0.00021 - 0.00385x + 0.00334x^2)T^2 \text{ Btu / lb} \quad \text{-----(3.2.2.1.1)}$$

$$h_{sv(T,T_2)} = 611 + 0.641T_1 - 0.398T_2 \text{ Btu / lb} \quad \text{-----(3.2.2.1.2)}$$

$$h_7 = c_p(T_7 - T_6) + h_6 \quad \text{-----(3.2.2.1.3)}$$

$$h_9 = c_p(T_9 - T_8) + h_8 \quad \text{-----(3.2.2.1.4)}$$

3.2.2.2 Heating and Cooling Loads

The heating and cooling loads are obtained from the following equations (see section 2.3.2.4):

Generator

Heating load of the generator:

$$Q_G = \dot{m}_8 h_8 + \dot{m}_1 h_1 - \dot{m}_7 h_7 \quad \text{-----(3.2.2.2.1)}$$

Condenser

Cooling load of the condenser:

$$Q_c = \dot{m}_2 h_2 - \dot{m}_1 h_1 \quad \text{-----(3.2.2.2.2)}$$

Evaporator

Cooling effect at the evaporator:

$$Q_E = \dot{m}_4 h_4 - \dot{m}_3 h_3 \quad \text{-----(3.2.2.2.3)}$$

Absorber

Cooling load at the absorber:

$$Q_A = \dot{m}_{10} h_{10} + \dot{m}_4 h_4 - \dot{m}_5 h_5 \quad \text{-----(3.2.2.2.4)}$$

Solution Heat Exchanger

Heat exchanged at the solution heat exchanger:

$$\dot{m}_r (T_7 - T_6) = \dot{m}_p (T_9 - T_8) \quad \text{-----(3.2.2.2.5)}$$

After the quantities of heat exchanged at the system components were obtained, the general design conditions were specified (see Table 3.5).

Table 3.5 General Design Conditions

General Design Condition of the Refrigeration System	
Design Temperature of Single Components	
Generator Temperature	73-83°C
Condenser Temperature	38°C
Evaporator Temperature	5°C
Absorber Temperature	38-46°C
Low Pressure	5.5bar
High Pressure	14.5 bar
Degassing Width in the Generator	8%
NH₃ Rich Solution Concentration	54%
NH₃ Poor Solution Concentration	46%
Heat Supplied	
Generator Q _g (required heat power)	0.5574 kW
Evaporator Q _c (designed cooling power)	0.111 kW
Heat Dissipated	
Condenser Q _c (required cooling)	0.533 kW
Absorber Q _a (required cooling)	0.294 kW

3.3 Sizing of Heat Exchangers

Approach to Heat Exchanger Design:

In a heat exchanger, heat energy is transferred from one body or stream to another. Temperature difference between the source of heat transfer and receiver of heat is the driving force in heat transfer. The heat passing from one body to another travels through a medium which in general offers resistance to the heat flow. Both these factors, the temperature difference and the resistance to heat flow, affect the rate of heat transfer. In the design of heat exchange equipment, heat transfer equations can be applied to calculate this transfer of energy so as to carry it out efficiently and under controlled conditions. The equation for the heat exchanger heat transfer :

$$Q = UA\Delta T \text{-----}(3.3.1)$$

Where

Q = heat transfer rate between the fluids

U = Overall heat transfer coefficient

A = heat transfer area

ΔT = log mean temperature difference

After accomplishing the two stages of design procedure (see Fig. 3.4), there are important decisions that need to be taken in the third stage i.e. heat exchanger sizing:

- 1- A starting point in sizing a heat exchanger is specifying the purpose of the exchanger, so the five exchangers included in the refrigeration cycle are designed to fulfill the need for **generator, condenser, evaporator, solution heat exchanger and absorber.**
- 2- What kind of construction is to be used, for example, double tube or shell and tube. Table 3.6 shows the type of exchanger construction chosen for each component of the system.
- 3- Then the other decision that need to be taken is fluid paths through the heat exchanger. Difference is made between a parallel flow, counter flow and cross flow. In designing this refrigeration unit, **a counter flow** is chosen where ever applicable.
- 4- The state of the media in the heat exchanger. For example, liquid-to-liquid, gas- to-gas or liquid-to-gas heat exchanger (or vice versa). The states of the media in this design are either liquid-to-liquid or gas-to-liquid (see table 3.1).
- 5- Mechanism of heat transfer: The basic mechanism of heat transfer are conduction, convection, boiling, condensation and radiation. Of these, radiation is usually significant only at temperatures higher than those ordinarily encountered in tubular process heat transfer equipment, therefore,

radiation will not be considered in this work . All of others play a vital role in equipment design. The mechanism of heat transfer for each heat exchanger will be given separately in the following sections, the emphasis will be upon a qualitative description of the process and the basic equation. Table 3.6 gives a summary of the correlation used to describe the mechanism of heat transfer.

The design of a process heat exchanger usually proceeds through the following steps:

- 1- Process conditions (stream compositions, flow rates, temperatures, pressure), must be specified.
- 2- Required physical properties over the temperatures and pressure ranges of interest must be obtained .
- 3- The type of heat exchanger to be employed is chosen.
- 4- A preliminary estimate of the size of the exchanger is made.
- 5- A first design is chosen, complete in all details necessary to carry out the design calculations.
- 6- The design chosen in step 5 is evaluated, or rated, as to its ability to meet the process specification with respect to heat transfer.
- 7- On the basis of result of step 6, a new configuration is chosen if necessary and step 6 is repeated. If the first design was not adequate to meet the required heat load, it is usually necessary to increase the size of the exchanger.
- 8- The final design should meet process requirement (within reasonable expectations of errors.

The design procedure of heat exchangers are presented in details in the following sections according to the following order.

- 1. Generator**
- 2. Condenser**
- 3. Evaporator**
- 4. Double Tube Exchanger**
- 5. Absorber**

Table 3.6 Flow Streams and Correlations


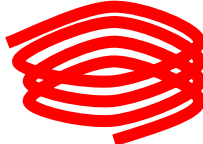

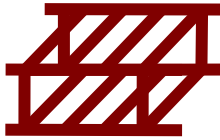

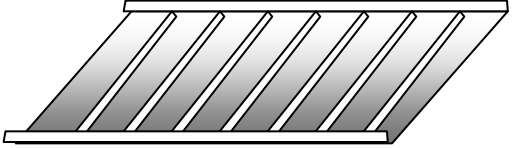
Component Name	Geometry	Refrigerant Phase (at state points referred to in 3.6)	Heating Agent	Cooling Agent	Correlation (see symbols definition in following sections)	Schematic Diagram
1 Generator	Shell & Tube	Strong Ammonia Solution	Hot Water (External Flow)	x	Internal Flow: Two Phase Forced Convective Boiling [5,6]: $h_i = \frac{k}{L} 1.86 \left(\frac{d_0 \text{Re Pr}}{L} \right)^{0.33} \quad \frac{h_o}{h_i} = 3.5 \left[\frac{1}{X_{tt}} \right]^{0.5}$	
					External Flow: Single Phase Forced Convection $h_o = \frac{k}{L} 1.86 \left(\frac{d_0 \text{Re Pr}}{L} \right)^{0.33}$	
2 Condenser	Coil in a Stagnant Pool	Superheated Ammonia Gas	x	Water	Internal Flow: Condensation of Superheated Vapor External Flow: Natural Convection [5] $h_i = \frac{k}{L} 1.86 \left(\frac{d_0 \text{Re Pr}}{L} \right)^{0.33} \quad h_i = 0.555 \left[\frac{g \rho_l (\rho_l - \rho_v) k_l^3 h'_{fg}}{\mu_l (T_{sat} - T_s) Di} \right]^{1/4}$ $h_o = c' \left(\frac{\Delta T}{d_i} \right)^n k \left(\frac{\beta g \rho^2 C_p}{\mu k} \right)^n$	
					Internal Flow: Heat Flux in Nucleate Boiling Regime [8] $q'' = \mu_l h_{fg} \left[\frac{g(\rho_l - \rho_v)}{\sigma} \right]^{1/2} \left[\frac{C_{p,l} \Delta T_e}{C_{S,f} h_{fg} \text{Pr}_l^n} \right]^3$	
3 Evaporator	Coil in a Stagnant Pool	Liquid Ammonia	x	Water	External Flow: Natural Convection $h_o = C' \left(\frac{\Delta T}{l} \right)^n k \left(\frac{\beta g \rho^2 C_p}{\mu k} \right)^n$	

Table 3.6 Flow Streams and Correlations (continued)

	Component Name	Geometry	Refrigerant Phase	Heating Agent	Cooling Agent	Correlation	Schematic Diagram
4	Absorber	Header-Footer in a Stagnant Pool	Weak Ammonia Solution	x	Water	Internal Flow: Transient Heat Transfer by conduction in a cylinder[8] $\frac{Q_o}{L} = \frac{\rho C_p \Pi l^2 L (T_{iNH_3} - T_{bH_2O})}{L}$	
						External Flow: Natural convection $h_o = C' \left(\frac{\Delta T}{l} \right)^n k \left(\frac{\beta g \rho^2 C_p}{\mu k} \right)^n$	
5	Solution Heat Exchanger	Double Tube	Strong Ammonia Solution	Weak ammonia solution	x	Internal Flow: Single Phase Forced Convection for Laminer flow. $h_i = \left(\frac{k}{D_i} \right) 1.86 \left(\frac{D_i Re Pr}{L} \right)^{0.33}$	
						External Flow: Single Phase Forced Convection for Laminer flow. $h_o = \left(\frac{k}{D_e} \right) 1.86 \left(\frac{D_e Re Pr}{L} \right)^{0.33}$	
6	Solar Warm up Cycle	Header-Footer	Strong Ammonia Solution	Solar Radiation	x	Internal Flow [1]: $T_s^+ = T_s + \frac{\Delta t}{m C_p} [Q_u - (UA)(T_s - T_a)]$	

3.3.1 Generator Design

Description: It consists of a shell on the outside and tubes placed inside the shell, the tubes are attached on the front and rear ends to tube sheets and by baffles which are placed to redirect the shell fluid past the tubes to enhance heat transfer (see Fig.3.7)

Mechanism of heat transfer:

1- **Inner Tubes:** The flow is a two phase flow in which the liquid and vapor are multi-components. The thermodynamic relationships are complex, the temperature, for example, being variable over a range values at a given pressure, but with a changing ratio of total liquid to total vapor and with changing composition of each phase. Prediction of the amount and composition of each phase is relatively well understood and easily done in few cases, as for mixtures of hydrocarbons, other cases require laboratory thermodynamic data.

For design consideration, the effective heat transfer coefficient can be considered to be made up of convective and nucleate boiling. The convective boiling coefficient is estimated using an equation for single phased forced convection heat transfer modified by a factor to allow for the effects of two phase flow (see flow correlation on table 3.6)

2- **Shell:** The flow in the shell is a forced convection flow. When a fluid is forced past a solid body and heat is transferred between the fluid and the body, this is called forced convection heat transfer (see flow correlation on table 3.6).

Calculation Procedure:

The sequence of calculations in shell and tube type heat exchanger are as follows:

a- Area of flows[8]:

(i) Through tubes, $A_1 = N \left(\frac{\pi}{4} \right) d_i^2$

Where, N is the number of tubes, d_i inner tube diameter.

(ii) Through shell, $A_2 = \frac{d_s C_t B}{P_T}$

Where, B is the baffle length, P_T is distance between tube centres, C_t is clearance between tube bundle and shell, d_s is shell diameter

b- Equivalent diameter for shell:

For triangular pitch[8],

$$D_s = 4 \left(\frac{0.86 P_T^2 / 2 - \frac{\pi d_o^2}{8}}{\pi d_o / 2} \right)$$

Where, d_o is outer diameter

c- Velocity of flow[8]:

(i) For flow through tubes, $V_1 = \frac{\dot{m}_{NH_3}}{\rho_{NH_3} A_1}$

(ii) For flow through shell, $V_2 = \frac{\dot{m}_w}{\rho_w A_2}$

d- Reynolds number[8]:

(i) For flow through tubes, $Re = \frac{d_i V_1 \rho_{NH_3}}{\mu_{NH_3}}$

(ii) For flow through shell, $Re = \frac{D_e V_2 \rho_w}{\mu_w}$

e- Individual heat transfer coefficient:

(i) Shell heat transfer[5,6,8],

$$h_o = \frac{k}{L} 1.86 \left(\frac{d_o Re Pr}{L} \right)^{0.33}$$

$$\frac{h_o}{h_L} = 3.5 \left[\frac{1}{X_{tt}} \right]^{0.5}$$

(ii) Tube side

$$h_i = \frac{k}{L} 1.86 \left(\frac{d_o Re Pr}{L} \right)^{0.33}$$

f- Overall heat transfer coefficient[8]:

$$\frac{1}{U} = \frac{r_o}{r_i h_i} + \frac{r_o \ln \frac{r_o}{r_i}}{k} + \frac{1}{h_o} + f$$

g- Log-mean temperature difference[8]:

$$\theta_m = \frac{(T_{wi} - T_{NH_3i}) - (T_{wo} - T_{NH_3o})}{\ln \frac{(T_{wi} - T_{NH_3i})}{(T_{wo} - T_{NH_3o})}}$$

Where, T_{wi} & T_{wo} are inlet and temperature of water, and T_{NH_3i} & T_{NH_3o} are inlet and outlet temperature ammonia solution

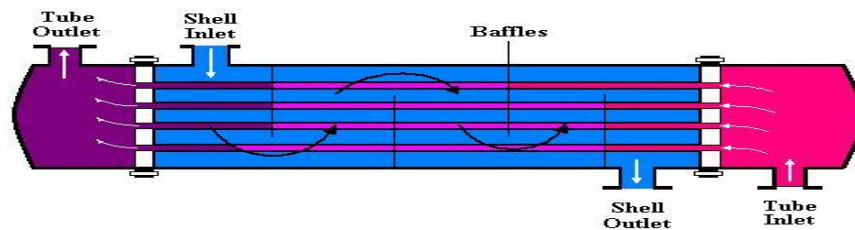


Fig. 3.7 Shell and Tube Heat Exchanger

The following tables shows the details of the calculation procedures and the resulting dimension specifications of the generator.
 Table 3.7 Generator Design Shell Side

Quantity	Heating Load Q_G	Overall Heat Transfer coefficient U	Specific heat capacity of water C_{pw}	Inlet water temperature T_{wi}	Outlet water temperature T_{wo}	Inlet aqueous Ammonia Temperature T_{NH3i}	Outlet aqueous Ammonia Temperature T_{NH3o}	Logarithmic Mean Temperature θ_m	Mass Flow of heating water \dot{m}_w	Heat transfer Area A
Numerical Value	0.3328 KW	100W/m ² K (preliminary estimation)	4.226 KJ/kgK (at mean temp 108 °C)	88 °C	80 °C	72 °C	83 °C	6.382	0.00994 kg/s	0.5215m ²
Remarks	Design		From tables(see Appendix)	Design	Design	Design	Design	See equation 3.3.1.2	See equation 3.3.1.1	See equation 3.3.1.3

Heat gained by ammonia solution = Heat lost by water

$$Q_G = \dot{m}_w (T_{wo} - T_{wi}) \text{-----}\{3.3.1.1\}$$

$$\theta_m = \frac{(T_{wi} - T_{NH3i}) - (T_{wo} - T_{NH3o})}{\ln \frac{(T_{wi} - T_{NH3i})}{(T_{wo} - T_{NH3o})}} \text{-----}\{3.3.1.2\}$$

$$Q_G = UA\theta_m \text{-----}\{3.3.1.3\}$$

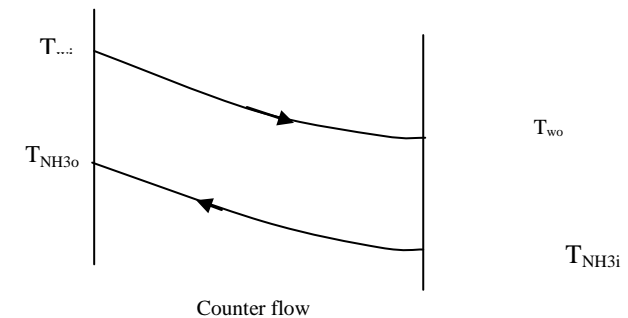


Table 3.8 Generator Design Shell Side (continued)

Quantity	Heat transfer Area A	Outer diameter of tube (d _o)	Inner diameter of tube ID	Tube length l	Surface Area of one tube A _t	No of Tubes N	Shell Equivalent diameter D _e	Bundle diameter d _b	Pitch	Diametrical Clearance between shell and tubes C _t [5]	Shell diameter d _s
Numerical Value	0.5215m ²	20 mm	14.8mm	1.6 m	0.10053 mm ²	5	14.22 mm	81 mm	Triangular pitch	9 mm	90 mm
Remarks			Design	Design	See equation 3.3.1.4	See equation 3.3.1.5	3.3.1.8	See equation 3.3.1.6	Design		See equation 3.3.1.7

$$A_t = d_i \pi l \text{-----} \{3.3.1.4\}$$

$$N = A / A_t \text{-----} \{3.3.1.5\}$$

$$N = a(d_b / d_o)^b \text{-----}\{3.3.1.6\}$$

$$d_s = d_b + C_t \text{-----} \{3.3.1.7\}$$

$$D_e = 4 \left(\frac{0.86 P_T^2 / 2 - \pi d_o^2}{\pi d_o / 2} \right) \text{-----} \{3.3.1.8\}$$

Where, $P_T = 1.25 d_o$, a & b are constants that take the values of 0.319 & 2.142 respectively for triangular pitch

Table 3.9 Generator Design Shell Side (continued)

Quantity	Shell flow area A_2	velocity of water V_2	Mean bulk temperature of water T_b	Density of water ρ_w	Viscosity of water μ_w	Thermal conductivity of water k	Prandtl number of water Pr	Reynold Number Of water Re	Shell side heat transfer coefficient h_o
Numerical Value	0.0018m ²	0.01262 m/s	357K	968.6 kg/m ³	343×10^{-6} N. s/m ²	673×10^{-3} W/m.K	2.068	506	184 W/m ² K
Remarks	See equation 3.3.1.9	See equation 3.3.1.10	See equation 3.3.1.11	From tables(see appendix	From tables(see appendix	From tables(see appendix	From tables(see appendix	See equation 3.3.1.12	See equation 3.3.1.13 3.3.1.14 3.3.1.15

$$A_2 = \frac{d_s C_t B}{P_T} \text{-----}\{3.3.1.9\}$$

$$V_2 = \frac{\dot{m}_w}{\rho_w A_2} \text{-----}\{3.3.1.10\}$$

$$T_b = \frac{T_{wi} + T_{wo}}{2} \text{-----}\{3.3.1.11\}$$

$$Re = \frac{D_e V_2 \rho_w}{\mu_w} \text{-----}\{3.3.1.12\}$$

$$h_i = \frac{k}{L} 1.86 \left(\frac{d_0 Re Pr}{L} \right)^{0.33} \text{-----}\{3.3.1.13\}$$

$$Nu = \frac{h_i D_e}{k} \text{-----}\{3.3.1.14\}$$

$$\frac{h_o}{h_L} = 3.5 \left[\frac{1}{X_u} \right]^{0.5} \text{-----}\{3.3.1.15\}$$

Where, B is the baffle length

Table 3.10 Generator Design Tube Side Ammonia Solution

Quantity	Ammonia Solution Velocity Of NH ₃ V ₁	Prandtl Number Pr Of NH ₃	Bulk Temp. of Ammonia solution T _b	Ammonia Solution density ρ _{NH₃}	Ammonia Solution conductivity k _{NH₃}	Ammonia Solution viscosity μ _{NH₃}	Reynold Number Of NH ₃ Re	Shell side Heat Transfer coefficient(Liquid Phase) h _{Li}	Tube side Heat Transfer coefficient(Gaseous Phase) h _{Li}	Fouling Factor f	Thermal Conduct-ivity of Steel K _w	Overall Heat Transfer Coefficient
Numerical Value	0.00892 m/s	1.423	78 °C (220 °F)	860 kg/m ³	0.526 w/mk	163x10 ⁻⁶ N. s/m ²	697	184 W/m ² K	831 W/m ² K	0.00018	15 W/mK	130 W/m ² K
Remarks	See equation 3.3.1.16	From tables(see appendix	Design	From tables(see appendix	From tables(see appendix	From tables(see appendix	See equation 3.3.1.18		See equation 3.3.1.19 3.3.1.20	From tables(see appendix	See table in appendix	See equation 3.3.1.21

$$V_1 = \frac{\dot{m}_{NH_3}}{\rho_{NH_3} A_1} \text{-----} \{3.3.1.16\}$$

$$A_1 = N \left(\frac{\pi}{4} \right) d_i^2 \text{-----} \{3.3.1.17\}$$

$$Re = \frac{d_i V_1 \rho_{NH_3}}{\mu_{NH_3}} \text{-----} \{3.3.1.18\}$$

$$Nu = \frac{h_i d_i}{k_{NH_3}} \text{-----} \{3.3.1.19\}$$

$$h_i = \frac{k}{L} 1.86 \left(\frac{d_o Re Pr}{L} \right)^{0.33} \text{-----} \{3.3.1.20\}$$

$$\frac{1}{U} = \frac{r_o}{r_i h_i} + \frac{r_o \ln \frac{r_o}{r_i}}{k} + \frac{1}{h_o} + f \text{-----} \{3.3.1.21\}$$

Table 3.11 Generator Specifications

Name:	Generator	Dimensional Specifications:
Type	Shell and Tube Heat Exchanger	Number of Tubes 5
Flow Type	Counter Flow	Inner Diameter 14.8mm
Operation Mode :		Outer Diameter 20.8
Component vaporizing	54%	Length of Tubes 1.6m
Inlet Temperature	72°C	Pitch Triangular
Outlet Temperature	83°C	Bundle Diameter 81 mm
Operating Pressure	14.5 bar	Shell Diameter 90mm
Heating Load	0.3328kW	Baffle Spacing 5cm
Heat Transfer Coefficient	130 W/m ² K	Shell Clearance 9mm
Thermodynamic Mode:		Material:
Vapor Phase	Superheated Vapor	Inner Tube Stainless Steel
Liquid Phase	Ammonia – Water Mixture	Shell Stainless Steel
Heating Agent:		
Agent Name	Water	
Rate	35kg/h	
Inlet Temperature	88°C	
Outlet Temperature	80°C	

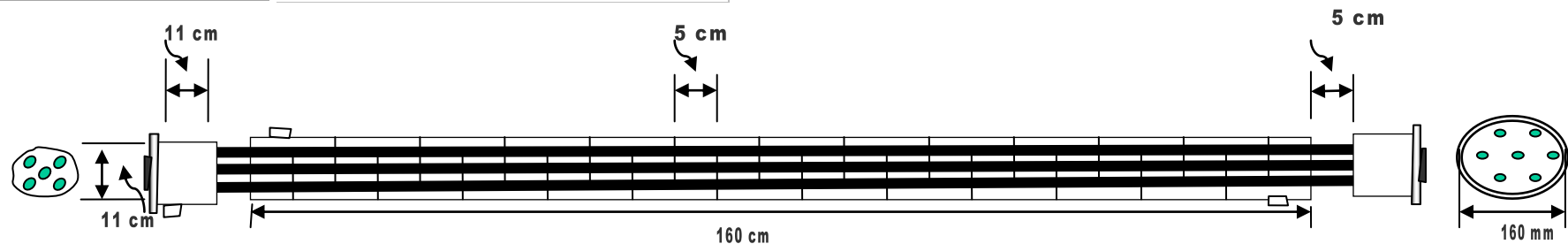


Fig. 3.8 Generator Dimensions

3.3.2 Condenser Design

Description: The condenser is a coil in stagnant water basin type.

Mechanism of heat transfer:

1. **Condenser Coil:** The superheated vapor enters the coil and the vapor is cooled to saturation temperature and then condensed as it loses heat to the water in the tank. The flow is subdivided into two regions: the superheated vapor region and the saturated vapor region.

a- The super heated vapor region: In the superheated region the flow is a forced convection flow in which heat is transferred from the vapor to the surrounding liquid.

Flow Correlation : Experimentally, it has been shown that forced convection heat transfer can be described in terms of these factors grouped in dimensionless numbers :

$$\text{Nusselt number (Nu)} = (hcD/k)$$

$$\text{Prandtl number (Pr)} = (c_p\mu/k)$$

$$\text{Grashof number (Gr)} = (D^3\rho^2g\beta\Delta T/\mu^2)$$

$$\text{Nu} = f(\text{Re and Pr})$$

(see flow correlation on table 3.6)

b- The saturated vapor region : The liquid and vapor are the same pure component. The pressure temperature relationship in this case is the vapor pressure curve for the components. The mode or mechanism of condensation is filmwise condensation inside horizontal tubes. The actual heat transfer mechanism that operates in the film wise condensation is closely related to the two phase flow mechanism described in the previous section. Conditions within the tube are complicated and depend strongly on the velocity of the vapor flowing through the tube. If this velocity is small, condensation occurs in the manner depicted by figure 3.9 for horizontal tube. That is, the condensate flow is from the upper portion of the tube to the bottom, from whence it flows in a longitudinal direction with the vapor(see flow correlation on table 3.6).

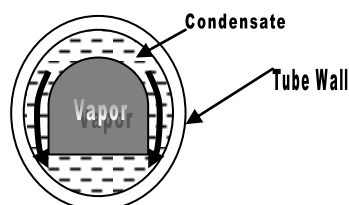


Fig.3.9 Film Condensation in Horizontal Tube (cross-section of condensate flow for low velocity vapor[10])

2. **Water tank :** Heat transfer in the water tank is by natural convection. Heat transfer by natural convection occurs when a fluid is in contact with a surface hotter or colder than itself. As the fluid is heated or cooled it changes its density. This difference in density causes movement in the fluid that has been heated or cooled and causes the heat transfer to continue

Flow Correlation: Experimentally, it has been shown that convection heat transfer can be described in terms of these factors grouped in dimensionless numbers :

$$\text{Nusselt number (Nu)} = (h_c D / \mathbf{k})$$

$$\text{Prandtl number (Pr)} = (c_p \mu / \mathbf{k})$$

$$\text{Grashof number (Gr)} = (D^3 \rho^2 g \beta \Delta T / \mu^2)$$

and in some cases a length ratio (L/D).

If we assume that these ratios can be related by a simple power function we can then write the most general equation for natural convection:

$$(\text{Nu}) = K(\text{Pr})^m (\text{Gr})^n (L/D)^p$$

In natural convection equations, the values of the physical constants of the fluid are taken at the mean temperature between the surface and the bulk fluid (see flow correlation on table 3.6)..

Quantity of water in the tank[5]

In case of a storage tank with liquor of mass m and specific heat C_p , heated by vapor condensing in a helical coil, it may be assumed that the overall transfer coefficient U is a constant. If T_s is the temperature of the condensing vapor, T_1 and T_2 the initial and final temperatures of the liquor at any time t , then the rate of transfer of heat is given by:

$$Q = m C_p \frac{dT}{dt} = UA(T_s - T)$$

$$\frac{dT}{dt} = \frac{UA}{m C_p} (T_s - T)$$

$$\int_{T_1}^{T_2} \frac{dT}{T_s - T} = \frac{UA}{m C_p} \int_0^t dt$$

$$\ln \frac{T_s - T_1}{T_s - T_2} = \frac{UA}{m C_p} t$$

The following tables show the details of the calculation procedures and the resulting dimension specifications of the condenser.

Table 3.12 Condenser Design (superheated coil /vapour side)

Quantity	Bulk Temp. of water T_b	Bulk Temp. of vapour T_s	Surface Temp. of Vapour T_s	Internal diameter of tube d_o	Thermal conductivity of Vapour K	Viscosity of Vapour μ	Specific Heat Capacity C_p	Reynold Number Re	Prandtl Number Pr	Cooling Load of Superheated vapour Coil $Q_{superheat}$	Vapour Flow Rate \dot{m}	Temp. Difference $\Delta\theta$	Surface Area of Coil A	vapour side Overall heat transfer coefficient U
Numerical Value	35 °C	60.5 °C	47.75 °C	0.03175m	0.0380512 w/mk	11.951 N. s/m ²	2.3012 kJ/kg	2134.49	0.723	0.0626 kW	0.0004240 74 Kg/s	60.5-35 °C	0.5089 m ²	5 w/m ² k
		$\frac{83 + 38}{2}$	$\frac{60.5 + 35}{2}$		Evaluated at Bulk Temp	Evaluated at Surface Temp.	Evaluated at Bulk Temp			$\frac{h_s - h_{sat}}{time(6hrs)}$	$\frac{9.16kg}{3600 \times 6hrs}$			
Remarks	Design			Design	From Tables(see Appendix)	From Tables(see Appendix)	From Tables(see Appendix)		From Tables(see Appendix)	$h_{superheat} = 1620.1$ $h_{saturated} = 1472.6$ KJ/Kg		See equation 3.3.2.2	See Equation 3.3.2.1	See Equation 3.3.2.3 Preliminary Value

$$A = \Pi d_o l \text{-----[3.3.2.1]}$$

$$\Delta\theta_m = T_{bNH_3} - T_{bw} \text{-----} \{3.3.2.2\}$$

$$Q = UA\theta_m \text{-----[3.3.2.3]}$$

Table 3.13 Condenser Design *continued* (superheated coil /vapour side)

Quantity	Length of Tube L	vapor side heat transfer coefficient h_i	vapor side heat transfer coefficient $h_{i\text{coil}}$	Coil Diameter d_c
Numerical Value	5.1 m	4.187 w/m ² k	5.73027 w/m ² k	0.3 m
		See Eqn3.3.2.4	See Eqn 3.3.2.5	Design

$$h_i = \frac{k}{L} 1.86 \left(\frac{d_0 \text{Re Pr}}{L} \right)^{0.33} \text{-----} \{3.3.2.4\}$$

$$h_{i\text{coil}} = h_i(\text{straightpipe}) \left(1 + 3.5 \frac{d}{d_c} \right) \text{-----} \{3.3.2.5\}$$

Table 3.14 Condenser Design *continued* (superheated coil/ water side)

Quantity	Bulk Temp. of water T_{bw}	Surface Temperature T_s	Superheated Ammonia Bulk Temp. T_{bv}	Thermal conductivity of Water K_w (at 42 °C)	Temperature Difference ΔT	Specific Heat Capacity of Water C_p	Density of Water ρ_w	Viscosity of Ammonia liquid μ_w	Prandtle Number Pr	Cubic Expansion β	Tube Diameter di	Grashof Number Gr	External transfer coefficient For helical tube h_o
Numerical Value	36 °C	48.25 °C	60.5 °C	0.634 w/m.k	12.25 °C	4.179KJ/kg	991 kg/m ³	631x10 ⁻⁶ N.S/m ²	4.16	400.4x10 ⁻⁶	0.03175 m	1.8544186 29x10 ¹² w/m ² k	667 w/m ² k
		$\frac{T_{bw} + T_{bv}}{2}$	See Table 3.3.2.1		48.25-36							$\Rightarrow c' = 0.13 \& n = 0.33$	
Remarks	Design			From Tables(see Appendix)		From Tables (see Appendix)	From Tables(see Appendix)	From Tables (see Appendix)	From Tables(see Appendix)		Design	See equation 3.3.2.6	See equation 3.3.2.7

Note : Evaluated at 42 °C $\frac{T_{bw} + T_s}{2}$

$$Gr = \frac{\beta g \Delta T d_i^3 \rho^2}{\mu} \text{-----} \{3.3.2.6\}$$

$$h_o = c' \left(\frac{\Delta T}{d_i} \right)^n k \left(\frac{\beta g \rho^2 C_p}{\mu k} \right)^n \text{-----} \{3.3.2.7\}$$

* c' & n are constants $c' = 0.13 \& n = 0.33$ see Appendix

Table 3.15 Condenser Design *continued* (superheated coil)

Quantity	Heat Transfer Area	Length of helical tube l	Internal Diameter of helical tube d_i	External Diameter of helical tube d_o	Condenser Load Q_c (superheated section)	Internal Heat Transfer Coefficient $h_{i\text{coil}}$	External Heat Transfer Coefficient h_o	External Scale factor R_o	Internal Scale factor R_i	Thermal Conductivity of Steel Wall k_w	Tube Wall Thickness x_w	Overall Heat Transfer Coefficient U	Temp. Difference $\Delta\theta$
Numerical Value	0.5089 m^2	5.1 m	0.02655 m	0.03175m	0.0626 KW	5.73027 w/m^2k	667 w/m^2k	0.0002	0.0002	15 W/mK	0.00026 m	5.62 W/ m^2K	60.5-35 $^{\circ}C$
Remarks			Design	Design	Design			From table(see appendix)	From table(see appendix)	From table(see appendix)	Design	Eqn. 3.3.2.8	

$$\frac{1}{U} = \frac{r_o}{r_i h_i} + \frac{r_o \ln \frac{r_o}{r_i}}{k} + \frac{1}{h_o} + f \text{-----} \{3.3.2.8\}$$

Table 3.16 Condenser Design *continued* (saturated vapour coil /vapour side)

Quantity	Bulk Temp. of water T_b	Bulk Temp. of vapour T_v	Surface Temp. of Vapour T_s	Density of water ρ_v	Density of Vapour ρ_w	Thermal Conductivity of Water K_L	Viscosity of Water μ_w	Tube Internal Diameter Di	Tube Internal Diameter Do	Internal Heat Transfer Coefficient h_{coil}	Cooling Load of Saturated vapour Coil $Q_{c,saturated}$	Specific Capacity Of Liquid C_{pL}
Numerical Value	36 °C	38 °C	37 °C	11.270 kg/m ³	583 kg/m ³	0.4514 W/mK	0.0001244 N. s/m ²	0.03175 m	0.03213 m	12971 w/m ² k	0.47093 KW	4.845072 KJ/Kg K
			$\frac{36 + 38}{2}$	Evaluated at Temp 37 °C	Evaluated at Temp 37 °C	Evaluated at Temp 37 °C	Evaluated at Bulk Temp				$\frac{h_g - h_f}{time(6hrs)}$	Evaluated at Temp 38 °C
Remarks	Design	Design		From Tables(see Appendix)	From Tables(see Appendix)	From Tables(see Appendix)	From Tables(see Appendix)	Design	Design	See equation 3.3.2.11	$h_g = 1472.6$ KJ/kg $h_f = 362.1$ KJ/Kg	From Tables(see Appendix)

$$h_i = 0.555 \left[\frac{g \rho_l (\rho_l - \rho_v) k_l^3 h'_{fg}}{\mu_l (T_{sat} - T_s) Di} \right]^{\frac{1}{4}} \text{-----} \{3.3.2.9\}$$

$$h'_{fg} = h_{fg} + \frac{3}{8} (T_{sat} - T_s) \text{-----} \{3.3.2.10\}$$

$$h_i (coil) = h_i (straightpipe) \left(1 + 3.5 \frac{d}{d_c} \right) \text{-----} \{3.3.2.11\}$$

Table 3.17 Condenser Design *continued* (saturated vapour coil/ water side)

Quantity	Prandtl Number Pr	Cubic Expansion β	Thermal Conductivity of Water K_w	Viscosity of Water μ_w	Viscosity of Vapour μ_v	Reynold Number Re	Specific Capacity Of Liquid C_{pw}	Grashof Number Gr	External Heat Transfer Coefficient h_o	Temp. Difference $\Delta\theta$	Surface Area of Coil A	Length of Condenser Coil L	Overall Heat Transfer Coefficient U
Numerical Value	4.62	361.9×10^{-6}	0.628 W/mK	695×10^{-6} N. s/m ²	11.905×10^{-6} N. s/m ²	1455	4.178 KJ/Kgk	1.071×10^{-7}	324.399 w/m ² k	2 °C	0.84397 m ²	8.5 m	279 w/m ² k
	Evaluated at Surface Temp 310k		Evaluated at Surface Temp 310k		Evaluated at Surface Temp.	$\frac{4\dot{m}}{\Pi\mu_v D}$		\Rightarrow C=0.53 & n=0.25		(38 -36) °C	0.84397		
Remarks						D=0.03123		See equation 3.3.2.12	See equation 3.3.2.13		Eqn. 3.3.2.15	See Equation 3.3.2.14	See equation 3.3.2.16

$$Gr = \frac{\beta g \Delta T d_i^3 \rho^2}{\mu} \text{-----} \{3.3.2.12\}$$

$$h_o = c' \left(\frac{\Delta T}{d_i} \right)^n k \left(\frac{\beta g \rho^2 C_p}{\mu k} \right)^n \text{-----} \{3.3.2.13\}$$

$$A = \Pi d_o l \text{-----} \{3.3.2.14\}$$

$$Q = UA \theta_m \text{-----} \{3.3.2.15\}$$

$$\frac{1}{U} = \frac{r_o}{r_i h_i} + \frac{r_o \ln \frac{r_o}{r_i}}{k} + \frac{1}{h_o} + f \text{-----} \{3.3.2.16\}$$

Table 3.18 Condenser Design *continued* (water tank/ superheated coil side)

Quantity	Temperature of Condensing Vapor T_{sv}	Initial Temperature of Water T_1	Final Temperature of Water T_2	Overall Heat Transfer Coefficient U	Heat Transfer Area A	Time For Raising Tank Temperature T	Specific Heat Capacity of Water C_p	Mass of Cooling Water m
Numerical Value	83°C	35°C	37°C	5.62	0.5089 m ²	6 hours	4200KJ/Kgk	345.6 kg
Remarks	Design	Design	Design	Table 3.15	Table 3.12	Design	From Tables	See equation 2.6.1

Table 3.19 Condenser Design *continued* (water tank/ saturated coil side)

Quantity	Temperature of Condensing Vapor T_v	Initial Temperature of Water T_1	Final Temperature of Water T_2	Overall Heat Transfer Coefficient U	Heat Transfer Area A	Time For Raising Tank Temperature T	Specific Heat Capacity of Water C_p	Mass of Cooling Water m
Numerical Value	38°C	35°C	37°C	279	0.84397 m ²	6 hours	4200KJ/Kgk	240.71kg
Remarks	Design	Design	Design	Table 3.17	Table 3.17	Design	From Tables	See equation 3.3.2.17

$$\ln \frac{T_v - T_1}{T_v - T_2} = \frac{UA}{mC_p} t \text{ ----- } \{3.3.2.17\}$$

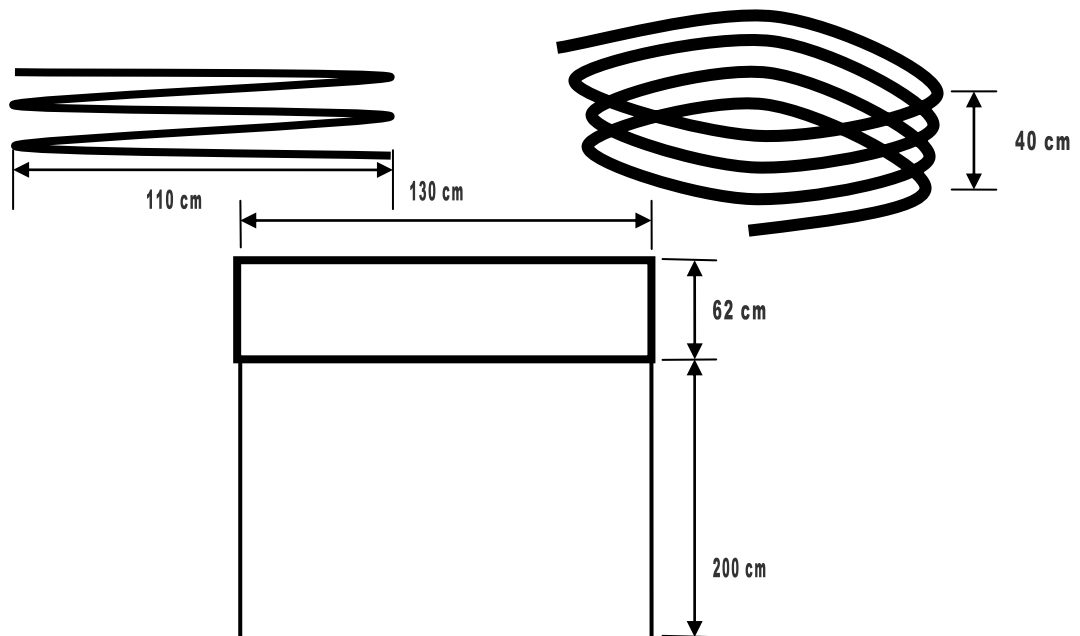


Fig. 3.10 Condenser Coil and Water Tank

Table 20 Condenser Specifications

Name: Condenser		Cooling Agent:	
Type	Coil in Stagnant Basin	Agent Name	Water
Operation Mode:		Initial Temperature	35°C
Condensing Component	99% Ammonia Vapor	Final Temperature	37°C
Operating Temperature	38 °C	Agent Quantity I	350 kg
Operating Pressure	14.5 bar	Agent Quantity II	250 kg
Cooling Load	0.53353kW	Dimensions:	
Heat Transfer Coefficient for Superheated Vapor	5.62 W/m ² K	Inner Diameter	31.23mm
Heat Transfer Coefficient for Saturated Vapor	279W/m ² K	Outer Diameter	31.75mm
Thermodynamic Mode:		Tube Length for Superheated Vapor	5.1m
Vapor Phase I	Superheated Ammonia Vapor	Tube Length for Saturated Vapor	8.5m
Vapor Phase II	Saturated Ammonia Vapor	Coil Diameter for Superheated Vapor	110 cm
Liquid Phase	Saturated Ammonia Liquid	Coil Diameter for Saturated Vapor Coil	110 cm
Material:			
Tubes	Stainless Steel		
Tank	Iron		

3.3.3 Evaporator Design

Description: It is a coil in stagnant water basin type.

Mechanism of Heat Transfer:

- 1. Evaporator Tube:** There are several mechanisms, or processes, through which a liquid at the saturation temperature may be converted to a vapor by the addition of heat. If the boiling or vaporization occurs on a hot surface in a container, in which the liquid is confined, the process is called "pool boiling". There are several quite different mechanisms by which pool boiling occurs depending upon the temperature difference between the surface and the liquid, and to a lesser extent upon the nature of the surface and liquid. The classic curve of heat flux vs. temperature difference between surface and liquid saturation temperature for saturated pool boiling is shown in Fig.3.11 There are various correlations that have been proposed in the literature for this region the correlation used in this design is for nucleate boiling((see flow correlation on table 3.6)..

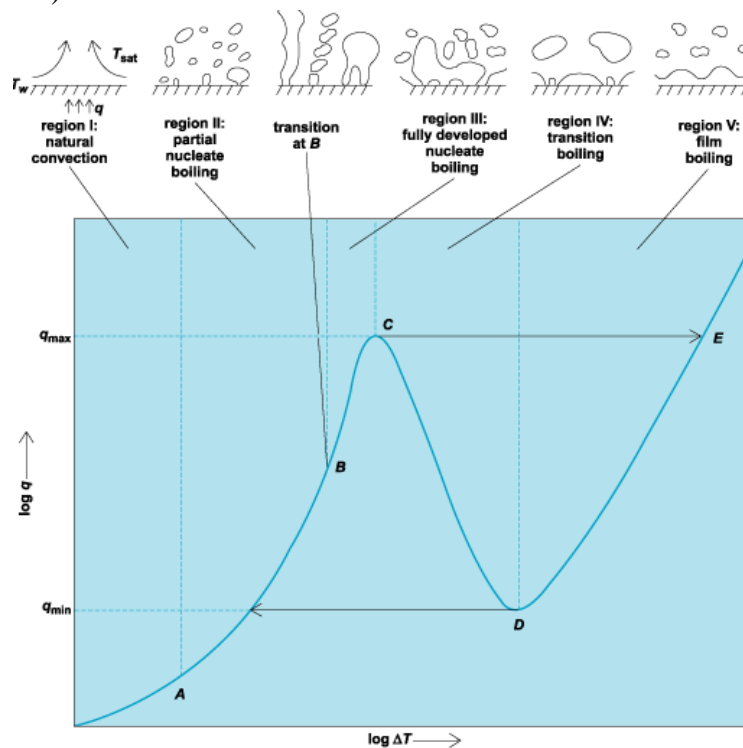


Fig.3.11 Curve of Heat Flux for Pool Boiling

- 2- Water Tank:** Heat Transfer in the water tank is by natural convection (refer to section 3.3.2 above)

The following tables show the details of the calculation procedures and the resulting dimension specifications of the evaporator.
Table 3.21 Evaporator Design (saturated liquid side)

Quantity	Density of Ammonia Liquid ρ_l	Density of Ammonia Vapour ρ_v	Enthalpy of Ammonia liquid h_f	Enthalpy of Ammonia vapour h_g	Latent Heat of Evaporation h_{fg}	Specific Heat capacity of Ammonia Liquid C_{pl}	Surface Tension σ	Prandtl Number of ammonia liquid Pr_l	Heat Flux [8] q''	Prandtl Number Pr	Viscosity of Ammonia liquid μ_l	Temperature Difference ΔT	Evaporator Area A
Numerical Value	633 kg/m³	3.9783 kg/m³	-319.27 KJ/kgK	216.72 KJ/kgK	1038 KJ/kg	4.184 KJ/kgK	55.7x10⁻³N/m	1.672	628.7 W/m²	1.58	0.00018065³ N. s/m²	2.5774 °C	0.027261462 m²
Remarks	From Tables(see Appendix)	From Tables(see Appendix)	From Tables(see Appendix)	From Tables(see Appendix)	h_g-h_f	From Tables(see Appendix)	From Tables(see Appendix)	From Tables(see Appendix)	See Equation 3.3.3.1		From Tables(see Appendix)		See Equation 3.3.3.2

$$q'' = \mu_l h_{fg} \left[\frac{g(\rho_l - \rho_v)}{\sigma} \right]^{\frac{1}{2}} \left[\frac{C_{p,l} \Delta T_e}{C_{s,f} h_{fg} Pr_l^n} \right]^3 \text{-----}\{3.3.3.1\}^*$$

$$A = \frac{Q_e}{q''} \text{-----}\{3.3.3.2\}$$

* $C_{s,f} = 0.013$ $n = 1.7$ $\Delta T_e = T_s - T_{evaporator}$ $T_s = \frac{T_{ambient} + T_{evaporator}}{2}$

Table 3.22 Evaporator Design *continued* (saturated liquid side)

Heat Flux q''	Evaporator Heat Transfer Area A	Internal Heat Transfer Coefficient h_i
4035.2 W/m ²	0.02726146 m ²	1566 W/m ² k
	Design	$Q = Ah_i\Delta t$

Table 3.23 Evaporator Design *continued* (water side)

Quantity	Water Reference Temperature T	Density of water ρ_w	Cubic Expansion β	Conductivity of Water K _w	Specific Heat Capacity of Water C_{p_w}	Prandtle Number Pr Of Water	Viscosity of Water μ_w	External Heat Transfer Coefficient h_o	Temperature Difference ΔT
Numerical Value	27	997 kg/m ³	0.0002761	0.613 W/mK	4.179 KJ/kgK	5.83	0.000855 N. s/m ²	651 W/m ² k	T _b -T _s
Remarks	$\frac{T_{surface} + T_{bulk}}{2}$	From Tables(see Appendix)	From Tables(see Appendix)	From Tables(see Appendix)	From Tables(see Appendix)		From Tables(see Appendix)	See Equation 3.3.3.3	

$$h_o = C' \left(\frac{\Delta T}{l} \right)^n k \left(\frac{\beta g \rho^2 C_\rho}{\mu k} \right)^n \text{-----} \{3.3.3.3\}$$

$C' = 0.53 \quad n = 0.25$

Table 3.24 Evaporator Design *continued*

Quantity	Internal Heat Transfer Coefficient h_i	External Heat Transfer Coefficient h_o	Internal Diameter Di	External Diameter Do	Stainless Steel Tube Thermal Conductivity K	Fouling factor f	Overall Heat Transfer Coefficient U	Evaporator Heat Transfer Area A	Length of Coil L
Numerical Value	1566 W/m ² k	651 W/m ² k	0.0148 m	0.02 m	15 W/mk	0.0002	326 W/m ² k	0.02726146 m ²	0.433 m
Remarks	See Table 3.22	See Table 3.23	Design	Design	From Tables(see Appendix)	From Tables(see Appendix)	See Eqn. 3.3.3.4	Design	See Eqn. 3.3.3.5

$$\frac{1}{U} = \frac{r_o}{r_i h_i} + \frac{r_o \ln \frac{r_o}{r_i}}{k} + \frac{1}{h_o} + \frac{f r_o}{r_i} + f \text{-----} \{3.3.3.4\}$$

$$A = \Pi D L \text{-----} \{3.3.3.5\}$$

Table 3.25 Evaporator Specifications

Name: Evaporator		Cooling Agent:	
Type	Coil in Stagnant Basin	Agent Name	Water
Operation Mode :		Initial Temperature	35°C
Evaporating Component	Saturated Ammonia Liquid	Final Temperature	37°C
Operating Temperature	5 °C	Agent Quantity	0.125m ³
Operating Pressure	5.5 bar	Dimensions	
Cooling Load	0.110kW	Inner Diameter	14.8mm
Heat Transfer Coefficient	326 W/m ² K	Outer Diameter	20mm
Thermodynamic Mode:		Tube Length for Superheated Vapor	0.433m
Vapor Phase	Saturated Ammonia Vapor	Material	
Liquid Phase	Saturated Ammonia Liquid	Tubes	Stainless Steel

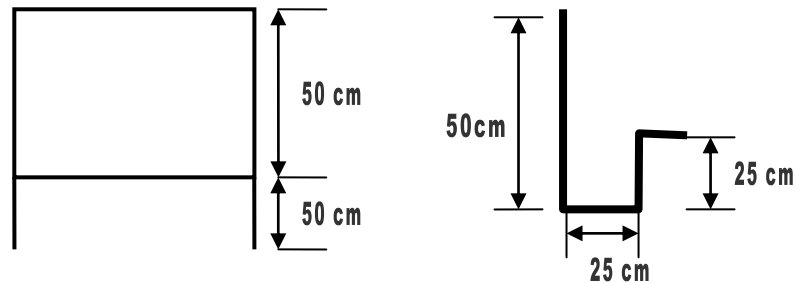


Fig. 3.12 Evaporator Coil and Cooling Tank

3.3.4 Double Pipe Heat Exchanger Design

Description:

A double-pipe heat exchanger consists of two concentric pipes or tubes. The outer tube is called the annulus. In one of the pipes a warmer fluid flows and in the other a colder one. Due to the temperature difference between the fluids, heat is transferred.

Mechanism of Heat Transfer

Inner Tubes & Outer Tubes : The flow in the annulus and inner pipes is a forced convection flow (see section 3.3.1 for details and see flow correlation on table 3.6).

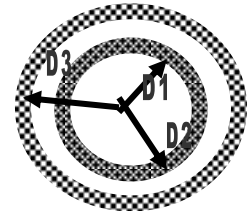
Calculation Procedure:

The sequence of calculations in double pipe heat exchanger are as follows:

a- Area of flow[8]:

(i) Through the pipe, $A_i = \frac{\Pi D_1^2}{4}$

(ii) Through the annulus $A_a = \frac{\Pi(D_3^2 - D_2^2)}{4}$



b- Equivalent diameter of the annulus[8]: $D_e = \frac{D_3^2 - D_2^2}{D_2}$

c- Velocity of flow[8]:

(i) For flow through pipe, $u_s = \frac{\dot{M}_s}{\rho_s A_i}$

(ii) For flow through annulus, $u_w = \frac{\dot{M}_w}{\rho_w A_a}$

Where \dot{M}_s, \dot{M}_w are mass flow rates of strong and weak ammonia ρ_s and ρ_w densities of strong and weak ammonia solutions respectively:

d- Reynolds number[8]:

(i) For through pipe, $Re_s = \frac{D_1 u_s \rho_s}{\mu_s}$

(ii) For flow through annulus, $Re_w = \frac{D_e u_w \rho_w}{\mu_w}$

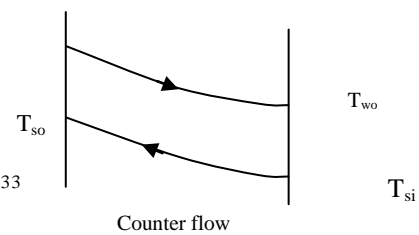
Where μ_s, μ_w are viscosities of strong and weak ammonia solution.

Individual heat transfer coefficient

(iii) For pipe, $h_i = \left(\frac{k}{D_i}\right) 1.86 \left(\frac{D_i Re Pr}{L}\right)^{0.33}$

(iv) For annulus, $h_o = \left(\frac{k}{D_e}\right) 1.86 \left(\frac{D_e Re Pr}{L}\right)^{0.33}$

Where L is the length of the heat exchanger k is thermal conductivity.



h- Overall transfer coefficient[8]: $\frac{1}{U} = \frac{1}{h_o} + \frac{1D_2}{h_i D_1} + f$

Where f is the fouling factor

i- Log mean temperature difference[8]: $\Delta T_m = \frac{(T_{wo} - T_{si}) - (T_{wi} - T_{so})}{\ln \left[\frac{T_{wo} - T_{si}}{T_{wi} - T_{so}} \right]}$

Where are inlet and outlet temperatures of strong and weak solutions

j- Area of heat transfer and length and length of pipe: $Q_t = UA\Delta T_m$

Where A area of heat exchanger.

The following tables show the details of the calculation procedures and the resulting dimension specifications of the double tube heat exchanger.

Table 3.26 Solution Heat Exchanger Design

Quantity	Strong Ammonia mass Flow Rate \dot{m}_s	Weak Ammonia mass Flow Rate \dot{m}_w	Bulk Temp. of of strong ammonia solution T_{bs}	Bulk Temp. of of weak ammonia solution T_{bw}	Density of strong ammonia solution ρ_s	Density of weak Ammonia solution ρ_w	Viscosity Of strong ammonia solution μ_s	Viscosity Of strong ammonia solution μ_w	Thermal Conductivity of Aqueous ammonia κ	Specific heat capacity of strong ammonia C_p	Specific heat capacity of weak ammonia C_p	Inlet Temperature of Strong Ammonia Solution T_{si}	Outlet Temperature of Strong Ammonia Solution T_{so}	Inlet Temperature of weak Ammonia Solution T_{wi}	Outlet Temperature of weak Ammonia Solution T_{wo}
Numerical Value	0.0066 kg/s	0.0057 kg/s	66 °C	75 °C	764 kg/m ³	788 kg/m ³	0.000188 N/m ² s	0.000214 Ns/m ²	0.5 WK/m	4614 J/kgK	4552 J/kgK	59 °C	73 °C	83 °C	66 °C
Remarks	Design	Design	Design	Design	From Tables(see Appendix)	From Tables(see Appendix)	From Tables(see Appendix)	From Tables(see Appendix)	From Tables(see Appendix)	From Tables(see Appendix)	From Tables(see Appendix)	Design	Design	Design	Design

Table 3.27 Double Pipe Heat Exchanger Design (continued)

Quantity	Log Mean Temperature Difference ΔT_m	Outer diameter of Inner tube D_2	Internal Diameter of Outer tube D_3	Internal Diameter of Inner tube D_1	Cross Sectional Area of inner Tube A_i	Cross Sectional Area of Annulus Tube A_o	Equivalent Diameter of Annulus D_e	Velocity through Inner tube u_s	Velocity through Annulus tube u_w	Reynold Number of strong Ammonia Re_s	Reynold Number of weak Ammonia Re_w	Prandtl Number of strong Ammonia Pr_s	Prandtl Number of weak Ammonia Pr_w
Numerical Value	8.4 °C	0.0254m	0.03256m	0.01986m	0.00031 m ²	0.00033 m ²	0.01633 m	0.0279 m/s	0.035099 m/s	2333	1507	1.74	4.047
Remarks	See equation 3.3.4.1	Design	Design	Design	$A_i = \frac{\Pi D^2}{4}$	See equation 3.3.4.2	See equation 3.3.4.3	See equation 3.3.4.4	See equation 3.3.4.5	See equation 3.3.4.6	See equation 3.3.4.7	See equation 3.3.4.8	See equation 3.3.4.9

$$\Delta T_m = \frac{(T_{wo} - T_{si}) - (T_{wi} - T_{so})}{\ln \left[\frac{T_{wo} - T_{si}}{T_{wi} - T_{so}} \right]} \dots\dots\dots \{3.3.4.1\}$$

$$A_o = \frac{\Pi(D_3^2 - D_2^2)}{4} \dots\dots\dots \{3.3.4.2\}$$

$$D_e = \frac{D_3^2 - D_2^2}{D_2} \dots\dots\dots \{3.3.4.3\}$$

$$u_s = \frac{\dot{M}_s}{\rho_s A_i} \dots\dots\dots \{3.3.4.4\}$$

$$u_w = \frac{\dot{M}_w}{\rho_w A_o} \dots\dots\dots \{3.3.4.5\}$$

$$Re_s = \frac{D_2 u_s \rho_s}{\mu_s} \dots\dots\dots \{3.3.4.6\}$$

$$Re_w = \frac{D_e u_w \rho_w}{\mu_w} \dots\dots\dots \{3.3.4.7\}$$

$$Pr_s = \frac{C_p \mu_s}{k} \dots\dots\dots \{3.3.4.8\}$$

$$Pr_w = \frac{C_p \mu_w}{k} \dots\dots\dots \{3.3.4.9\}$$

Table 3.28 Double Pipe Heat Exchanger Design *continued*

Quantity	Heat Exchanger Load Q	Mass Flow Rate through Inner Tube \dot{m}	Temperature Difference ΔT	Overall Heat Transfer Coefficient U	Heat Transfer Coefficient of Strong Solution Side h_i	Heat Transfer Coefficient of weak solution side h_o	External Scale factor R_f	Overall Heat Transfer Coefficient U	Overall Heat Transfer Area A	Total Tube Length L
Numerical Value	426W	0.0066 Kg/s	17 °C	68 W/m ² K	87.8 W/m ² K	85.94 W/m ² K	0.0002	47.6 W/m ² K	0.7487 m ²	12m
Remarks	$Q = \dot{m}cp\Delta t$	Design	$T_{so} - T_{si}$	Preliminary Value	See equation 3.3.4.10	See equation 3.3.4.11	From Tables(see Appendix)	see equation 3.3.4.12	See equation 3.3.4.13	See equation 3.3.4.14

$$h_i = \left(\frac{k}{D_i}\right) 1.86 \left(\frac{D_i \text{ Re Pr}}{L}\right)^{0.33} \text{-----} \{3.3.4.10\}$$

$$h_o = \left(\frac{k}{D_e}\right) 1.86 \left(\frac{D_e \text{ Re Pr}}{L}\right)^{0.33} \text{-----} \{3.3.4.11\}$$

$$\frac{1}{U} = \frac{1}{h_o} + \frac{1}{h_i D_1} + R_f \text{-----} \{3.3.4.12\}$$

$$Q_t = UA\Delta T_m \text{-----} \{3.3.4.13\}$$

$$A = \Pi D_2 L \text{-----} \{3.3.4.14\}$$

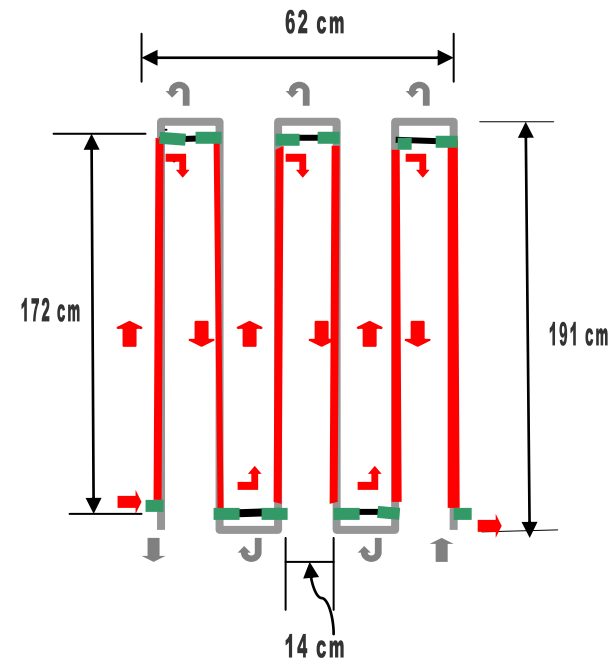


Fig. 3.13 Double Tube Heat Exchanger

Table 3.29 Double Pipe Heat Exchanger Specifications

Name: Heat Exchanger		Thermodynamic Mode:	
Type	Double Tube /Counter Flow	Liquid Phase	Ammonia- Water Mixture
Heating Specification:		Dimensions:	
Component Heated	54% Ammonia Mixture	Inner Diameter of Inner Tube	19.86 mm
Flow Rate	23.76kg/hr	Outer Diameter of Outer Inner Tube	25.4mm
Exit Temperature	73°C	Inner Diameter of Outer Tube	32.56 mm
Inlet Temperature	59°C	Tube Length	12m
Heat Transfer Coefficient	47.6 W/m ² K	Material:	
Heating Load	o.426KW	Tubes	Stainless Steel
Heating Agent			
Agent Name	46% Weak Ammonia Solution		
Initial Temperature	83°C		
Final Temperature	66°C		
Agent Rate	20.52 kg/hr		

3.3.5 Absorber Design

Description: The absorber is a header-riser type cooled by stagnant water in a tank. The weak ammonia solution is distributed in the rows and columns of the absorber. Ammonia vapor is distributed through nozzles which are located in the rows of the absorber.

Heat Transfer Mechanism.

1. **Flow Inside Tubes:** Unsteady state heat flow exists in tubes. The solution in tubes is stagnant and its temperature changes with time as it is cooled by the water in the tank. The problem is treated as a transient heat conduction in a cylinder..

The form of the solution is:

$$f(\theta) = F\{(\tau)(Bi)\}$$

where f and F indicate functions of the terms following, θ is dimensionless temperature, τ is called the Fourier number (this includes the factor k/c_p the thermal conductance divided by the volumetric heat capacity, which is called the thermal diffusivity) and Bi is the Biot number.

The exact analytical solution is very complicated. However, an approximate solution can be obtained by using graphical tools. The graphs allow you to find the centerline temperature at any given time, and the temperature at any location based on the centerline temperature((see flow correlation on table 3.6)..

2. **Water Tank:** Heat Transfer in the water tank is by natural convection (refer to section 3.3.2 above)

The following tables show the details of the calculation procedures and the resulting dimension specifications of the absorber.

Table 3.30 Absorber Design (Aqueous Ammonia Solution)

Quantity	Bulk Temp. of weak ammonia solution T_{bw}	Density of weak ammonia solution ρ_w	Prandtl Number Pr	Viscosity Of weak ammonia solution μ_w	Thermal Conductivity of Aqueous ammonia κ	Specific heat capacity of weak ammonia C_p	Volume of Absorber V_a	Diameter of Absorber Tubes D	Total Length of Tube L	Surface Area A
Numerical Value	52 °C	822.2 kg/m ³	2.47	0.000315 Ns/m ²	0.5 WK/m	4879 J/kgK	0.0965	0.1282m	7.5 m	3.0206 m ²
Remarks	$\frac{66 + 38}{2}$	From Tables(see Appendix)	From Tables(see Appendix)	From Tables(see Appendix)	From Tables(see Appendix)	From Tables(see Appendix)	$\frac{110\%Mass}{\rho}$	$V = \frac{\pi D^2 L}{4}$	Design	Design

Table 3.31 Absorber Design (Cooling Water Side)

Quantity	Bulk Temp. of Water T_{bH_2O}	Specific Expansion β	Density of Water ρ_{H_2O}	Prandtl Number Pr	Viscosity Of Water μ_{H_2O}	Thermal Conductivity of Water κ	Specific heat capacity of weak ammonia C_p	Volume of Absorber V_a	Diameter of Absorber Tubes D	Grashof Number Gr	Nusslet Nu	External Heat Transfer Coefficient h_o
Numerical Value	35 °C	$320.6 \times 10^{-6} K^{-1}$	995 kg/m ³	5.2	0.000769 Ns/m ²	0.62WK/m	4879 J/kgK	0.0965	0.1282m	7.7×10^4	16.52	79.9152 W/m ² K
Remarks	$\frac{37 + 35}{2}$	From Tables(see Appendix)	From Tables(see Appendix)	From Tables(see Appendix)	From Tables(see Appendix)	From Tables(see Appendix)	From Tables(see Appendix)	$\frac{110\% Mass}{\rho}$	$V = \frac{\Pi D^2 L}{4}$	See Equation. 3.3.5.1	See Equation 3.3.5.2	See Equation 3.3.5.3

$$Gr = \frac{\beta g \Delta T l^3 \rho^2}{\mu^2} \text{-----} \{3.3.5.1\}$$

$$Nu = 0.683 Gr^{0.25} Pr^{0.25} \left(\frac{Pr}{0.861 + Pr} \right)^{0.25} \text{-----} \{3.3.5.2\}$$

$$Nu = \frac{hl}{k} \text{-----} \{3.3.5.3\}$$

Table 3.32 Absorber Design *continued*

Quantity	Bulk Temperature Of Ammonia Solution T_{iNH_3}	Density of Water ρ_{NH_3}	Viscosity Of Water μ_{NH_3}	Thermal Conductivity of Water κ	Specific heat capacity of weak ammonia C_p	Characteristic Length of the Tube l_c	Thermal Diffusivity α	Biot Number Bi	Time	Fourier Number τ	External Heat Transfer Coefficient h_o	Dimensionless Heat Transfer $\frac{Q}{Q_o}$	Total Length of Tube L	Total Heat Transferred Q
Numerical Value	52 °C	822.23 kg/m ³	0.000769 Ns/m ²	0.5WK/m	4879 J/kgK	0.064m	0.124×10	10.243	6 Hours	0.65186	79.9152 W/m ² K	0.9	7.5 m	6355872.18 J 0.294KW
Remarks	$\frac{66 + 38}{2}$	From Tables(see Appendix)	From Tables(see Appendix)	From Tables(see Appendix)	From Tables(see Appendix)	$\frac{D}{2}$	$\alpha = \frac{k}{c_p \rho}$	$Bi = \frac{hl}{K}$	Design	$\tau = \frac{\alpha t}{l^2}$	See section 5.2	From Graphs [8]	Design	See Equation 3.3.5.4 $\frac{Q}{6 \times 3600}$

$$\frac{Q_o}{L} = \frac{\rho C_p \Pi l^2 L (T_{iNH_3} - T_{bH_2O})}{L} \text{-----} \{3.3.5.4\}$$

Total heat need to be removed = $m\Delta TC_p = 61(66-38)4879 = 8.3MJ$

Table 3.33 Absorber Design *continued*

Quantity	Heat Transfer Q	Heat Transfer Area A	Bulk Temperature of Weak Ammonia T_{bNH_3}	Bulk Temperature of Water	Surface Temperature T_s	Temperature Difference ΔT	Heat Transfer Coefficient U
Numerical Value	0.294KW	3.0206m ²	52 °C	36 °C	44 °C	8°C	12.17 W/m ² K
Remarks	See Section 5.3				$\frac{T_{bNH_3} + T_{bw}}{2}$	$T_s - T_{bw}$	See Equation 3.3.5.5

$$Q = AU\Delta T \text{ ----- } \{3.3.5.5\}$$

Table 3.34 Absorber Design *continued* (Water Tank side)

Quantity	Temperature of Weak Ammonia T_{bNH_3}	Initial Temperature of Water T_1	Final Temperature of Water T_2	Overall Heat Transfer Coefficient U	Heat Transfer Area A	Time For Raising Tank Temperature T	Specific Heat Capacity of Water C_p	Mass of Cooling Water m
Numerical Value	52°C	35°C	37°C	12.17 W/m ² K	3.0206m ²	6 hours	4200KJ/kgK	1511kg
Remarks	Design	Design	Design	See table 3.33	See table 3.33	Design		See equation 2.6.1 See equation 3.3.5.6

$$\ln \frac{T_{bNH_3} - T_1}{T_{bNH_3} - T_2} = \frac{UA}{mC_p} t \text{ ----- } \{3.3.5.6\}$$

Table 3.35 Absorber Specifications

Name: Absorber		Thermodynamic Mode	
Type	Riser Header	Liquid Phase	Ammonia- Water Mixture
Cooling Specification		Dimensions	
Component Cooled	46% Ammonia Mixture	Inner Diameter	0.1282 mm
Flow Rate	20.33kg/hr	Total Length of Absorber	7.5m
Bulk Temperature	52°C	Material	
Heat Transfer Coefficient	12.17 K W/m ² K	Tubes	Galvanized Steel
Cooling Load	o.2943kW	Tank	Polyethylene
Cooling Agent			
Agent Name	Water		
Bulk Temperature	35°C		
Agent Quantity	1500 kg		

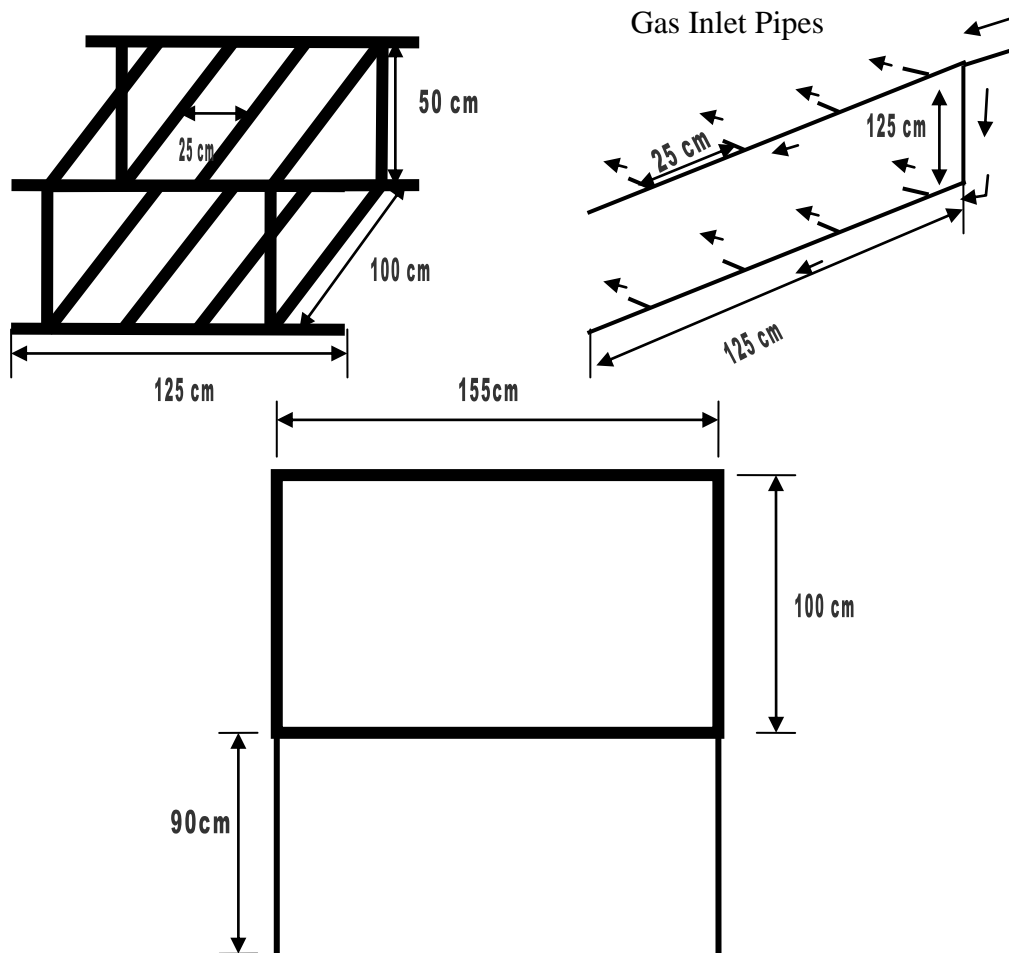


Fig. 3.14 Absorber Components (Header-Riser pipes, Ammonia vapor Inlet Pipes and Water Tank)

3.4 Sizing and Performance Prediction of Solar Collectors

3.4.1 Solar Collectors Sizing

3.4.1.1 Flat Plate Collector Design

Description: The flat plate collector field consists of two collectors of header-riser type with storage tanks of different capacities.

Basic Flat-Plate Energy Balance

There are three parameters which need to be specified in designing a solar collector: optical efficiency (transmittance-absorbance factor), collector heat loss coefficient and heat removal factor. The useful energy output, Q_u , of a collector area, A_c , is the difference between the absorbed solar radiation, S , and the thermal loss, U_L and is given by the following equation:

$$Q_u = A_c F_r [S - U_L (T_i - T_a)] \quad [1]$$

Where $S = [\tau\alpha]_{av}$ (optical efficiency) $\times I_i$ (incident solar radiation)

$$U_L = U_s \text{ (side-losses)} + U_b \text{ (bottom-losses)} + U_t \text{ (top Losses)}$$

T_i & T_a are inlet fluid and ambient temperatures respectively.

The following tables show the details of the calculation procedures and the resulting dimension specifications of the collector.

Table 3.36 Flat Plate Collector Design (Overall Heat Loss Coefficient Evaluation)

Quantity	Internal Convection Coefficient h_1	Plate to Cover Radiation Coefficient h_2	External Convection Coefficient h_3	External Radiation Coefficient h_4	Top Loss Coefficient U_t	Back Surface Coefficient U_B	Edge Heat Coefficient U_E	Overall Heat Transfer Coefficient U_L
Numerical Value	4 W/m ² K	7 W/m ² K	7.3 W/m ² K	5.5 W/m ² K	5.915 W/m ² K	0.45 W/m ² K	1.75 W/m ² K	8.04 W/m ² K
Remarks	Design	Design	Design	Design	See Eqn. 3.4.11	Design	Design	See Eqn. 3.4.1.2

$$U_T = \frac{1}{\frac{1}{h_1 + h_2} + \frac{1}{h_3 + h_4}} \text{-----} \{3.4.1.1\}$$

$$U_L = U_T + U_B + U_E \text{-----} \{3.4.1.2\}$$

Table 3.37 Flat Plate Collector Design *continued*(Collector Parameters)

Quantity	Overall Loss Coefficient U_L	Tube Spacing W	Tube Inside Diameter D_i	Plate Thickness δ	Plate Thermal Conductivity K	Collector Efficiency F	Heat Transfer Coefficient Inside Tubes h_f	Collector Efficiency Factor F'	Mass Flow Rate \dot{m}	Specific Heat Capacity C_p	Collector Area A_c	Heat Removal Factor F_r
Numerical Value	8 W/m ² K	150 mm	31.75 mm	1.5 mm	237 W/mK	0.95418578 8	57.64W/m ² K	0.782	0.0066 kg/s	3540 J/kgK	2 m ²	0.782
Remarks	See Previous Section	Design	Design	Design	From Tables	See Eqn. 3.4.1.3	See Eqn. 3.4.1.4	See Eqn. 3.4.1.4	Design	From Tables	Design	See Eqn. 3.4.1.5

$$F = \frac{\tanh[m(W - D)/2]}{m(W - D)/2} \text{-----}\{3.4.1.3\}^*$$

$$F' = \frac{1}{U_L W \left\{ \frac{1}{U_L [D + (W - D)F]} + \frac{1}{C_B} + \frac{1}{\Pi D h_f} \right\}} \text{-----}\{3.4.1.4\}^*$$

$$F_r = \frac{\dot{m} C_p}{A_c U_L F'} \left[1 - \exp \left(\frac{A_c U_L F'}{\dot{m} C_p} \right) \right] \text{-----}\{3.4.1.5\}$$

$$Nu = \frac{h_f D_i}{k} = 3.66 \quad , \quad m^2 = \frac{U_L}{k\delta} \quad C_B = \frac{k_b b}{\gamma}$$

Table 3.38 Collector Specifications

Name:	Solar Collector	Dimensional Specifications:	
Type	Flat Plate	Length of Riser Tubes	1m
Flow Type	Thermosyphon	Riser Tube Diameter	0.03175m
Structure	Riser –Header	Riser Tube Thickness	2.5 mm
Operating Pressure	5.5 bar	Number of Riser Tubes	14
Collector Tilt Angle	15 °	Tube center to center distance	15 cm
Heat Transfer Fluid	Strong Ammonia Solution 54%	Length of Header Tubes	210 cm
Specific Heat Capacity of Ammonia Solution	3540J/kgK	Header Tube Inner Diameter	0.03175m
Heat Removal Factor	0.605	Header Tube Thickness	2.5mm
Transmittance –Absorptance Factor	0.55	Absorber Plate Thickness	2.7mm
Overall Heat Transfer Coefficient	8.04 W/m ² K	Collector Case Dimensions LxWxH	210x125x32cm
Storage Tank Heat Loss Coefficient	7.838 W/m ² K	Insulating Material Thickness(collector/storage)	5cm
Absorber Plate Thermal Conductivity	237 W/mK		
Materials:			
Riser Tubes	Stainless Steel		
Header Tubes	Stainless Steel		
Transparent Cover	Window Glass		
Case	Iron + Galvanized Steel Sheets		
Storage Tank	Stainless Steel		
Insulation	Glass Wool		

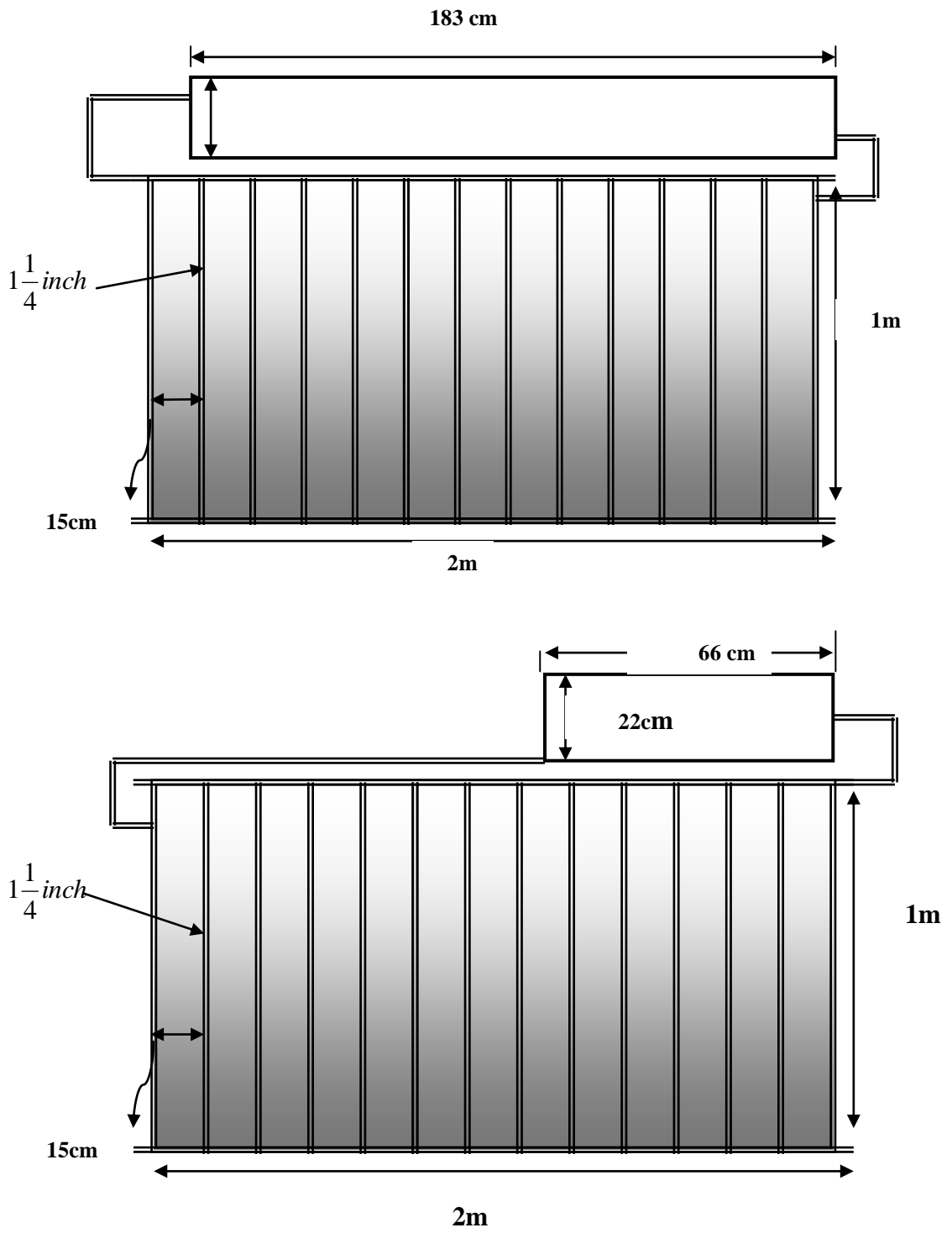


Fig. 3.15 Flat Plate Collectors Field

3.4.1.2 Evacuated Collector Specification

Description: The evacuated collector field consists of two all-glass collector type connected in series. The storage capacity of each collector is around 95 liter and hot water is delivered from the collector field to the generator by a hot water circulation pump. The specification of collector is presented in Table 3.39.

Table 3.39 Evacuated Collector Specification

Type	All Glass Evacuated Tube Collector	Length of Evacuated Tubes	1.5 m
Flow Type	Thermosyphon	Inner Tube Diameter	37mm
Structure	All glass coaxial double-layer tubes	Outer Tube Diameter	47mm
Operating Pressure	1MPa	Tube Thickness	1.6 mm
Collector Tilt Angle	45°	Number of tubes	16/15
Heat Transfer Fluid	Water	Volume of Tank	100 L
Absorption	0.94~0.96	Insulating Layer Thickness	5cm
Emittance	0.04~0.06	Materials	
Vacuum	$P \leq 5 \times 10^{-3} \text{Pa}$	Evacuated Glass Tubes	borosilicate
Transmittance of Outer Tube	0.91	Solar Selective Surface	AIN/AIN-SS/Cu
Collector Heat Loss Coefficient	$\leq 0.6 \text{W/m}^2\text{K}$	Insulation	Foaming polyurethane
Storage Tank Heat Loss Coefficient	$10 \text{W/m}^2\text{K}$	Storage Tank	Stainless Steel

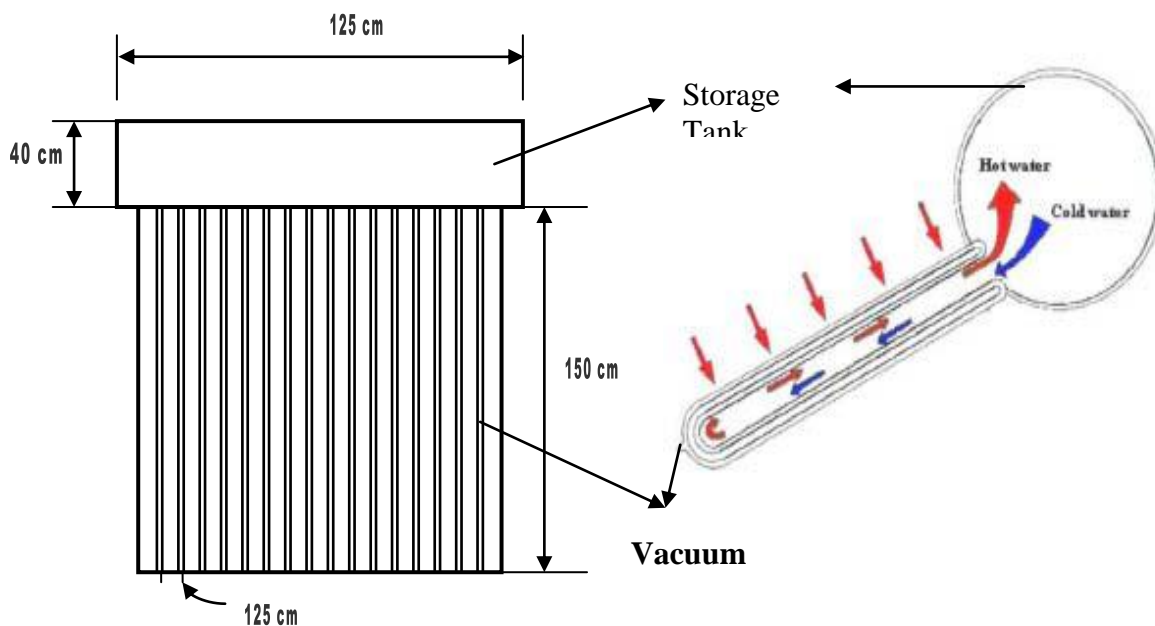


Fig. 3.16 Flat Plate Collectors Field

3.4.2 Performance Predication of Solar Collectors

The solar energy collection system consists of the evacuated collectors which provides hot water to heat the generator, and flat plate collectors which preheat the rich ammonia before been pumped to the generator. Both collector fields have storage units attached to them. To

Estimation of Hourly Radiation on a Sloped Surface Using Isotropic Theory

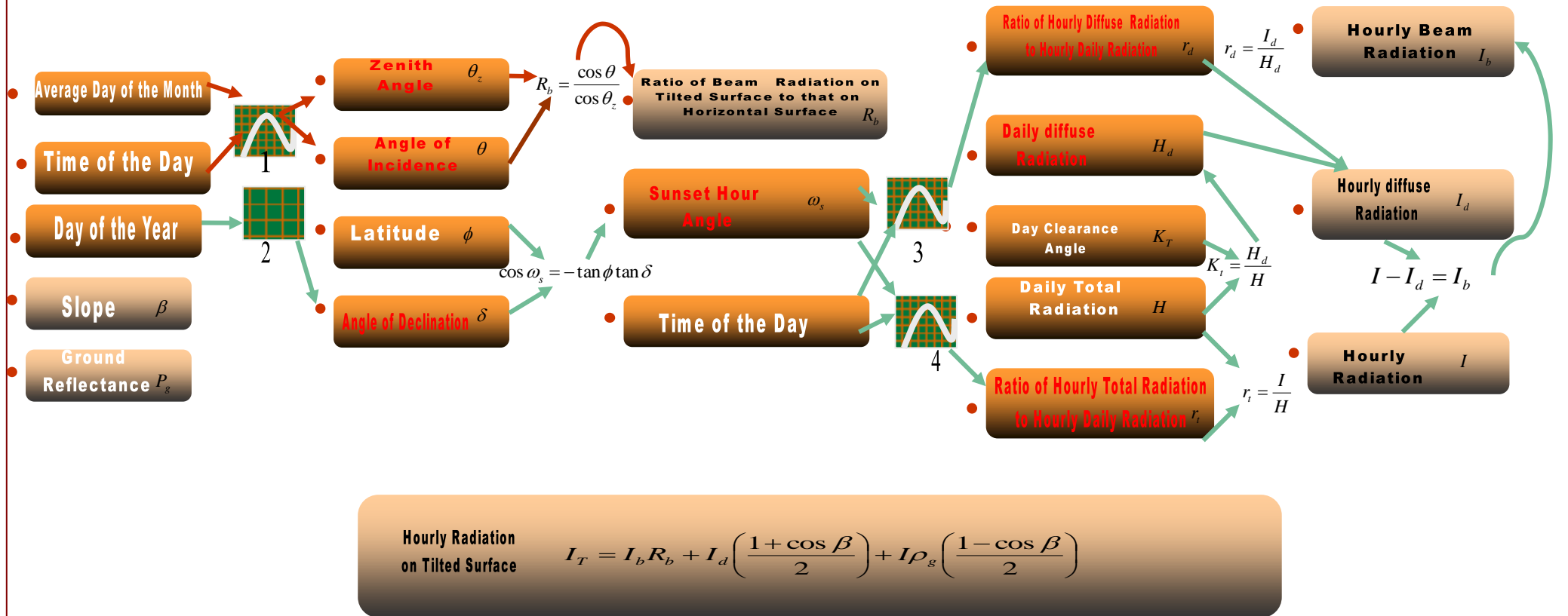


Fig. 3.17 Estimation of Hourly Radiation using the Isotropic Sky Correlation

check the system delivery capacity at the specified design temperature under the local meteorological conditions, the variables that must be considered are daily thermal energy delivery (load), mean inlet and delivery temperature, storage size & heat loss, irradiation on the collectors, ambient temperature. The variation of storage temperature with time were predicted using an expression for the change in storage tank temperature for the specified time period (hourly) in terms of the above mentioned quantities (see equation below).

$$T_s^+ = T_{si} + \frac{\Delta t}{2(m_s C_s)} F_r A_c [(\alpha\tau)I(t) - U(T_m - T_a)] + (UA)_s (T_s - T_a) + \dot{m}_l C_l (T_s - T_{l,r}) \quad [1]$$

Estimation of Incident Radiation

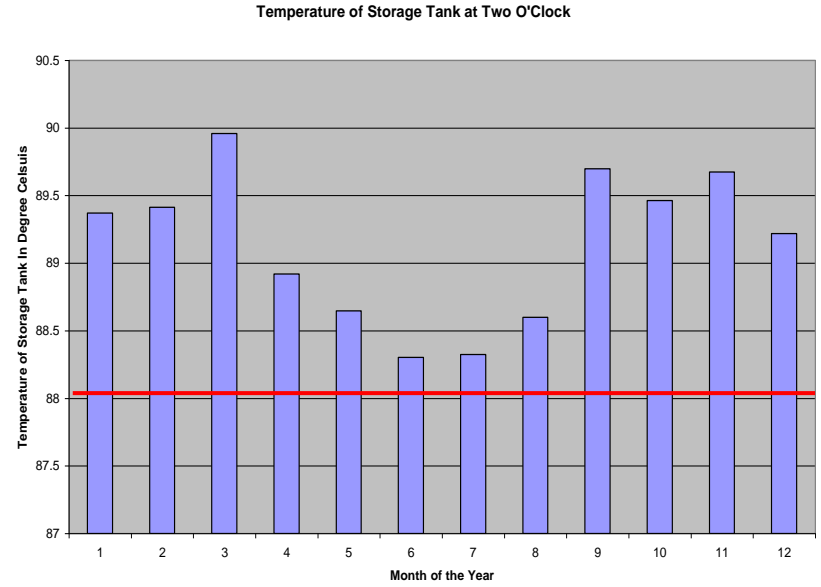
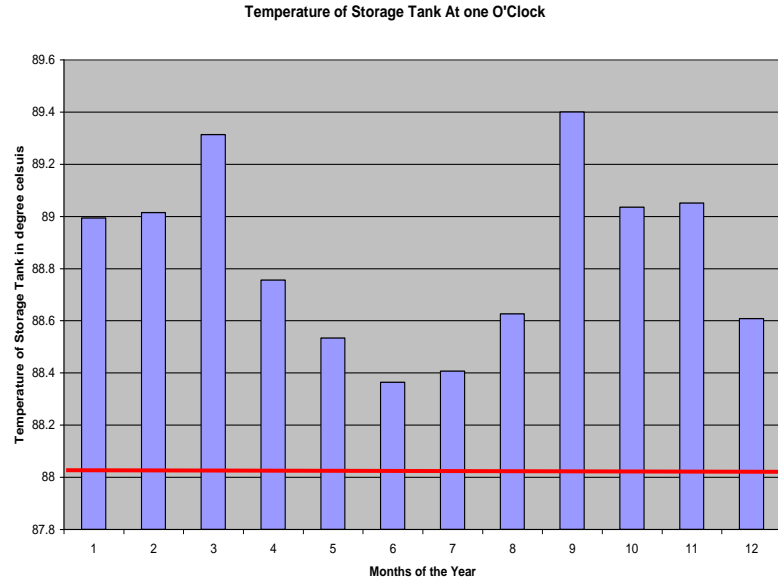
Hourly values of solar radiation in the above mentioned performance prediction equation were estimated from daily values using the Isotropic Sky correlation. Several terms related to solar geometry and basic concepts referring to solar radiation are used, but not explained (to obtain more details refer to specific textbooks[1]). The procedure of hourly radiation estimation is illustrated in Fig. 3.17.

3.4.2.1 Long Term Performance of Evacuated Tube Collector

The evacuated collector field supplies the generator with hot water at a temperature of 88 °C and a fixed flow rate of 35kg/hr and returns water back to the tank at 80° C. The performance of the collector field was predicted under the above mentioned conditions throughout the year for the period from one to four O'clock afternoon using recorded meteorological data(monthly average). The result of performance prediction is presented in the following charts(see Fig. 3.18) and the calculation procedure is presented in tables 3.40 &3.41 According to the result obtained it was decided to use two evacuated collectors to supply the load with the hot water needed at the generator.

3.4.2.2 Performance Prediction of Flat Plate Collector

The function of the flat plate collector field is to preheat the strong ammonia solution before delivery to the generator. The performance was predicted under storage capacity of 65, 45 and 15 kg for December only because, according to Sudan meteorological statistics, December is the month with the minimum radiation level. The performance prediction procedure is presented in Tables 3.42 and 3.43 According to the result obtained it was decided to use two collectors with 65 and 15 kg capacity to supply the system with preheated strong ammonia solution necessary to operate the refrigeration unit.



■ Storage Tank Temperature

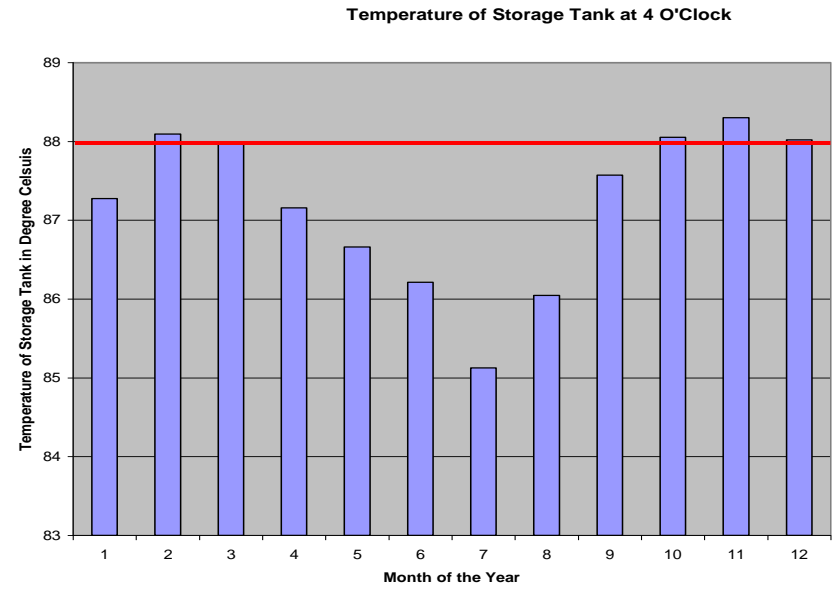
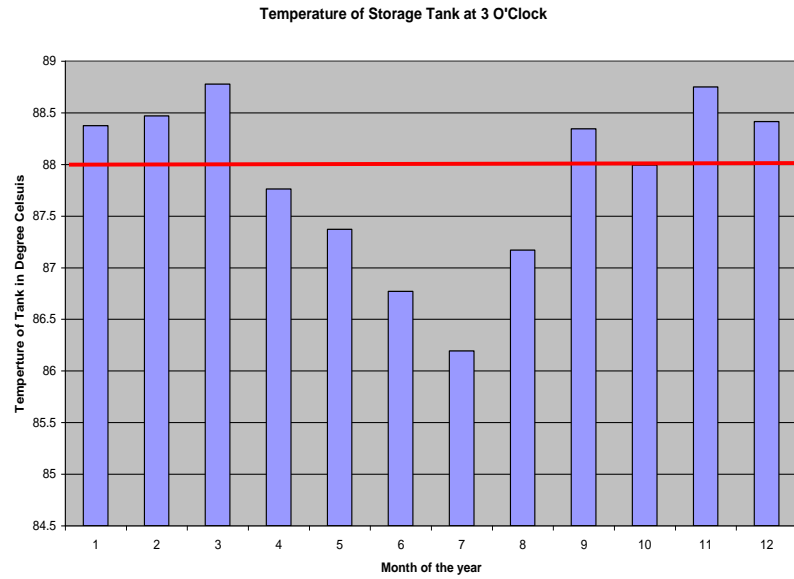


Fig. 3.18 Predicted Storage Tank Temperature

Table 3.40 Radiation on Tilted Surface for the Period for Evacuated Collector from 12 to 4 O`Clock

Quantity	Hourly Radiation on Tilted Surface I_T	Sunset Hour Angle ω_s	Latitude ϕ	Angle of Declination δ	Ratio of Hourly Total Radiation To Daily Total Radiation r_t	Ratio of Hourly Diffuse Radiation to Daily Diffuse Radiation r_d	Hourly Total Radiation I	Daily Total Radiation H	Hourly Diffuse Radiation I_d	Daily Diffuse Radiation H_d	Day Clearance Angle K_T	Hourly Beam Radiation I_b	Ground Reflectance P_g	Slope β	Ratio of Beam Radiation on Tilted Surface to that on Horizontal Surface R_b	Zenith Angle θ_z	Angle of Incidence θ
Numerical Value	See Eqn 3.4.2.1	See eqn. 3.4.2.2	15.5°	See Table	From Graphs	From Graphs	See Eqn. 3.4.2.4	From Tables	See Eqn 3.4.2.5	From Graphs	From Tables	See Eqn 3.4.2.6	0.2	65°	See Eqn 3.4.2.3	From Graphs	From Graphs
Units							MJ/m^2	$MJ/m^2/Day$	MJ/m^2	MJ/m^2		MJ/m^2					
Hourly Radiation Estimation					12 to 1 O`Clock I_{12-01}	1 to 2 O`Clock I_{01-02}	2 to 3 O`Clock I_{02-03}	3 to 4 O`Clock I_{03-04}	12 to 1 O`Clock I_{T12-01}	1 to 2 O`Clock I_{T12-01}	2 to 3 O`Clock I_{T12-01}	3 to 4 O`Clock I_{T12-01}					
Month	δ	ω_s	K_T	H													
Jan	-21.27	83.80	0.70	20.30	3.2886	3.842	2.194	1.1774	3.8665	3.3608	2.7355	1.1978					
Feb	-13.29	86.24	0.72	23.10	3.6498	3.234	2.541	1.571	3.8287	3.3178	2.7348	1.8542					
March	-2.28	89.37	0.69	24.50	3.969	3.43	2.646	1.421	4.0238	3.4913	2.4995	1.3594					
April	9.41	92.63	0.69	25.90	3.95	3.45	2.7	1.65	3.3066	2.7864	2.1693	1.2954					
May	18.79	95.414	0.65	24.70	4.0508	3.555	2.717	1.5808	3.0098	2.5949	1.8915	1.0426					
June	23.31	96.86	0.62	23.60	4.1536	3.5872	2.596	1.3216	2.8883	2.4895	1.6724	1.2115					
July	21.52	96.28	0.60	23.00	3.0554	2.5933	1.2121	0.7648	3.0515	2.5933	1.2121	0.7648					
August	13.78	93.9	0.61	22.80	4.1602	3.527	2.487	1.7572	3.2676	2.7347	1.9090	0.8724					
September	2.22	90.62	0.64	22.90	3.6084	3.034	2.3977	1.2830	3.6084	3.0304	2.3977	1.2830					
October	-9.60	87.31	0.67	21.90	3.5478	3.066	2.3652	1.2702	3.6113	3.1168	1.9964	1.0516					
November	-19.15	84.47	0.71	21.00	3.318	2.898	2.268	1.386	3.8102	3.495	2.7515	1.7686					
December	-23.24	83.160	0.72	20.10	3.4617	3.5062	2.863	1.8904	3.4617	3.5062	2.8634	1.8905					

$$I_T = I_b R_b + I_d \left(\frac{1 + \cos \beta}{2} \right) + I_g \left(\frac{1 - \cos \beta}{2} \right) \text{-----} \{3.4.2.1\} [1]$$

$$R_b = \frac{\cos \theta}{\cos \theta_z} \text{-----} \{3.4.2.3\}$$

$$r_d = \frac{I_d}{H_d} \text{-----} \{3.4.2.5\}$$

$$\cos \omega_s = -\tan \phi \tan \delta \text{-----} \{3.4.2.2\}$$

$$r_t = \frac{I}{H} \text{-----} \{3.4.2.4\}$$

$$I - I_d = I_b \text{-----} \{3.4.2.6\}$$

Table 3.41 Storage Tank Temperature Variation with Radiation for Evacuated Collector.

Quantity	Number of Collectors	Total Collectors Area A_c	Surface Area of Storage Tank A_s	Mass of Water in the Storage Tank M	Heat Removal Factor F_r	Absorptance-Transmittance Factor $\tau\alpha$	Heat Loss Coefficient Of Storage Tank U_L		
Numerical Value	2	1.62 m ²	4.032 m ²	190 kg	0.9	0.5	0.78		
Remarks	Design	Collector Area = 0.81	Tank Surface Area = 2.016	Each Storage Tank = 95 kg	Design	Design	From Tables (apply a Safety factor of 2)		
	Flow Rate of Hot Water = 35.8kg/hr Load Temperature Return = 80°C				Flow Rate of Hot Water = 26.8kg/hr Load Temperature Return = 80°C				
Month	Storage Tank Temperature at 12 0'Clock T_{s12}	Storage Tank Temperature at 1 0'Clock T_{s01}	Storage Tank Temperature at 2 0'Clock T_{s02}	Storage Tank Temperature at 3 0'Clock T_{s03}	Storage Tank Temperature at 12 0'Clock T_{s12}	Storage Tank Temperature at 1 0'Clock T_{s01}	Storage Tank Temperature at 2 0'Clock T_{s02}	Storage Tank Temperature at 3 0'Clock T_{s03}	Storage Tank Temperature at 3 0'Clock T_{s04}
Jan	88 °C	88.7405	88.8757	88.375	88	88.9932	89.3173	89.0859	87.2733
Feb	88	88.7618	88.9169	88.4679	88	89.0144	89.413	89.1859	88.0922
March	88	89.0604	89.4552	88.7766	88	89.313	89.96	89.5137	87.966
April	88	88.5027	88.4314	87.76	88	88.7553	88.9196	88.4529	87.1548
May	88	88.2812	87.1668	87.37	88	88.5338	88.6477	88.0481	86.6614
June	88	88.1106	87.8273	86.77	88	88.3632	88.3029	87.434	86.2102
July	88	88.1537	87.846	86.194	88	88.4063	88.3229	86.856	85.1232
August	88	88.3736	88.1702	87.1709	88	88.6262	88.5983	87.7971	86.0464
September	88	88.7874	88.8883	88.3443	88	89.4094	89.6983	89.3282	87.572
October	88	88.7828	88.9668	87.9938	88	89.0354	89.4636	88.7085	88.0526
November	88	88.798	89.1755	88.7504	88	89.0514	89.6734	89.4727	88.2982
December	88	88.3547	88.7343	88.4129	88	88.6073	89.2176	89.1086	88.0202

$$T_s^+ = T_{si} + \frac{\Delta t}{2(m_s C_s)} F_r A_c [(\alpha\tau)I(t) - U(T_m - T_a)] + (UA)_s (T_s - T_a) + \dot{m}_l C_l (T_s - T_{l,r})$$

Table 3.42 Estimation of Hourly Radiation on a Sloped Surface from Daily Data for Flat Plate Collector (Constant Values)

Quantity	Declination Angle δ	Latitude ϕ	Sunset Hour Angle ω_s	The Monthly Average Clearance Angle K_T	Average Daily Radiation H(June)	Diffuse Component of Daily Radiation H_D	Tilt Angle β	Ground Diffuse Reflectance Factor P_g
Numerical Value	-23	15.5	83.24	0.72	20.10 MJ/day/m ²	3.892869711	15.5	0.2
Remarks	From Tables	From Tables	$\cos \omega_s = -\tan \phi \tan \delta$	From Tables	From Tables	From Graphs	Design	Constant

Table 3.43 Estimation of Hourly Radiation on a Sloped Surface from Daily Data for Flat Plate Collector *continued*(Time Dependent Variables)

Quantity	Angle of Incidence θ	Zenith Angle θ_z	Geometric Factor R_b	Ratio of hourly Total Radiation to Daily Total r_t	Ratio of hourly Diffuse Radiation to Daily Total r_d	Hourly Radiation I	Hourly Diffuse Radiation I_d	Hourly Beam Radiation I_b	Hourly Radiation On Tilted Ground I_T		
Remarks	From Graphs	From Graphs	$R_b = \frac{\cos \theta}{\cos \theta_z}$	From Graphs	From Graphs	$r_t = \frac{I}{H}$	$r_d = \frac{I_d}{H_d}$	$I_b = I - I_d$	MJ	W	
Time of the Day	7---8	0.35	0.25	1.4	0.03	0.04	0.603	0.1556	0.4474	0.7813	217W
	8---9	0.55	0.45	1.22	0.07	0.078	1.407	0.30342	1.10358	1.649	458W
	9--10	0.725	0.6	1.21	0.106	0.11	2.1306	0.4279	1.7027	2.488	619W
	10-11	0.85	0.725	1.172	0.132	0.13	2.6532	0.5057	2.1475	3.023	840W
	11-12	0.925	0.775	1.194	0.15	0.14	3.015	0.5446	2.4704	3.495	971W
	12--1	0.925	0.775	1.194	0.15	0.14	3.015	0.5446	2.4704	3.495	971W
	1---2	0.85	0.85	1.172	0.132	0.13	2.6532	0.5057	2.1475	3.023	840W
	2---3	0.725	0.6	1.21	0.106	0.11	2.1306	0.4279	1.7027	2.488	691
3---4	0.55	0.45	1.22	0.07	0.078	1.407	0.30342	1.10358	1.649	458	
4---5	0.35	0.25	1.4	0.03	0.04	0.603	0.1556	0.4474	0.7813	217	

Table 3.44 Storage Tank Temperature Variation with Radiation for Flat Plate Collector (June)

Quantity	Specific Heat Capacity of Ammonia Solution C_p	Transmittance –Absorptance Factor $\tau\alpha$	Heat Removal Factor Fr	Overall Heat Transfer Coefficient U_L	Storage Tank Heat Loss Coefficient UA	Tilt Angle β	Average Daily Radiation H	Latitude ϕ
Numerical Value	3540J/KgK	0.55	0.605	8.04 W/m ² K	7.838 W/mk	15.5	20.10 MJ/day/m ²	15.5
Remarks	From Tables	Design	Design	See Table 6.1	From Tables After Applying a Safety Factor of 2	Design	(December) From Tables	From Tables
Quantity	Hourly Radiation On Tilted Ground I_T	Ambient Temperature T_a	Initial Tank Temperature T_s	Final Tank Temperature T_s^+	Initial Tank Temperature T_s	Final Tank Temperature T_s^+	Initial Tank Temperature T_s	Final Tank Temperature T_s^+
Remarks	Table 6.2	From Tables	Storage Tank Mass 45 kg	Storage Tank Mass 15k	Storage Tank Mass 65kg			
Time of the Day	7---8		27	27.8	27	29.6	27	27.6
	8---9	20.9	27.85	32.7	29.6	42.071	27.6	31.03
	9--10	22.7	32.7	39.9	42.071	52.6	31.03	36.49
	10-11	24.7	39.9	47.4	52.6	60.08	36.49	42.63
	11-12	27	47.4	54.8	60.08	67.2	42.63	49.05
	12--1	29.2	54.8	59.8	--	--	--	--
	1---2	30.55	59.8	61.3	--	--	--	--
	2---3	31.7	61.3	60.21	--	--	--	--
3---4	32.3	--	--	--	--	--	--	--

$$T_s^+ = T_s + \frac{\Delta t}{mC_p} [Q_u - (UA)(T_s - T_a)]$$

Chapter 4

4. Construction and Performance Testing

This section describes the construction, assembly and reports the measured performance of the absorption components.

4.1 Construction and Assembly

The components of the experimental unit were constructed at Khartoum University Workshop. After construction, the unit was assembled and tested on the roof of Engineering College at Khartoum University. The following figures (4.1&4.2) show the refrigeration unit after assembly. The piping lines that join the system components together were connected by threaded fittings, and a special pipe binding material for high pressure pipe connection were used. All components, expect few fittings and piping in very limited locations, are made of stainless steel. Electric welding machine and stainless steel welding material were used in fabrication of components. Among the components, generator and absorber experienced some changes from their original designs due to technical and financial limitations. All components fabricated at the University Workshop have been subjected to pressure tests using an air compressor before assembly. Leakages revealed during the pressure tests were treated using cold welding materials.

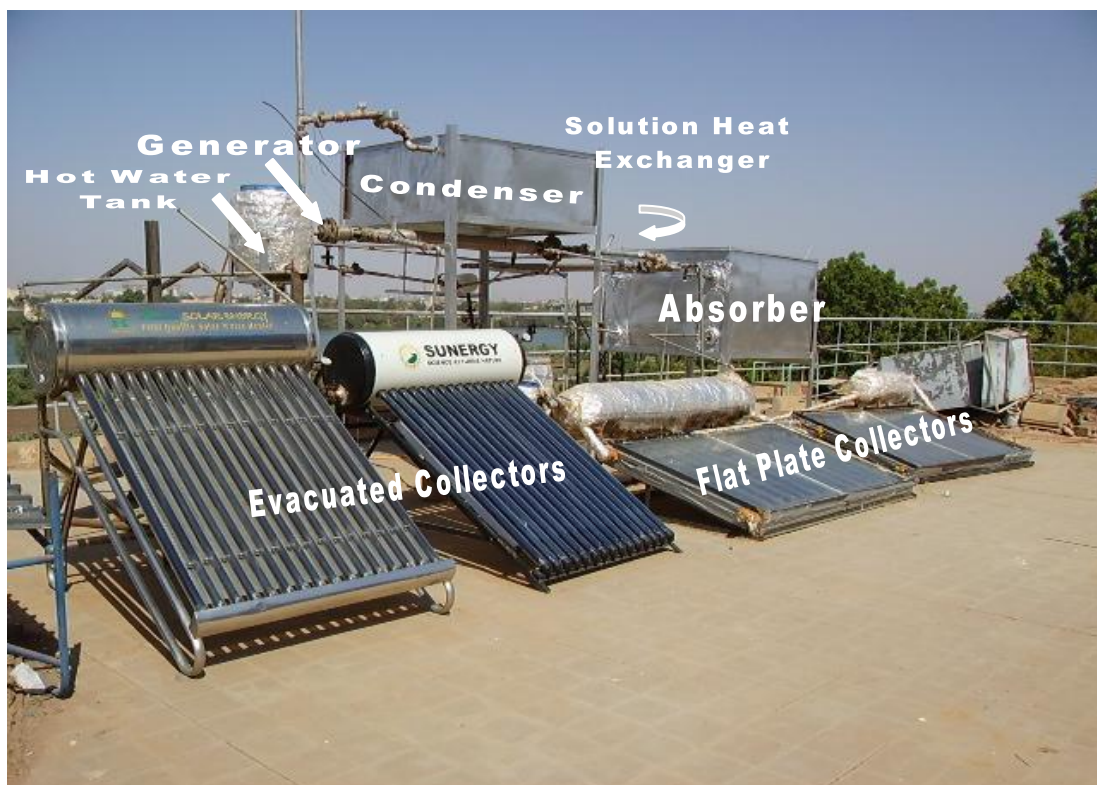


Fig. 4.1 The Absorption Refrigeration Unit after Assembly

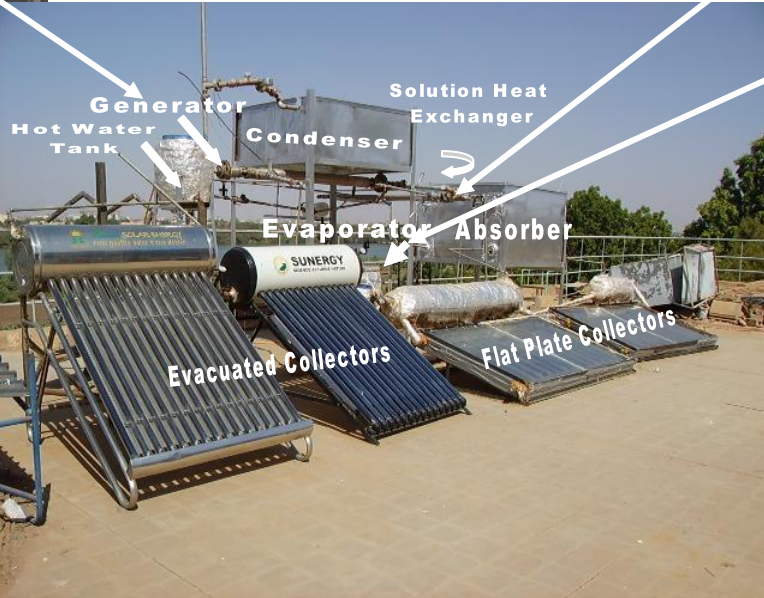
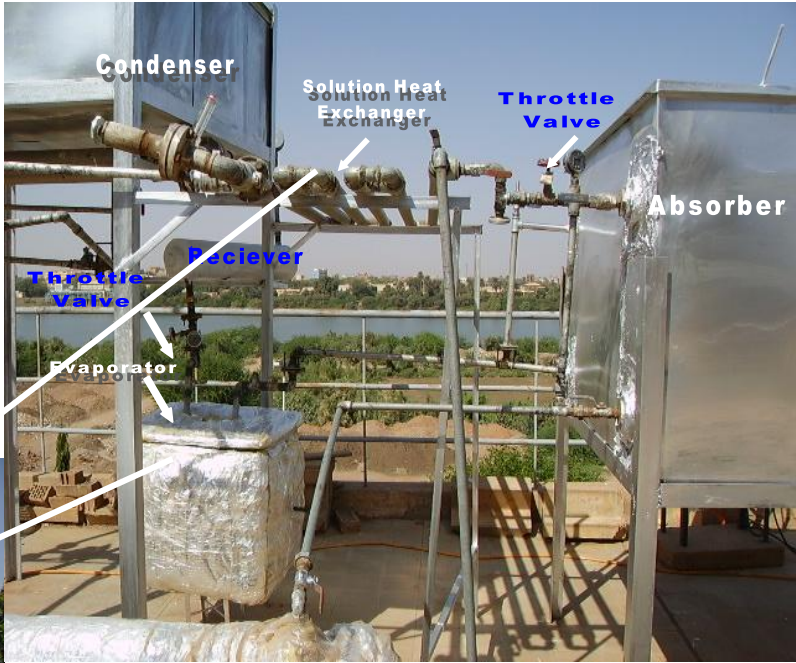
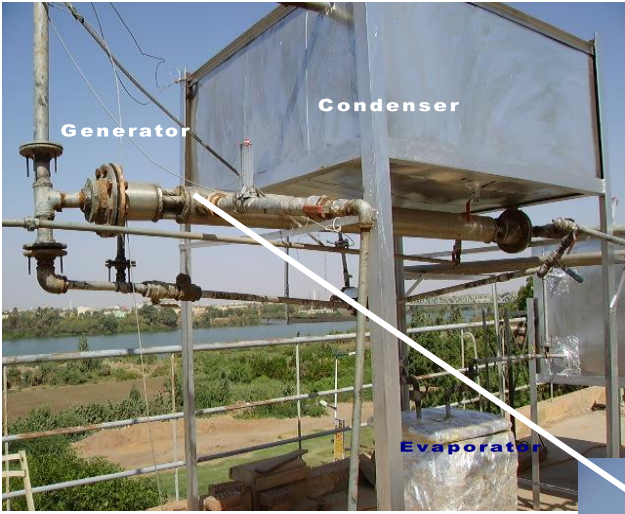
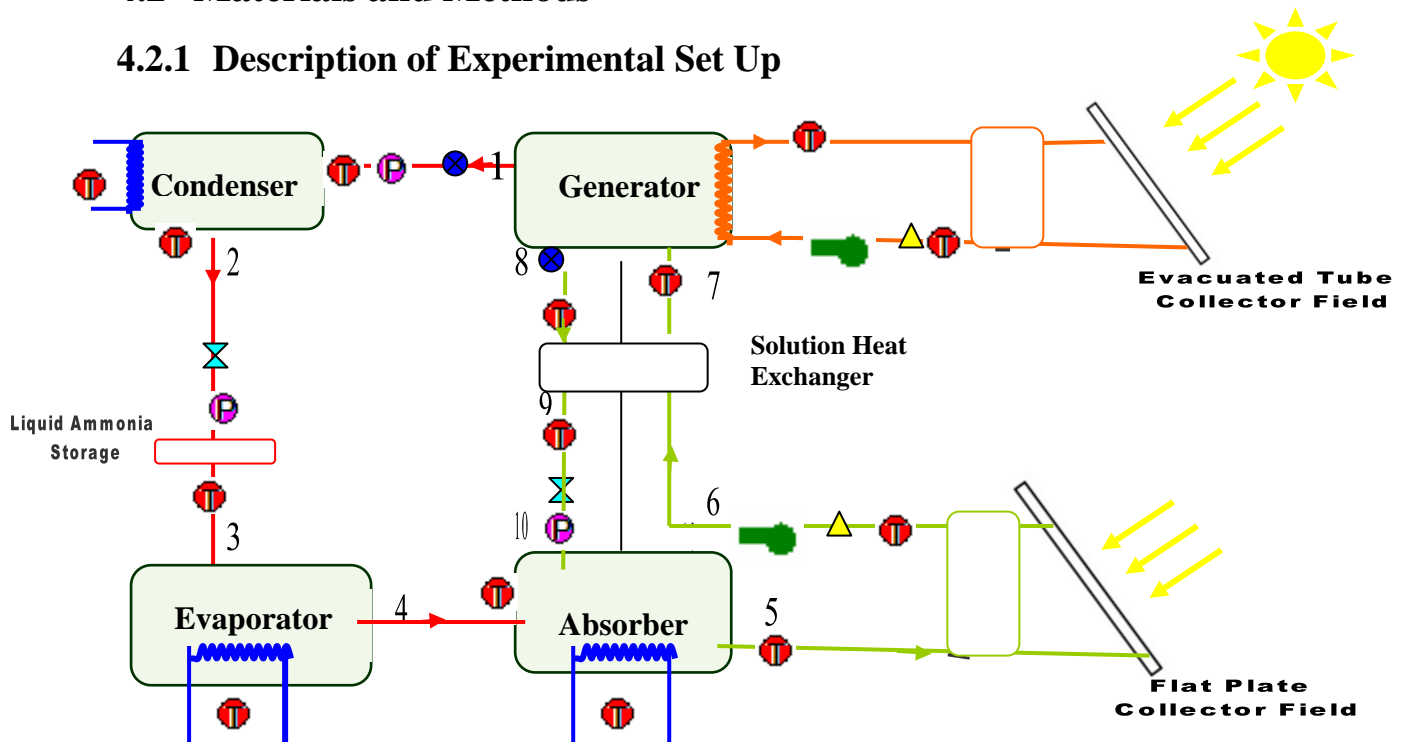


Fig. 4.2 The Absorption Refrigeration Unit After Assembly

4.2 Materials and Methods

4.2.1 Description of Experimental Set Up



	Dial Thermometer		Direction of Flow
	Pressure Gauge		Hot Water Circulation
	Pitot Tube Flow Meter		Ammonia Solution Circulation
	Non-return Valve		Refrigerant Circulation
	Circulation Pump		Cooling Water
1,2,...etc.	State points as described in chapter 3		Solar Radiation

Fig. 4.3 Layout of the Experimental Unit and Positions of Testing Instruments

4.2.1.1 Overall Description of Experimental Unit

Figure 4.3 illustrates the main components of the absorption refrigeration cycle and positions of the measuring instruments. Rich ammonia solution in the storage of the flat collector field is pumped to the generator (7) through the solution heat exchanger, where it is heated by hot water from the evacuated collector field and then the refrigerant in it is boiled off and rise to the condenser. High-pressure liquid refrigerant (2) from the condenser passes into the evaporator (4) through an expansion valve (3) that reduces the pressure of the refrigerant to the low pressure existing in the evaporator. The liquid refrigerant (3) vaporizes in the evaporator by absorbing heat from the material being cooled (water in a tank). The resulting low-pressure vapor (4) passes to the absorber, where it is absorbed by the poor ammonia solution coming from the generator (8). The poor ammonia flows to the absorber, after passing through

a solution heat exchanger (9), and giving off heat to the rich solution coming from the flat plate collector field to the generator. At the absorber a rich ammonia solution is thus formed (5). The rich solution (5) will accumulate in the absorber and ammonia vapor from the evaporator continues to dissolve in the poor ammonia solution even after the unit is shut down after six hours of operations. The next day at sun shine, the rich solution in the absorber is allowed to flow to the storages of the flat plate collector fields, where it starts to gain heat as a result of exposure to solar radiation. When both the evacuated and flat plate collector fields have reached the unit operating temperature, the cycle is powered on and the operation continues for 6 hours. The following figures displays the flow streams in the heat exchangers. Table 4.1 and photos (Fig. 4.4 to 4.9) describe the flow streams directions and the corresponding state points.

Table 4.1 Direction and State of Flow Streams in the Heat Exchangers

→	Ammonia Vapor from generator to condenser	→	Hot water from generator to evacuated collector
→	Liquid Ammonia from condenser	→	Rich ammonia solution from double tube heat exchanger to generator
→	Hot Water from evacuated collector to generator	→	Rich ammonia solution from flat plate collectors to solution heat exchanger
→	Ammonia vapor from evaporator to absorber	→	Strong ammonia solution from absorber to flat plate collector
→	Poor ammonia from generator to solution heat exchanger	→	Poor Ammonia solution from solution heat exchanger to absorber



Fig.4.4 Flow of Rich Ammonia from Absorber to Flat Plate Collectors (greater storage capacity) at sun shine.

Fig. 4.5 Flow of Rich Ammonia Solution to Flat Plate Collector (smaller storage capacity) at Sunshine.



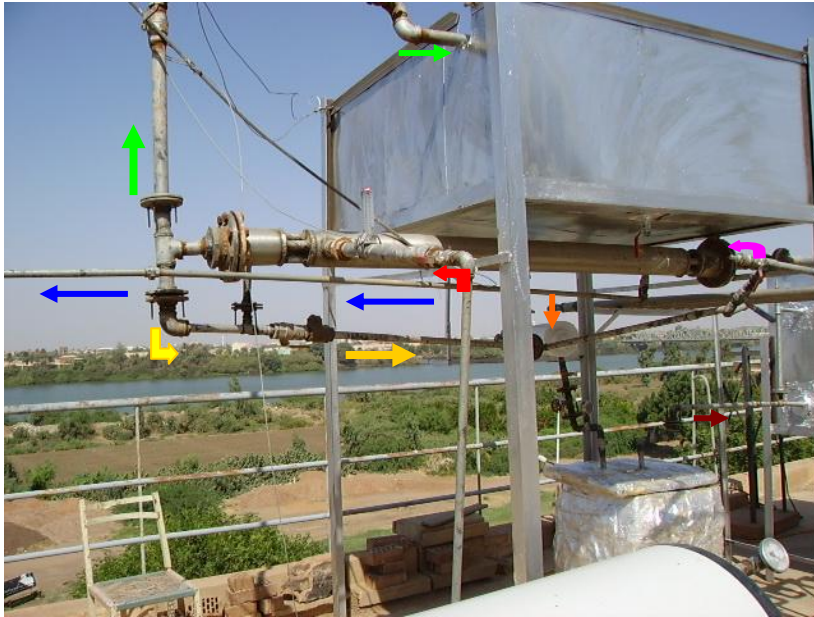


Fig.4.6 Flow of Poor Ammonia Solution , Ammonia Vapor and Hot Water(from evacuated collectors) to and from Generator.



Fig. 4.7 Flow of Rich & Poor Ammonia Solutions to and from Solution Heat Exchanger and Absorber.



Fig.4.8 Circulation of Hot Water from Evacuated Collector to Generator and back to Collector.



Fig.4.9 Flow of Rich Ammonia Solution From Absorber to Flat Plate Collectors

4.2.1.2 Measuring Instruments

The positions of the instruments used in testing of the absorption unit are shown in figure 4.3, and instruments are shown in figure 4.10 , all measuring instruments are inserted in the pipe lines except the digital thermometers are inserted in evaporator and absorber water tanks:



Fig. 4.10 Measuring Instruments of the Experimental Unit

4.2.1.3 Detailed Description of the Test Components

(i) Generator

The generator is the main component of this absorption unit, in which rich ammonia solution is heated until ammonia vapor is driven off to the condenser. A shell and tube heat exchanger has been designed and constructed to undertake the generation process. The tube bundle (see Fig.4.13) consists of 5 Stainless tubes (3/4"OD) and 25 baffles (see Fig. 4.11). The generator has double tube sheets so that any leaks can be detected immediately. The tube sheets(6mm thickness) are made of stainless steel round plates(see Fig.4.12). The rich ammonia flows in the tubes and the hot water flows in the shell (see Fig.14). *Note: Section 3.3 contains more details about heat exchangers specifications.*

(ii) Condenser and Receiver

In the condenser, the ammonia vapor coming from the generator is condensed into liquid by cooling water in a tank(Fig16). The condenser coil(see Fig.4.15) is made up of stainless steel pipe 13 m long (1.25"OD). After condensation the ammonia liquid passes to the receiver(see Fig.4.17) m long ("OD).

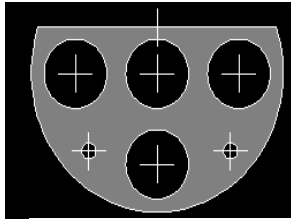


Fig. 4.11 Baffles

Fig. 4.12 Tube Sheet

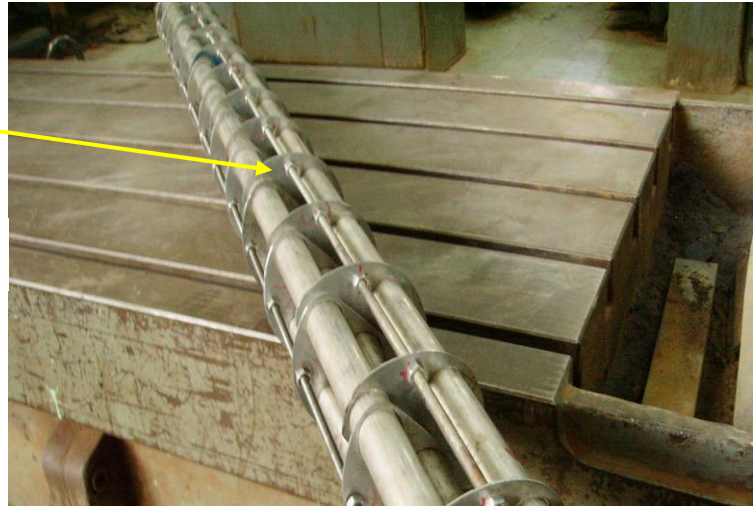
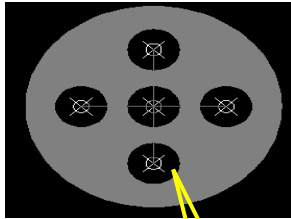


Fig. 4.13 Tube Bundle



Fig. 4.14 Shell and Tube Heat Exchanger

Condenser Coil



Fig.4.15 Condenser Coil in Tank

Condenser Cooling Water Tank



Fig.4.16 Water Tank

Ammonia Liquid Receiver



Fig. 4.17 Ammonia Receiver

(iii) Evaporator

In the evaporator the liquid ammonia expands through a throttle valve(see Fig.4.18) changing from liquid to vapor , in doing so it removes heat from the water tank (see. Fig.4.18). The evaporator coil(see Fig.4.19) is made of a stainless steel U shape pipe (0.75"OD).



Fig.4.18 Evaporator coil in the insulated water Tank

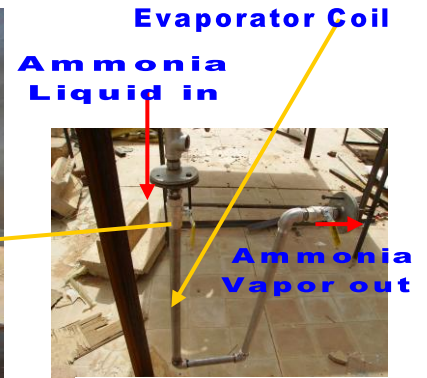


Fig.4.19 Evaporator coil

(iv) Solution Heat Exchanger

The solution heat exchanger preheats the rich ammonia solution flowing to the generator by cooling the weak ammonia solution exiting it. This heat exchanger reduces the generator heat duty requirement by preheating the rich ammonia solution, and the absorber heat duty by reducing the poor ammonia solution temperature entering the absorber. A Double tube exchanger is used as the solution heat exchanger(see Fig4.20). The rich ammonia solution flow in the inner tube(1"OD) and the weak ammonia solution flows in the outer tube(1.5"OD).

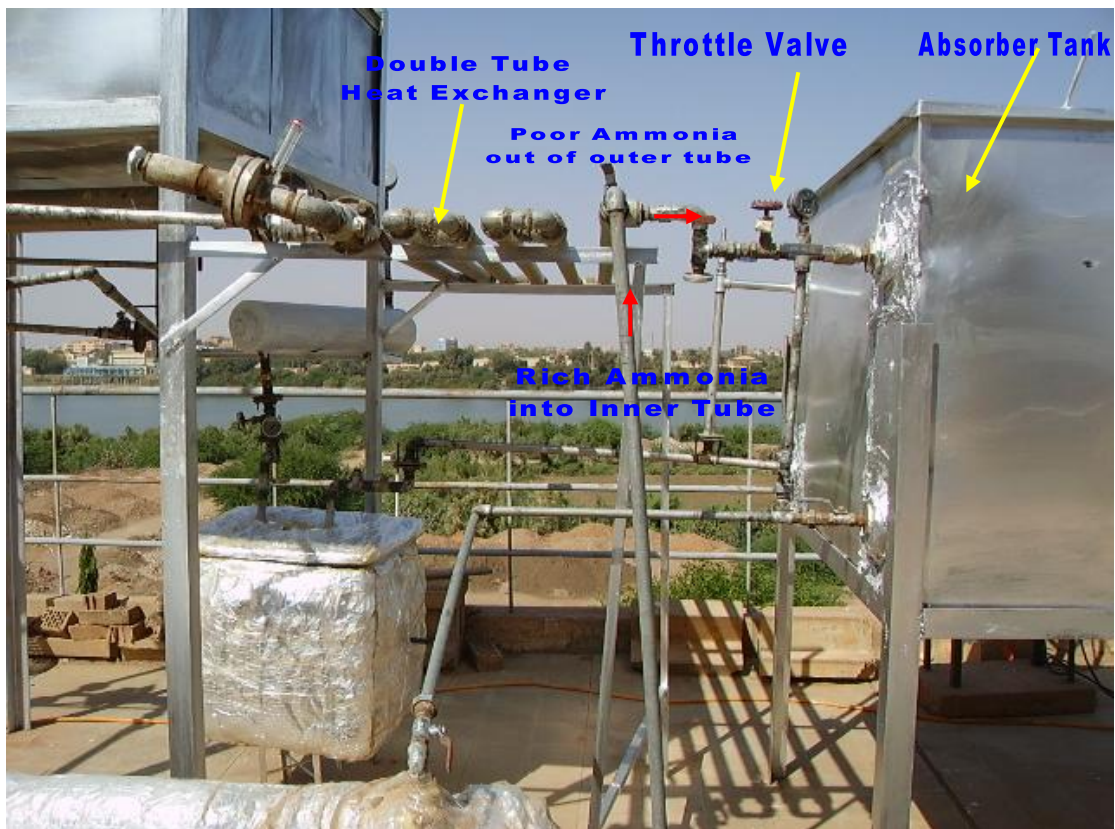


Fig. 4.20 Solution Heat Exchanger

(v) **Absorber**

In the absorber ammonia vapor flowing from the evaporator is absorbed by the poor solution from the generator, rejecting its heat to cold stagnant water in a tank(see Fig.4.21). A header-riser tube arrangement is used as an absorber (see Fig.4.21 –a). It consists of two rows (upper & lower) of tubes (4"OD). Poor ammonia solution flows from the solution heat exchanger to the header of the upper row(see Fig.4.21-a)and then flows by gravity to the tubes of lower rows. Ammonia vapor from the evaporator enters the header of the upper and lower rows simultaneously through nozzles fixed to tubes (see Fig.4.21-c). The nozzles distribute the ammonia equally among the risers (see Fig.4.21-b) of the absorber. Then the rich ammonia solution flows to the flat plate collectors through opening in the lower header of the absorber. Stream Flows to and from the absorber are shown in figure. 4.22.

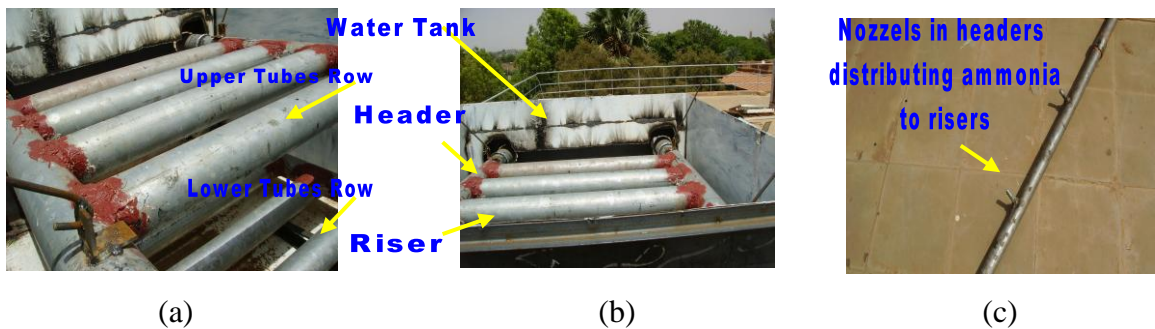


Fig. 4.21 Absorber

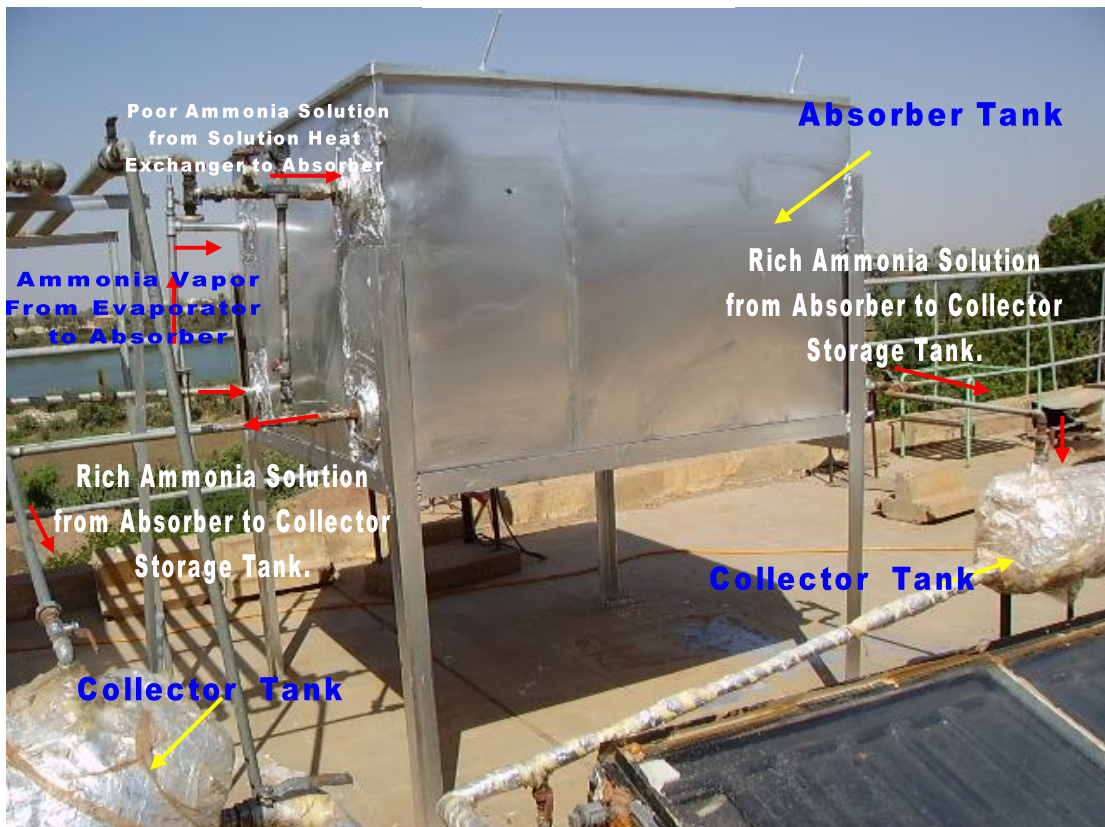


Fig. 4.22 Stream Flows in the Absorber

(vi) Flat Plate Collectors

In the flat plate collectors field (solar warm up cycle), the rich ammonia, after being discharged from the absorber at sunshine, would be left to warm up in the collectors before the system operation. The flat plate collector field is riser-header type and consists of two (2×1m) collectors. Each collector consists of single-glazed absorber plate coated with dull-black commercial paint. The flat-plate absorber was inclined at 15° to the horizontal and facing due south (latitude of Khartoum=15°). It was made from 2.7 mm thick iron sheet and has 14 tubes (each 1m long (1.25"OD). The absorber plate is encased in a metallic box insulated by 5cm thick fiber wool on the bottom and sides. One collector has 110 liter capacity storage tank (see Fig. 4.23), while the other has 36 (see Fig. 4.24) liter storage capacity. The storage tanks are insulated and fitted with insulated pipeline connections for the circulation of the working fluid from the collector to the solution heat exchanger, and back from the absorber to the collectors. A pump (see Fig.4.25) is used to drive the rich ammonia solution from the collectors to the solution heat exchanger. The ammonia solution will be withdrawn from the collector with smaller capacity (36 liter) first and then from the collector with bigger (110 liter), since it would have higher temperature due to the less quantity of ammonia solution.

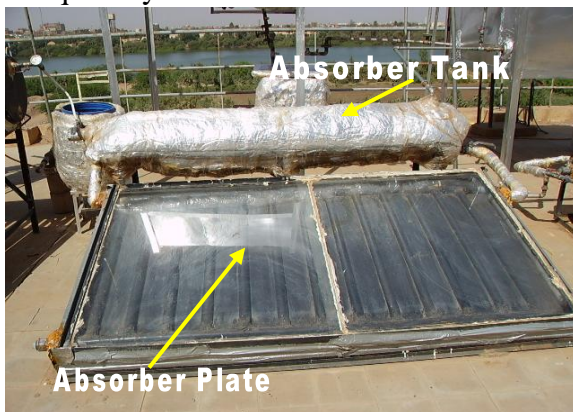


Fig. 4.23 Flat Plate Collector 110 Liter Storage

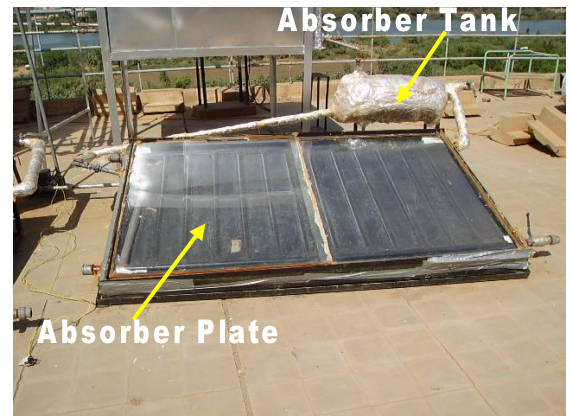


Fig.4.24 Flat Plate Collector 36 liter Storage



Fig. 4.25 Rich Solution Pump

(vii) **Evacuated Tube Collectors.**

In order to evaporate ammonia from the rich ammonia solution flowing in the generator, hot water in the range of 80-88 °C is passed through the shell of the generator in a counter current flow. The hot water comes from the evacuated tube field (Dewar Flask type) which consists of two collectors with storage capacity of 90 liter each. The maximum operating temperature of the collector is 100°C. The two collectors are connected in series (parallel connection is possible too). The hot water flowing out of the generator discharges to a upper hot water tank (see Fig.4.26). Then the hot water flows by gravity from the tank to the evacuated collector 1, then from the evacuated collector 1 to evacuated collector 2. Next it flows by gravity to the lower storage tank (see Fig.4.26). From there it is pumped up to the generator shell by hot water circulation pump (see Fig.4.27) and then to the hot water tank.

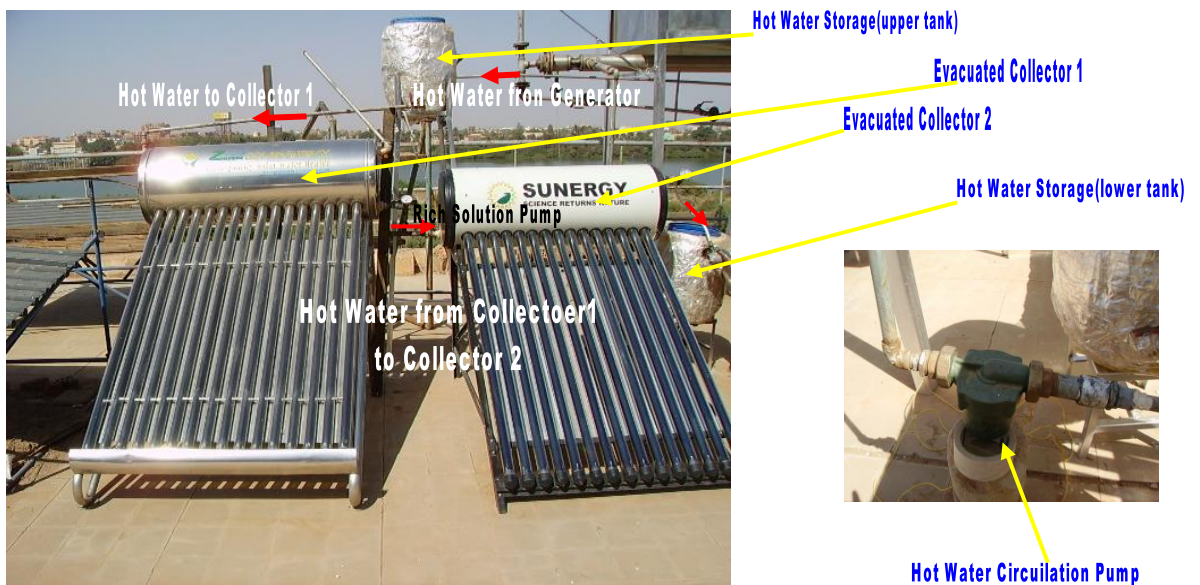


Fig.4.26 Evacuated Collector Field



Fig. 4.27 Hot Water Pumping from Storage to Generator

4.2.2 Test Procedure and Result

4.2.2.1 Initial Observed Operation of the System Components

(i) Evacuated Collector Test

Pre-design performance test was conducted on the evacuated collector which had been purchased from local market. The test objective was to study the variation of temperature of the storage tank through the day under no load conditions. The test result was used to predict the long term performance and to decide the number of collectors needed to operate the system(see Table 4.2 and Fig.4.28).

Table 4.2 No Load Test Result of Evacuated Collector

Time	Ambient Temperature (°C)	Outlet Water Temperature(°C)	Date:
9:00	28.5	73	5/4/2005
10:00	29	72	
11:00	30.1	72	
12:00	32.4	80	Weather Condition: Wind &Dust
1:00	35.2	81.2	
2:00	35.7	89	
3:00	37.8	91	
4:00	37.5	93.3	

Time	Ambient Temperature (°C)	Outlet Water Temperature(°C)	Date:
9:00	31.7	75	10/4/2005
10:00	32.9	76.9	
11:00	36.0	82.7	
12:00	38.0	86.7	Weather Condition: Sunny
1:00	37.5	90.4	
2:00	39.5	93.4	
3:00	41.7	96.5	
4:00	43.1	98	

Time	Ambient Temperature (°C)	Outlet Water Temperature(°C)	Date:
9:00	25.4	77.4	19/4/2005
10:00	27.4	76.4	
11:00	29.8	72.4	
12:00	32	83	Weather Condition: Sunny
1:00	33	85	
2:00	32.8	90	
3:00	34	95	
4:00	34.6	98.6	

Time	Ambient Temperature (°C)	Outlet Water Temperature(°C)	Date:
9:00	33.2	75	24/4/2005
10:00	31.8	75.4	
11:00	29	76	
12:00	28.7	79.9	Weather Condition: Cloudy
1:00	42.2	80.4	
2:00	34.3	83.5	
3:00	33.3	85	
4:00	41	85	

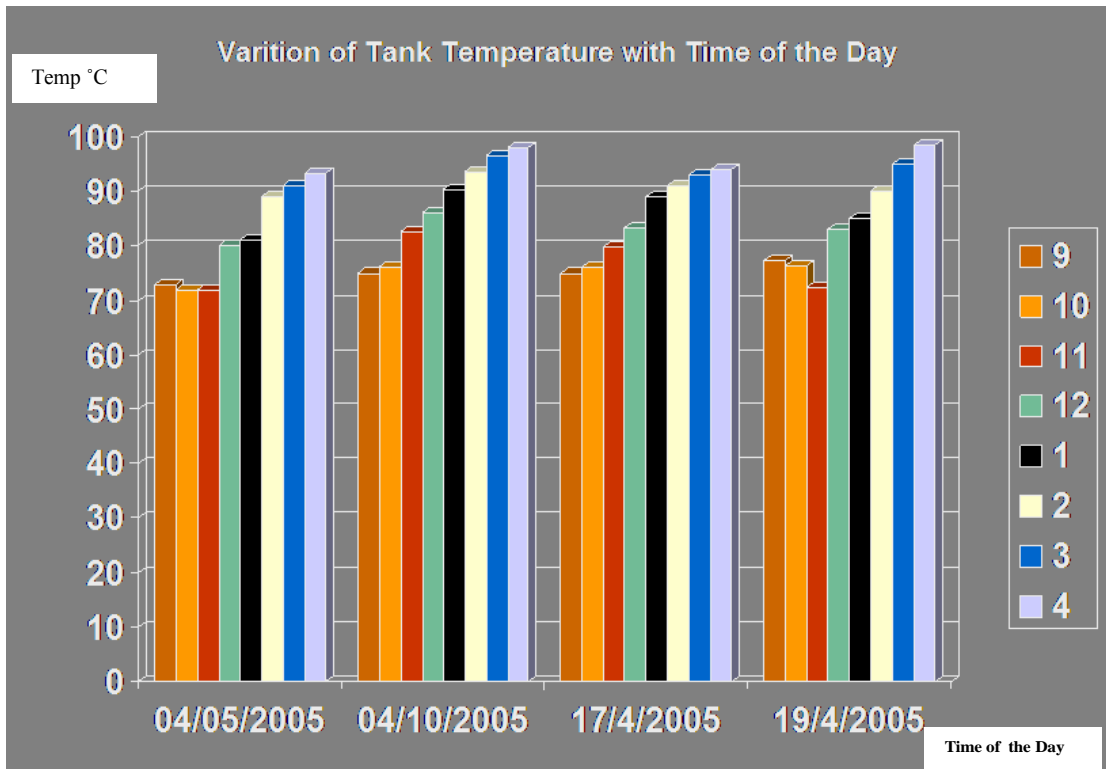


Fig.4.28 Variation of Tank Temperature with Time Under No-Load Condition

(ii) Flat Plate Collector Test

The performance of flat plate solar collectors field (the preheating solar components) was observed (from December to March) and it was found that:

- The flat plate collector with 36 liter capacity recorded 100° C temperature at 3 0'clock (time for maximum yield for systems with storage) and the designed temperature was 67°C with 15 liters.
- The flat plate collector with 110 liter capacity recorded a temperature of 80° at 3 0'clock and the designed temperature was 60 °C with 65 litre capacity

(iii) Testing of the Experimental Unit.

After assembly of the experimental setup , tests had been conducted using compressed air to detect leakages and water to test the proper functioning of pumps. .

4.2.2.2 Test Procedure of Experimental Unit and Result

It was decided to carry out experiments on the heat exchangers of the prototype and the solar collector fields individually , so the absorption machine will be used as a test bank to validate the design procedure and to evaluate the impact of the system components performance on the overall performance of the absorption machine. The arrangement of components of the experimental setup was relatively flexible and some minor modifications had to be applied to carry out experiments on the different

components separately. These special arrangements would be described for each component separately. The main characteristics of the different cases under study are shown in Table 4.3 below. The suggested test procedure for each component and result obtained would be presented in the following sections.

Table 4.3 Overview of Cases under Study.

Cases under Study	Parameters Tested	Components under Study			
		Shell and Tube Heat Exchanger	Double Tube Heat Exchanger	Flat Plate Collector Field	Evacuated Collector Field
Case 1	Optimum Flow Rate	×	×		×
Case 2	Compliance with Designed Temperature range	×	×	×	×
Case 3	Efficiency			×	
Case 4	Ability to meet Designed Load	×	×	×	×
Case 5	Effect on Overall System Performance	×	×	×	×

(i) Testing of the Shell and Tube Heat Exchanger

Experimental Set up: Experiments were conducted on the shell and tube heat exchanger described in section 4.2.1.3(i) above. Hot water was supplied by the evacuated collector field (see Fig.4.27) and colder water was supplied by the flat plate collector with 110 liter capacity (see Fig.4.23)

Experimental Procedure:

The solution pump (see Fig.4.25 above) delivered water from the flat plate collector to the heat exchanger tube bundle , while the hot water circulation pump(see Fig.4.27 above) delivered hot water from the evacuated collector field to the shell of the heat exchanger. It was waited until the steady state had been reached. At steady state, all the four temperatures and flow rates of cold and hot fluid do not change. The readings recorded are shown below (see Table 4.4).

Operational Problems and Special Arrangements:

- Dial thermometers malfunction occurred in 4 of the measuring points, so a portable digital thermometer was used to measure temperatures at those positions.
- The flow meter inserted between the flat plate collector field and the tank was damaged, and a measuring jar and stop watch was used to measure the flow rate from a discharge valve.

- The flow of water from the flat plate collector could not be adjusted due to inability of the pump to deliver liquid at the designed flow rate, so the solution pump in figure 4.25 was replaced by a hot water circulation pump similar to the evacuated collector field pump (see Fig. 4.27)
- A portable submersible pump was used to supply water at ambient temperature (37-39) since the flat plate collector could not deliver water at this temperature.
- According to the previous arrangement, an additional valve was inserted in the delivery line of the solution pump so as to supply the shell and tube heat exchanger with hot water from the flat plate collector field (without passing through the double tube heat exchanger). A flexible tube was used to connect this valve to a side valve that led the flow to the inner tube bundle (see Fig.4.30) A flexible tube was connected to the discharge line of the tube bundle so as to redirect flow to the flat plate collector storage tank (see Fig.3.29) instead of the outer tube of the double heat exchanger.

Note: the first four above arrangements were also applied in the following test.

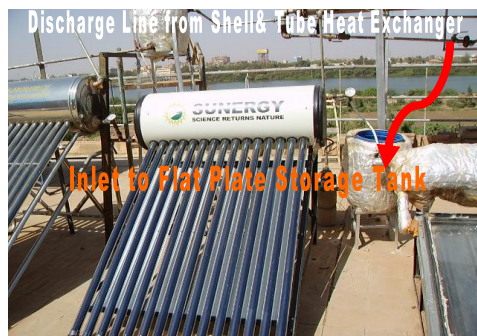


Fig. 4.29 Connection of Tube Bundle Discharge Line to Flat Plate Collector.

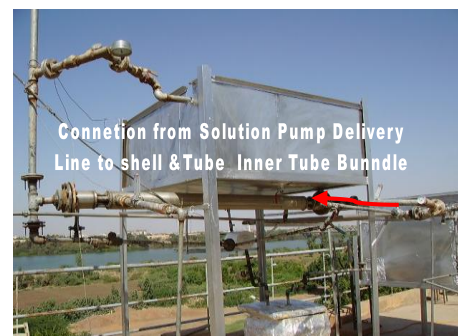


Fig. 4.30 Connection of Solution Pump Delivery Line to Tube Bundle

Table 4.4 Hot Water –Water Test Result of Shell and Tube Heat Exchanger

Date of Experiment	Volumetric Flow Rate of Hot Water (lpm)	Volumetric Flow Rate of Cold Water (lpm)	Fluid Temperatures (°C)			
			Cold Fluid Inlet	Cold Fluid Outlet	Hot Fluid Inlet	Hot Fluid Outlet
23/7/2009	0.5/3	0.5	51	59	66	62
23/7/2009	4	1.6	50	55	67	48
27/7/2009	2	0.67	45	52	64	59
13/8/2009	0.63	0.74	38	46	60	50
18/8/2009	0.4	0.55	39	50	71	54
19/8/2009	1.36	0.5	58	57	65	61

(ii) Testing of Double Tube Heat Exchanger

Experimental Set up: Experiments were conducted on the Double Tube Heat Exchanger described in section 4.2.1.3(iv) above. Hot water was supplied by the evacuated collector field (see Fig.4.27) and colder water was supplied by the flat plate collector with 110 liter capacity (see Fig.4.23)

Experimental Procedure:

The solution pump (see Fig.4.25) delivered water from the flat plate collector to the heat exchanger inner tube, while the hot water circulation pump(see Fig.4.27) delivered hot water from the evacuated collector field to the outer tube of the heat exchanger. It was waited until the steady state had been reached.. The readings recorded are shown (see Table 4.5).

Operational Problems and Special Arrangements:

- The first four special arrangement in section 4.2.2.2.(i) above were applied in addition to the following arrangements.
- In the original experimental set up the inner tube of the double tube heat exchanger admitted fluid flow from flat plate collector and discharge it to the generator. In the modified experimental set up the flow from the inner tube of the double heat exchanger was directed to discharge in the flat plate collector(see Fig 4.32).
- A flexible tube was made to connect the hot pump delivery line to the inlet of outer tube of the double heat exchanger (see Fig.4.31). In this way the evacuated collector field can supply double tube heat exchanger in addition to the shell and tube heat exchanger. Then the fluid coming out of the outlet of the outer tube, would flow to the evacuated collector (see Fig.4.33)

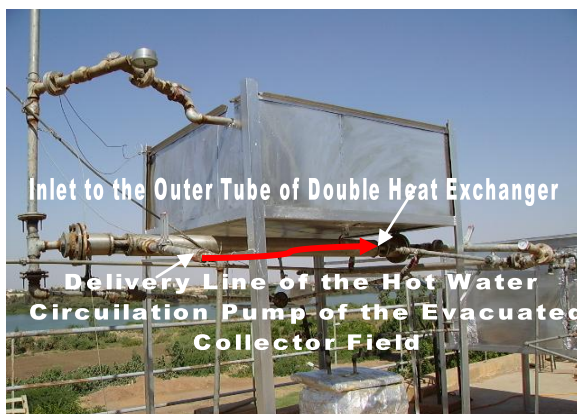


Fig. 4.31 Connection of Evacuated Collector Field to Outer Tube Double Tube Heat Exchanger.



Fig. 4.32 Connection of Outlet of Inner Tube of Double Heat Exchanger to Flat Plate Collector



Fig. 4.33 Connection of Outlet Tube of Double Heat Exchanger to Evacuated Collector

Table 4.5 Hot Water –Water Test Result of Double Tube Heat Exchanger

Day of the Experiment	Volumetric Flow Rate of Hot Water (lpm)	Volumetric Flow Rate of Cold Water (lpm)	Fluid Temperatures (°C)			
			Cold Fluid Inlet	Cold Fluid Outlet	Hot Fluid Inlet	Hot Fluid Outlet
23/7/2009	0.57	0.9	51	57	66	51
26/7/2009	1.8	2.4	50	54	67	56
27/7/2009	1.5	2.7	45	49	64	45
10/8/2009	3.3	2.5	34	55	72	59
10/8/2009	2.5	0.8	37	50	64	58
19/8/2009	0.625	0.7	38	46	60	50
29/7/2009	0.6	0.7	47	57	71	49
13/8/2009	0.55	0.6	38	55	69	41
13/8/2009	0.625	0.5	38	50	61	42
18/8/2009	0.65	0.41	37	59	71	42
19/8/2009	0.5	0.65	58	58	65	55.6

(iii) Testing of Flat Plate Collector

a) Test of Absorber Plate of Flat Plate Collector

Experimental Set up: Experiments were conducted on the flat plate collector (with 36 liter capacity) described in section 4.2.1.3(vi) above. The storage tank was isolated from the absorber plate (see Fig. 4.34). Stream flows in and out of the collector absorber plate are shown in figure 4.34. Water was supplied from the lower hot water storage tank of the evacuated collector field and passed through flexible tubes to the inlet of the lower header of the absorber plate (see Fig. 4.35).

Experimental Procedure: The standard procedure for collector testing is to operate the collector under conditions in which operation is nearly steady i.e. the

radiation and other conditions are essentially constant for a time long enough for the outlet temperature and useful gain to become steady. In order to achieve the above conditions water at a constant temperature was supplied to the collector absorber plate at constant flow rate temperature . Tests were made with a range of inlet temperature conditions. To minimize effects of heat capacity of collectors, tests are usually made in nearly symmetrical pairs, one before and one after solar noon, with results of pairs averaged. Instantaneous efficiencies are determined from $\eta_i = \dot{m}C_p(T_o - T_i)/A_c G_T$ for the averaged pairs. The flow rate of water at outlet of the collector was measured using a stop watch and a measuring cylinder. A digital thermometer was used to measure the inlet and outlet temperature (see Table 4.6).

Operational Problems and Special Arrangements:

- In order to obtain different inlet temperatures at constant flow rate, the lower hot water tank of the evacuated field was used to supply water at different inlet temperatures (see Fig.4.35). That was accomplished by mixing water at ambient temperature with hot water from the collector field inside the tank. Then the mixed water would delivered to the collector absorber plate through the hot water circulation pump (see Fig.4.35).

Table 4.6 Efficiency Test of Flat Plate Collector

Time of the Day	Ambient Temperature	Radiation	Flow Rate	Inlet and Outlet Heat Transfer Fluid Temperature °C	
	°C T _a	W/m ² G	\dot{m}	T _i	T _o
1:00	33	709	2liters/min	40	50
1:20	37			47	53
1:30		785			
1:35	37			54	59
2:00		739			



Fig. 4.34 Inlet and Outlet flow through the Collector Plate



Fig. 4.35 Mixing of Hot Water with cold Water to Obtain Water with Different Temperature

Water Delivered by Circulation Pump to Inlet of The Lower Header of the Absorber Plate

Water at Different Temperatures from Lower Tank of Evacuated Collector to Absorber Plate of the Flat Plate Collector.

Hot Water Circulation Pump

b) Observation of Storage Tank Variation

Experimental Set up and Procedure: The storage tank temperature variation with weather conditions of the collector field described in section 4.2.1.3.(vi) was observed at different times of the year and result is shown in Table 4.7

Table 4.7 Variation of Tank Temperature with Weather Conditions of Flat Plate Collectors

Experimental Device		Temperature(°C) at Different Times of the Day												Date		
		10:00	10:30	11:00	11:30	12:00	12:30	1:00	1:30	2:00	2:30	3:00	3:30		4:00	4:30
Collector Tank with 150 liter Storage Tank	Test no.1	34		46		48		63		72						
	Test no.2	65		67		70 ¹		70		68						17/8/2009
	Test no.3		50		58		62		70		76		78		78	March
	Test no.4	44		47		56		60		66		68				2/8/2009
	Test no.5	56		58		64		70								5/8/2009
	Test no.6	42		44		52		58								
Collect or with 36	Test no.1	38		38		42		96		100						
Absorber Plate without Storage Tank	Test no.1	41		58		81		89		97		100				2/8/2009
	Test no.1		51		66		81		87							5/8/2009

(iv) Testing of Evacuated Collector Field

a) Effect of Hot Water Withdrawal on Storage Tank Temperature

Experimental Set up: Experiments were conducted on the evacuated collector field which consists of two collectors connected in series(parallel connection is also possible). The stream flows in and out of the collectors field are described in figure 4.26 &4.27 above. Hot Water from the shell and tube heat exchanger enters the upper storage tank and flows by gravity to collector 1, through collector 2 and finally discharges through the upper tank port of collector 2 to the lower storage tank (see Fig.4.26 &4.27).

Experimental Procedure: To study the effect of hot water withdrawal rate on the collector field average delivery temperature, hot water was withdrawn at a fixed flow rate from the collector field to supply the load of shell and tube heat exchanger and then returned back the collector through the upper storage tank. The flow rate and return tank temperature were measured at the inlet of the upper storage tank, while the

outlet temperature of the field was measured at the inlet of the lower storage tank. Ambient temperature and general weather conditions were also recorded (see Table 4.8)

Table 4.8 Effect of Hot Water Withdrawal on Storage Tank Temperature of Evacuated Collector.

Date: 17/8/2009	17/8/2009 Time	Evacuated Collector Tank Temperature	Ambient Temperature °C	Temperature of Water Inlet to Tank of Evacuated
Before Hot Water Withdrawal	10:00	81	39	
	11:00	82	38	
	12:00	85	40	
Start of Hot Water of 0.5L/min Flow Rate	1:00)	88	32	45
	2:00	87	39.6	55
	3:00	86	41	48
	4:00	84	42	49

b) Observation of Storage Tank Variation

Experimental Set up and Procedure: The storage tank temperature variation with weather conditions of the collector field described in section 4.2.1.3.(vii) was observed at different times of the year and result is shown in Table. 4.9

Table 4.9 Variation of Tank Temperature with Weather Conditions of Evacuated Collector

Experimental Device		Temperature(°C) at Different Times of the Day												Date		
		10:00	10:30	11:00	11:30	12:00	12:30	1:00	1:30	2:00	2: 30	3:00	3:30		4:00	4:30
Evacuated Collector Tank Storage Tank	Test no.1	81		82		85		88								17/8/ 2009
	Test no.2		55		65		72		79		80		81		83	March
	Test no.3	75		79		80		84		85						2/8/ 2009
	Test no.4	70		73		77		81								5/8/ 2009
	Test no.5	72		72		75		77								5/8 /2009

4.3 Analysis of Result

Several tests have been carried out on the absorption machine components in order to investigate a range of operating conditions. The experimental data has been compared with the design parameters. The conclusions reported will lead to the future revisions of design and improvements to be implemented in order to achieve a better performance and reliability.

4.3.1 Shell and Tube Heat Exchanger

Operating parameters under investigation are:

- Energy delivered or gained by flow streams
- Temperature ranges
- Flow Rates
- Heat Transfer Coefficient

Table 4.10 & 4.11 below shows the test result of the shell and tube heat exchanger and the designed operating parameters respectively.

Table 4.10 Experimental Data of Shell and Tube Heat Exchanger

Flow Rate of Hot Water (lpm)	Flow Rate of Cold Water (lpm)	Cold Water Inlet Temperature (°C)	Cold Water Outlet Temperature (°C)	Hot Water Inlet Temperature (°C)	Hot Water Outlet Temperature (°C)	Log Mean Temperature Difference	Heat Energy Lost By Hot Stream (Kw)	Heat Energy Gained By Cold Stream (Kw)	Heat Transfer Coefficient (W/m ² k)
2	0.67	45	52	64	59	12.97	0.704	0.330	48.83
0.63	0.74	38	46	60	50	12.97	0.443	0.416	61.64
0.4	0.55	39	50	71	54	17.82	0.4789	0.426	45.83

Table 4.11 Designed Operating Parameters of Shell and Tube Heat Exchanger

Flow Rate of Hot Stream (lpm)	Flow Rate of Cold Stream (lpm)	Cold Stream Inlet Temperature (°C)	Cold Stream Outlet Temperature (°C)	Hot Stream Inlet Temperature (°C)	Hot Stream Outlet Temperature (°C)	Log Mean Temperature Difference	Heat Energy Lost By Hot Stream (Kw)	Heat Energy Gained By Cold Stream (Kw)	Heat Transfer Coefficient (W/m ² k)
0.5964	0.396	72 °C	83C	88 °C	80 °C	6.382	0.3328 KW	0.3328 KW	130

4.3.1.1 Energy Gain and Loss between Cold and Hot Streams

Referring to table 4.10 above there is a difference between the heat gained by cold stream and heat lost by hot stream which shows that there is heat loss to the surrounding (see Fig.4.36). This difference between heat gained and loss means that

the insulation was insufficient and more insulating material is needed to isolate the shell and the connecting pipes from surroundings.

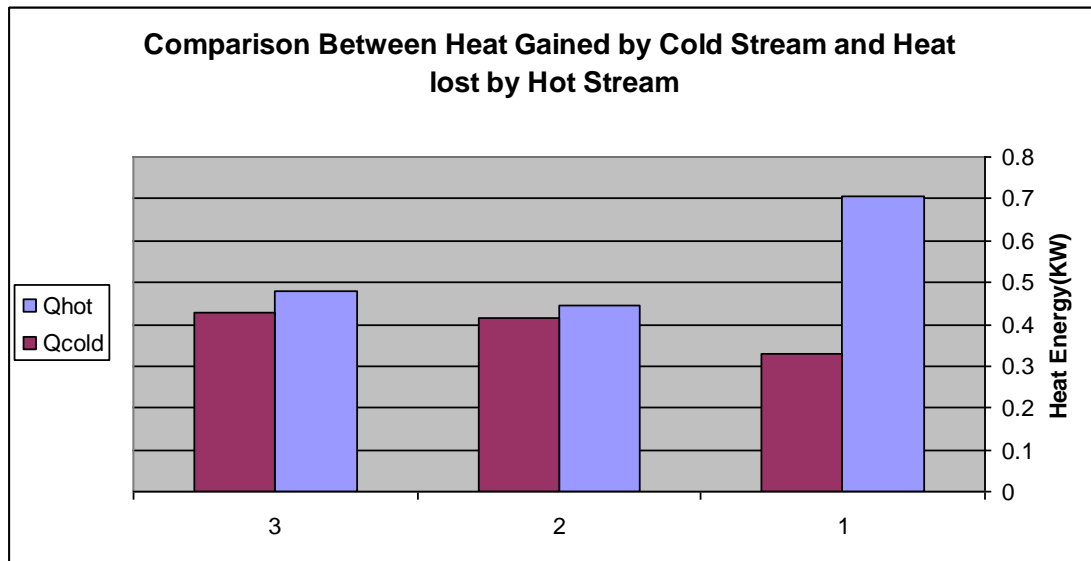


Fig. 4.36 Heat Gain and Loss by Cold and Hot Streams in Shell & Tube Heat Exchanger

4.3.1.2 Temperature Ranges

The test was conducted in July and August and weather was always cloudy. Due to the almost permanent cloud cover and heat losses in piping and lower storage tank of the evacuated collector field (see Fig. 4.26), the evacuated collector failed to attain the designed operating conditions during the above mentioned testing period. The shell & tube heat exchanger was supplied by a hot stream of lower temperature. That necessitated the use of cold water of lower temperature (ambient temperature) so as to test the ability of the heat exchanger to provide the rise in temperature required in the cold stream.

Referring to table 4.10 (2nd and 3rd rows), it appears that the heat exchanger can deliver the required heat capacity at the designed flow rate (*approximately*) only at a minimum log mean temperature of 12.97 which is twice the designed value. This result indicates that the temperature difference between inlet and outlet streams should be increased accordingly. Figure 4.37 illustrate the effect of difference between inlet temperatures of the two streams on the increase in temperature of cold stream.

4.3.1.3 Flow Rates

The system was designed to work at relatively low flow rates so as to minimize the quantity of hot water required and consequently the size of the evacuated collector field. Difficulties were encountered in adjusting the control valves to deliver the

designed flow rate required. The solution pump (see Fig 4.25) was replaced by a variable speed circulation pump in order to operate the system at the designed flow rate. Due to the above mentioned difficulties, the flow rates were adjusted as close as possible to the designed values (*but not exactly equivalent to them*). Fewer operational problems could have been met, if the system was designed to operate at higher flow rates.

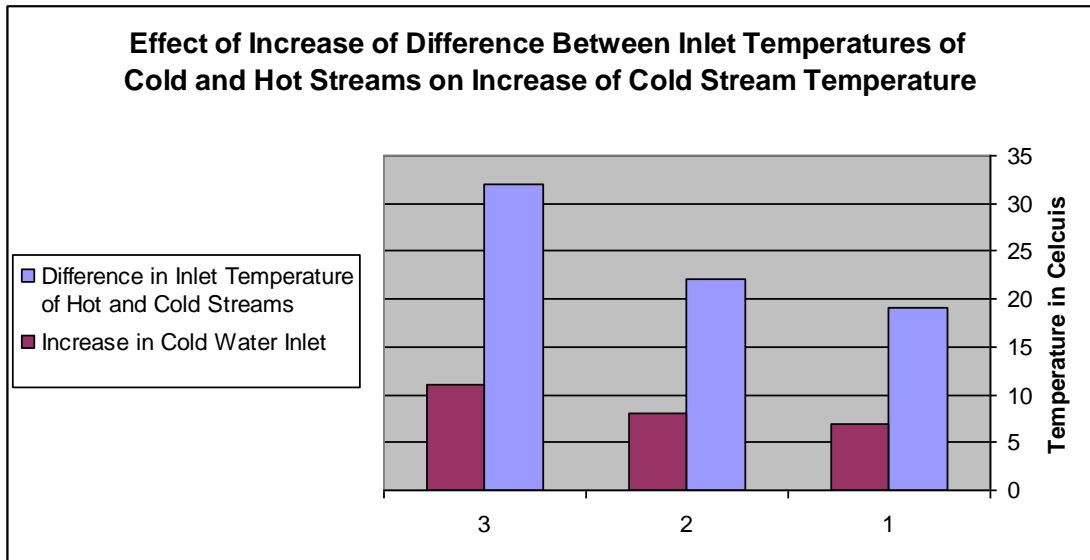


Fig. 4.37 Effect of Flow Streams Inlet Temperature on Temperature Rise of Cold Stream.

4.3.1.4 Heat Transfer Coefficient

It is evident from tables, 4.10 & 4.11 that the experimental heat transfer coefficient was lower than the designed value. It is worth mentioning that the experimental values of the heat transfer coefficient were obtained from calculations based on heat gained by cold stream not heat lost by hot stream, which explains the low values obtained. In addition, the designed value was based on two-phase flow in the cold stream and not a single phase flow.

4.3.2 Double Tube Heat Exchanger

Operating parameters under investigation are:

- Energy delivered or gained by flow streams
- Temperature ranges
- Flow Rates
- Heat Transfer Coefficient

Table 4.12 & 4.13 below shows the test result of the double tube heat exchanger and the designed operating parameters respectively.

4.3.2.1 Energy Gain and Loss between Cold and Hot Streams

Referring to Table 4.12 below, it appears that there is a difference between heat gained by cold water and heat lost by hot water, which necessitates the use of more insulating material around the heat exchanger and pipe lines. It can be noticed that heat losses are more serious than at the shell and tube heat exchanger (see Fig.4.38)

Table 4.12 Experimental Data of Double Heat Exchanger

Flow Rate of Hot Water (lpm)	Flow Rate of Cold Water (lpm)	Cold Water Inlet Temperature (°C)	Cold Water Outlet Temperature (°C)	Hot Water Inlet Temperature (°C)	Hot Water Outlet Temperature (°C)	Log Mean Temperature Difference	Heat Energy Lost By Hot Stream (Kw)	Heat Energy Gained By Cold Stream (Kw)	Heat Transfer Coefficient (W/m ² k)
1.8	2.4	50	54	67	56	9.05	1.3947	0.6762	99.78
2.5	0.8	37	50	64	58	17.26	1.0566	0.7325	56.67
0.625	0.7	38	46	60	50	12.97	0.4402	0.3944	40.61
0.6	0.7	47	57	71	49	6.16	0.9298	0.493	106.76
0.55	0.6	38	55	69	41	7.14	1.0847	0.7184	134.36
0.625	0.5	38	50	61	42	6.91	0.8364	0.4226	81.57
0.65	0.41	37	59	71	42	7.99	1.3277	0.6353	106.11

Table 4.13 Designed Operating Parameters of Double Tube Heat Exchanger

Flow Rate of Hot Stream (lpm)	Flow Rate of Cold Stream (lpm)	Cold Stream Inlet Temperature (°C)	Cold Stream Outlet Temperature (°C)	Hot Stream Inlet Temperature (°C)	Hot Stream Outlet Temperature (°C)	Log Mean Temperature Difference	Heat Energy Lost By Hot Stream (Kw)	Heat Energy Gained By Cold Stream (Kw)	Heat Transfer Coefficient (W/m ² k)
0.396	0.342	59	73	83	66	8.4	0.426KW	0.426Kw	47.6

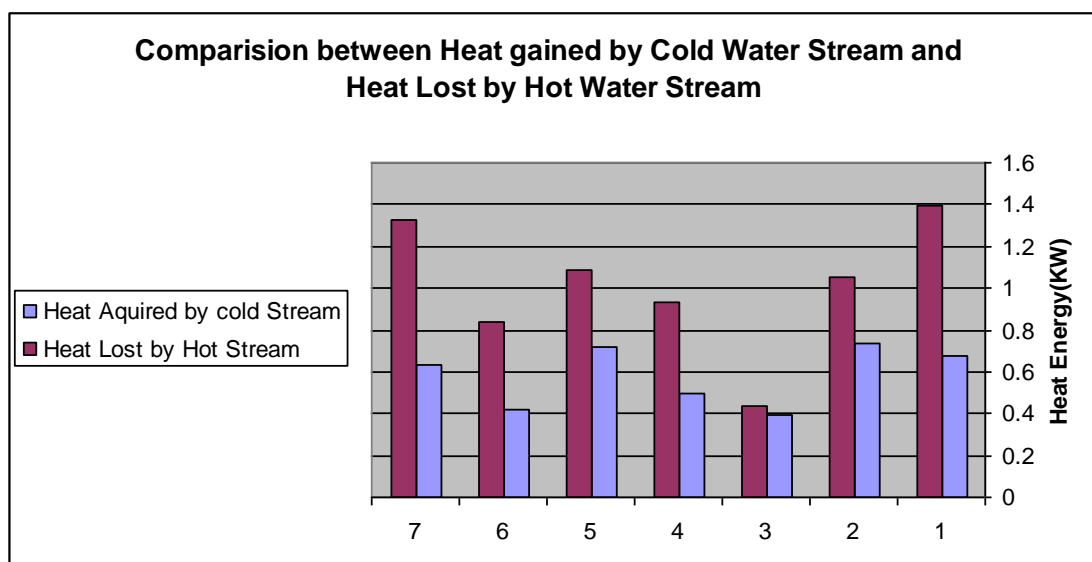


Fig. 4.38 Heat Gain and Loss by Cold and Hot Streams in Double Tube Heat Exchanger

4.3.2.2 Temperature Ranges

Again, as in the case of shell & tube heat exchanger, the tests were conducted at off designed operating parameters due to unfavorable weather conditions. As it is shown in Table 4.12 above, the heat exchanger can meet the designed load at log mean temperature difference lower than the designed log mean temperature difference. But the experimental flow rates are slightly higher than designed flow rates. The effect of difference of inlet stream temperatures on the increase of cold water temperature can be clearly shown by figure 4.39.

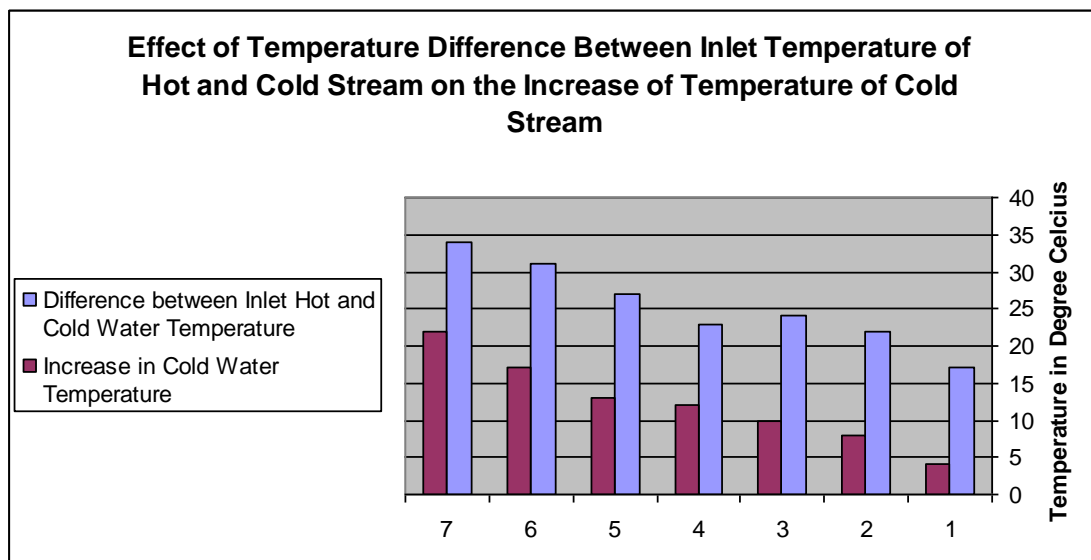


Fig. 4.39 Effect of Flow Streams Inlet Temperature on Temperature Rise of Cold Stream.

4.3.2.3 Flow Rates

Difficulties were met at trying to operate the exchanger at the designed flow rates, so tests were conducted with flow rates as close as possible to the designed flow rates.

4.3.2.4 Heat Transfer Coefficient

As shown by table 4.12 and 4.13 the values of the experimental heat transfer coefficient are higher than the designed values, which means that the heat exchanger can meet greater load than the designed load.

4.3.3 Flat Plate Collector Field

Operating parameters under investigation are:

- Efficiency of the absorber plate of the flat plate collector.
- Storage Tank Temperature variation with weather condition.

Table 4.14 shows the test result of the flat plate collector.

4.3.3.1 Efficiency Test of Flat Plate Collector

Referring to table 4.14 below, the average collector efficiency was found to be 65.9% which is remarkable for a flat plate collector without selective surface. It appears also that the instantaneous efficiency is highest when the temperature difference between inlet temperature and ambient temperature is the lowest. This result is in agreement with that reported in literature.

Table 4.14 Efficiency Test of Flat Plate Collector

Ambient Temperature T_a (°C)	Radiation Intensity I (W/m ²)	Inlet Temperature T_i (°C)	Outlet Temperature T_o (°C)	Heat Gain(W) $Q = \dot{m}c(T_o - T_i)$	efficiency $\eta = \frac{Q}{AI}$	$T_i - T_a$	Average Efficiency
33	709	40	50	1407.258	0.94194	7	
37	747	47	53	844.3548	0.565164	10	0.659
37	762	54	59	703.629	0.47097	17	

4.3.3.2 Variation of Storage Tank Temperature with Ambient Conditions

(i) Flat Plate Collector with 110 liter Storage

The designed operating parameters and the experimental data (summarized from Table 4.7) are shown in table 4.15.

Table 4.15 Comparison between Design and Experimental Data for Flat Plate Collector with 110 Liter Capacity

No.	Parameters	Designed Values	Experimental Values
1	Quantity of liquid to be preheated	65 liter	110 liter
2	Temperature to be attained prior to operation	59°C	58* up to 70

**Reading obtained at very cloudy weather condition*

Table 4.15 shows the flat plate collector can preheat almost twice the quantity of fluid to temperatures greater than the designed temperatures by up to 10 degrees and it can fulfill the preheating duty even at the worst weather conditions. At clear sky conditions the storage tank temperature can reach 80 °C at 3 O'clock p.m.

(ii) Flat Plate Collector with 36 liter Capacity

The purpose of the flat plate collector was to preheat the strong ammonia solution to temperature higher than that of the flat plate collector with 110 liter capacity to provide the system with preheated fluid for the first hour of operation till operation stability was attained. The performance of the collector was observed from December till March and it was evident that the storage tank temperature could reach 100 °C at 3O'clock p.m. Table 4.16 compare the designed parameter with the experimental data.

It shows that the collector can preheat more than double the heat transfer fluid to temperatures higher than up to 30 degrees.

Table 4.16 Comparison between Design and Experimental Data for Flat Plate Collector with 36 Liter Capacity

No.	Parameters	Designed Values	Experimental Values
1	Quantity of liquid to be preheated	15 liter	36 liter
2	Temperature to be attained prior to operation i.e. one O'clock local time	67°C	80 up to 96 (from December 2008 to March 2009)

4.3.4 Evacuated Collector Field

Operating parameters under investigation are:

- Variation of storage tank temperature under constant load withdrawal.
- Attaining operating temperature under different weather conditions.

4.3.4.1 Effect of Constant Load Withdrawal On Storage Tank Temperature Variation.

Table 4.3.4.1. compares the designed parameters to the experimental data. As shown by the table, there is a slight difference between the experimental and designed delivery temperature but there is a big difference between the experimental and designed temperature. This difference is attributed to the following:

- Heat losses in pipe lines and upper & lower storage tanks (see Fig. 4.26)
- Difficulties in controlling the heat exchange process between the hot and cold streams at the shell and tube heat exchanger which was used as the load of the experiment.
- Presence of cloud covers during the testing period prevented the collector field from receiving adequate radiation to meet the load

4.3.4.2 Variation of Storage Tank Temperature under Different Weather Conditions

As shown by Fig. 3.16, failure of the collector field to meet the load was predicted to occur at 3 and 4 O'clock from April till September. Although observations of the collector field temperature showed that it can attain temperatures higher than the designed delivery temperature during period from Decemeber 2008 to March 2009,

the storage tank temperature observation during July and August showed that the collector field would not attain the operating temperature at time of system operation(see Table 4.8)

Table 4.17 Comparison of Experimental Data with Design Parameters of Effect of Constant Load withdrawal on the Evacuated Collector Field

Parameters		Experimental Data	Design Parameters
Hot Water Delivery Temperature	Time (p.m.)		
Hot Water Delivery Temperature	1:00	88	88
	2:00	87	88
	3:00	86	88
	4:00	84	88
Hot Water Return Temperature	Time		
	1:00	45	80
	2:00	55	80
	3:00	48	80
	4:00	49	80
Mass Flow Rate of Hot Water(lpm)		0.55	0.59

Chapter 5

5. Conclusion and Recommendation

5.1 General Conclusion and Recommendation

Within the course of this study, a continuous absorption refrigeration machine has been designed and constructed. Performance tests were conducted on the components of the experimental unit. In view of the previous result analysis, the following can be concluded:

- The performance of the shell and tube heat exchanger and double tube heat exchanger could be improved, if greater log mean temperature difference and higher flow rates could be used.
- The temperature of the hot water delivered by the evacuated collector field need to be increased by at least 10 to 15 °C. This rise in temperature is necessary to compensate for pipe line losses and unfavorable weather conditions. In addition, it will increase the value of the log mean temperature difference of the heat exchangers. Since the water in glass collector operating temperature is below this temperature range, a different type of evacuated collector should be inserted between the evacuated collector and the shell& tube heat exchanger. The duty of this suggested evacuated collector is to provide the rise in temperature necessary to improve system performance.
- The performance of the flat plate collector field was excellent and obviously it can accomplish the preheating duty even under unfavorable weather condition.

5.2 Further Work

- Testing of heat exchangers using higher flow rates and different temperature ranges to define the maximum power capacity of the system.
- Subjecting the evacuated collector field to withdrawal different mass flow rates to determine the variation of storage tank temperatures under different load patterns.

References

- 1- Duffie, J.A. and Beckman, W.A., *Solar Engineering of Thermal Processes*, Wiley, New York, 1980.
- 2- Ursula Eicker, *Solar Technologies for Buildings*, Wiley, England, 2003.
- 3- Marcel Bogart, *Ammonia Absorption Refrigeration in Industrial Processes*, Gulf Publishing Company, Texas, 1981.
- 4- Tiwari, G.N., *Solar Energy*, Narosa, New Delhi, 2003.
- 5- Coulson, J.M., Richardson, J.F., Backhurst, J.R., Harker, J.H., *Chemical Engineering*, Vol.1, Butterworth Heinmann, CCC, 000
- 6- Coulson, J.M., Richardson, J.F., Backhurst, J.R., Harker, J.H., *Chemical Engineering*, Vol.2, Butterworth Heinmann, CCC.
- 7- Morrison G.L., *Solar Energy - The State of the Art*, Gordon J. James and James, 2001.
ASHRAE. ASHRAE HANDBOOK Fundamentals 1985.
- 8- Tiwari, D.P., *Heat Transfer*, Umesh Publication, Delhi.
- 9- Jan F. Kreider and Frank Kreith, *Solar Energy Handbook*, Mc-Graw-Hill Book Company.
- 10- Frank P. Incropera and David P. Dewitt, *Fundamentals of Heat and Mass Transfer*, Wiley, New York.
- 11- Robert H. Perry, Don W. Green and James O. Maloney, *Perry's Chemical Engineering Handbook*, McGraw-Hill Company.
- 12- Charles F. Kutcher, Roger L. Davenport and Douglas A. Dougherty, *Design Approaches for Solar Industrial Process Heat Systems*, National Technical Information Service, 1982.
- 13- Abdeen Mustafa Omer, *Compilation and Evaluation of Solar and Wind Energy Resources in Sudan*. *Journal of Renewable Energy*, Vol. 12, No. 1, Elsevier Science Ltd. 1997.
- 14- Jim A. Clark, *An investigation of Solar-Powered Continuous Ammonia- Water Absorption Air Conditioner for Residential Dwelling*, M.Sc. Thesis, University of Florida, 1976.
- 15- Paul J. Wilbur and Susumu Karkai, *Solar Cooling*,
- 16- Kim D.S., *Solar Absorption Cooling*, Ph.D Thesis, Delft Technical University, 2007
- 17- Nathan Rona, *Solar Air-Conditioning Systems*, Building Services Engineering, Gotenborg, Sweden 2005.
- 18- Dwipen Boruah, *Solar Adsorption Cooling*, Master Thesis, Oldenburg University, 2007
- 20- Jakob Uli (2002), *Design of solar Driven Cooling Unit based on the Diffusion Principle*. Technical report IEA-SHC International Energy Agency (IEA) pp. 33-39
- 21- ASHRAE, *Solar Refrigeration*, ASHRAE Journal, (Vol. 47, No. 9, September 2005).
- 22- Thévenot, R., 1979, *A history of refrigeration throughout the world*, Int. Inst. Refrigeration, Paris
- 23- Budihardjo I., Morrison G. L. and Behnia M. (2003) *Measurement and simulation of flow rate in a water-in-glass evacuated tube solar water heater* Proc. IEES 2003 World Congress: Göteborg, June 14-19 2003

Appendix

Thermophysical Properties of Saturated Water

Temperature, T (K)	Pressure, P (bars) ^a	Specific Volume (m ³ /kg)		Heat of Vaporization, h_{fg} (kJ/kg)	Specific Heat (kJ/kg · K)		Viscosity (N · s/m ²)		Thermal Conductivity (W/m · K)		Prandtl Number	Surface Tension, $\sigma_f \cdot 10^3$ (N/m)	Expansion Coefficient, $\beta_f \cdot 10^6$ (K ⁻¹)	Temperature, T (K)	
		$v_f \cdot 10^3$	v_g		$c_{p,f}$	$c_{p,g}$	$\mu_f \cdot 10^6$	$\mu_g \cdot 10^6$	$k_f \cdot 10^3$	$k_g \cdot 10^3$					Pr_f
273.15	0.00611	1.000	206.3	2502	4.217	1.854	1750	8.02	569	18.2	12.99	0.815	75.5	-68.05	273.15
275	0.00697	1.000	181.7	2497	4.211	1.855	1652	8.09	574	18.3	12.22	0.817	75.3	-32.74	275
280	0.00990	1.000	130.4	2485	4.198	1.858	1422	8.29	582	18.6	10.26	0.825	74.8	-40.04	280
285	0.01387	1.000	99.4	2473	4.189	1.861	1225	8.49	590	18.9	8.81	0.833	74.3	114.1	285
290	0.01917	1.001	69.7	2461	4.184	1.864	1080	8.69	598	19.3	7.56	0.841	73.7	174.0	290
295	0.02617	1.002	51.94	2449	4.181	1.868	959	8.89	606	19.5	6.62	0.849	72.7	227.5	295
300	0.03531	1.003	39.13	2438	4.179	1.872	855	9.09	613	19.6	5.83	0.857	71.7	276.1	300
305	0.04712	1.005	29.74	2426	4.178	1.877	769	9.29	620	20.1	5.20	0.865	70.9	320.6	305
310	0.06221	1.007	22.93	2414	4.178	1.882	695	9.49	628	20.4	4.62	0.873	70.0	361.9	310
315	0.08132	1.009	17.82	2402	4.179	1.888	631	9.69	634	20.7	4.16	0.883	69.2	400.4	315
320	0.1053	1.011	13.98	2390	4.180	1.895	577	9.89	640	21.0	3.77	0.894	68.3	436.7	320
325	0.1351	1.013	11.06	2378	4.182	1.903	528	10.09	645	21.3	3.42	0.901	67.5	471.2	325
330	0.1719	1.016	8.82	2366	4.184	1.911	489	10.29	650	21.7	3.15	0.908	66.6	504.0	330
335	0.2167	1.018	7.09	2354	4.186	1.920	453	10.49	656	22.0	2.88	0.916	65.8	535.5	335
340	0.2713	1.021	5.74	2342	4.188	1.930	420	10.69	660	22.3	2.66	0.925	64.9	566.0	340
345	0.3372	1.024	4.683	2329	4.191	1.941	389	10.89	668	22.6	2.45	0.933	64.1	595.4	345
350	0.4163	1.027	3.846	2317	4.195	1.954	365	11.09	668	23.0	2.29	0.942	63.2	624.2	350
355	0.5100	1.030	3.180	2304	4.199	1.968	343	11.29	671	23.3	2.14	0.951	62.3	652.3	355
360	0.6209	1.034	2.645	2291	4.203	1.983	324	11.49	674	23.7	2.02	0.960	61.4	679.9	360
365	0.7514	1.038	2.212	2278	4.209	1.999	306	11.69	677	24.1	1.91	0.969	60.5	707.1	365
370	0.9040	1.041	1.861	2265	4.214	2.017	289	11.89	679	24.5	1.80	0.978	59.5	728.7	370
373.15	1.0133	1.044	1.679	2257	4.217	2.029	279	12.02	680	24.8	1.76	0.984	58.9	750.1	373.15
375	1.0815	1.045	1.574	2252	4.220	2.036	274	12.09	681	24.9	1.70	0.987	58.6	761	375
380	1.2869	1.049	1.337	2239	4.226	2.057	260	12.29	683	25.4	1.61	0.999	57.6	788	380
385	1.5233	1.053	1.142	2225	4.232	2.080	248	12.49	685	25.8	1.53	1.004	56.6	814	385
390	1.794	1.058	0.980	2212	4.239	2.104	237	12.69	686	26.3	1.47	1.013	55.6	841	390
400	2.455	1.067	0.731	2183	4.256	2.158	217	13.05	688	27.2	1.34	1.033	53.6	896	400
410	3.302	1.077	0.553	2153	4.278	2.221	200	13.42	688	28.2	1.24	1.054	51.5	952	410
420	4.370	1.088	0.425	2123	4.302	2.291	185	13.79	688	29.8	1.16	1.075	49.4	1010	420
430	5.699	1.099	0.331	2091	4.331	2.369	173	14.14	685	30.4	1.09	1.10	47.2	1070	430
440	7.333	1.110	0.261	2059	4.36	2.46	162	14.50	682	31.7	1.04	1.12	45.1	1130	440
450	9.319	1.123	0.208	2024	4.40	2.56	152	14.85	678	33.1	0.99	1.14	42.9	1190	450
460	11.71	1.137	0.167	1989	4.44	2.68	143	15.19	673	34.6	0.95	1.17	40.7	1250	460
470	14.55	1.152	0.136	1951	4.48	2.79	136	15.54	667	36.3	0.92	1.20	38.5	1310	470
480	17.90	1.167	0.111	1912	4.53	2.94	129	15.88	660	38.1	0.894	1.23	36.2	1370	480
490	21.83	1.184	0.0922	1870	4.59	3.10	124	16.23	651	40.1	0.87	1.25	33.9	1430	490
500	26.40	1.203	0.0766	1825	4.66	3.27	118	16.59	642	42.3	0.86	1.28	31.6	1490	500
510	31.66	1.222	0.0631	1779	4.74	3.47	113	16.95	631	44.7	0.85	1.31	29.3	1550	510
520	37.70	1.244	0.0525	1730	4.84	3.70	108	17.33	621	47.5	0.84	1.35	26.9	1610	520
530	44.58	1.268	0.0445	1679	4.95	3.96	104	17.72	608	50.6	0.85	1.39	24.5	1670	530
540	52.38	1.294	0.0375	1622	5.08	4.27	101	18.1	594	54.0	0.86	1.43	22.1	1730	540
550	61.19	1.323	0.0317	1564	5.24	4.64	97	18.6	580	58.3	0.87	1.47	19.7	1790	550
560	71.08	1.355	0.0269	1499	5.43	5.09	94	19.1	563	63.7	0.90	1.52	17.3	1850	560
570	82.16	1.392	0.0228	1429	5.68	5.67	91	19.7	548	76.7	0.94	1.59	15.0	1910	570
580	94.51	1.433	0.0193	1353	6.00	6.40	88	20.4	528	96.7	0.99	1.68	12.8	1970	580
590	108.3	1.482	0.0163	1274	6.41	7.35	84	21.5	513	124.1	1.05	1.84	10.5	2030	590
600	123.5	1.541	0.0137	1176	7.00	8.75	81	22.7	497	159.9	1.14	2.15	8.4	2090	600
610	137.3	1.612	0.0115	1068	7.85	11.1	77	24.1	467	219.3	1.30	2.60	6.3	2150	610
620	159.1	1.705	0.0094	941	9.35	15.4	72	25.9	414	311.7	1.52	3.46	4.5	2210	620
625	169.1	1.778	0.0085	858	10.6	18.3	70	27.0	430	430	1.65	4.20	3.5	2270	625
630	179.7	1.856	0.0075	781	12.6	22.1	67	28.0	412	600	2.0	4.8	2.6	2330	630
635	190.9	1.935	0.0066	683	16.4	27.6	64	30.0	392	800	2.7	6.0	1.5	2390	635
640	202.7	2.075	0.0057	560	26	42	59	32.0	367	1100	4.2	9.6	0.8	2450	640
645	215.2	2.351	0.0045	361	90	—	54	37.0	331	1700	12	26	0.1	2510	645
647.3 ^c	221.2	3.170	0.0032	0	∞	∞	45	45.0	238	238	∞	∞	0.0	2570	647.3

^aAdapted from Reference 19.
^b1 bar = 10⁵ N/m².
^cCritical temperature.

Refrigerant 717 (Ammonia) Properties of Liquids and Saturated Vapor

Temp F	Pressure		Volume	Density	Enthalpy**		Entropy**		12	14	16	18	20	22	24	26	28	30	34	38	42	46	50	54	58	62	66	70	72	74	76	78	80	82	84	86	88	90	92	94	96	98	100	110	120	125	130	140	150	160	170	180	190	200	210	220	230	240	250	260	270	271*	280	290	300	320	360	400	440	500			
	lb/in ²		cu ft/lb	lb/cu ft	Liquid	Vapor	Liquid	Vapor																																																																	
	psia	psig	v _g	l/v _f	h _f	h _g	s _f	s _g																																																																	
-105	0.996	27.9*	223.2	45.71	-68.5	570.3	-0.1774	1.6243	40.31	42.18	44.12	46.13	48.21	50.36	52.59	54.90	57.28	59.74	64.91	70.43	76.31	82.55	89.19	96.23	103.7	111.6	120.0	128.8	133.4	138.1	143.0	148.0	153.0	158.3	163.7	169.2	174.8	180.6	186.6	192.7	198.9	205.3	211.9	217.0	228.4	237.1	246.4	255.1	264.4	273.1	282.4	291.1	300.8	310.5	320.2	330.0	340.0	350.0	360.0	370.0	380.0	390.0	400.0	410.0	420.0	430.0	440.0	450.0	460.0	470.0	480.0	490.0	500.0

*From National Bureau of Standards Circular No. 142 (1945) and Circular No. 472 (1948).
 **Based on 0 for the saturated liquid at -40 F.
 †Standard cycle temperatures.
 ‡Inches of mercury below one standard atmosphere.

Temp, F	Viscosity, lb _m /ft · h			Thermal Conductivity, Btu/h · ft · F				Specific Heat, c _p , Btu/lb _m · F				Temp, F
	Sat. Liquid	Sat. Vapor	Gas, P = 1 atm × 10 ⁻² ‡	Sat. Liquid	Sat. Vapor	Gas, P = 1 atm × 10 ⁻² ‡	Sat. Liquid	Sat. Vapor	Gas (c _p) _{0.1 atm}	Gas (c _p) _{1 atm}		
-100				0.410			1.030				-100	
-80				0.395			1.044				-80	
-60				0.380			1.056	0.523	0.477		-60	
-40				0.365			1.066	0.543	0.480		-40	
-20	0.629	0.0227	2.02	0.350	0.011	11.1	1.075	0.565	0.483	0.547	-20	
0	0.558	0.0237	2.11	0.335	0.012	11.7	1.083	0.590	0.486	0.536	0	
20	0.494	0.0246	2.20	0.321	0.012	12.2	1.092	0.620	0.489	0.528	20	
40	0.437	0.0256	2.29	0.306	0.013	12.9	1.103	0.655	0.493	0.522	40	
60	0.386	0.0266	2.39	0.291	0.015	13.5	1.118	0.698	0.496	0.519	60	
80	0.341	0.0277	2.48	0.276	0.016	14.2	1.135	0.750	0.500	0.517	80	
100	0.301	0.0288	2.58	0.261	0.018	14.9	1.158	0.814	0.504	0.517	100	
120	0.268	0.0299	2.67	0.246	0.020	15.6	1.187	0.866	0.508	0.518	120	
140	0.238	0.0312	2.77	0.231	0.022	16.3	1.222		0.512	0.520	140	
160	0.213	0.0325	2.87	0.216	0.025	17.1	1.265		0.517	0.523	160	
180	0.190	0.0340	2.97	0.201	0.029	17.8	1.317		0.521	0.527	180	
200	0.171	0.0358	3.06	0.186	0.034	18.6	1.379		0.526	0.532	200	
220	0.154	0.0380	3.16	0.169	0.039	19.4	1.452		0.530	0.536	220	
240	0.124	0.0411	3.26	0.149	0.044	20.2	1.536		0.535	0.542	240	
250	0.110	0.043	3.31	0.137	0.049	20.7	1.59		0.537	0.544	250	
260	0.094	0.046	3.36	0.120	0.060	21.1	1.65		0.540	0.547	260	
270			3.41	0.102	0.081	21.5			0.542	0.550	270	
271*	0.060	0.060	3.42	0.087	0.087	21.5			0.542	0.550	271*	
280			3.46			21.9			0.544	0.552	280	
290			3.51			22.3			0.547	0.555	290	
300			3.56			22.8			0.549	0.557	300	
320			3.66			23.7			0.554	0.562	320	
360			3.86			25.4			0.564	0.572	360	
400			4.06			27.3			0.574	0.581	400	
440			4.27			29.1			0.584	0.590	440	
500			4.57			32.0			0.599	0.602	500	

*Critical Temperature. Tabulated properties ignore critical region effects.
 ‡Actual value = (Table value) × (Indicated multiplier).

Specific Volume of Saturated Ammonia Solution

Temp, F	Concentration, % Weight Ammonia										Temp, F	
	0	10	20	30	40	50	60	70	80	90		100
20	0.0160	0.0165	0.0170	0.0176	0.0182	0.0190	0.0197	0.0207	0.0217	0.0230	0.0245	20
40	0.0160	0.0165	0.0171	0.0177	0.0184	0.0191	0.0200	0.0209	0.0221	0.0236	0.0253	40
60	0.0160	0.0166	0.0172	0.0178	0.0186	0.0193	0.0202	0.0212	0.0225	0.0241	0.0260	60
80	0.0161	0.0167	0.0173	0.0180	0.0188	0.0196	0.0205	0.0216	0.0230	0.0247	0.0267	80
100	0.0161	0.0168	0.0174	0.0182	0.0190	0.0198	0.0208	0.0220	0.0235	0.0254	0.0275	100
120	0.0162	0.0169	0.0176	0.0184	0.0192	0.0201	0.0211	0.0224	0.0241	0.0261	0.0284	120
140	0.0163	0.0170	0.0177	0.0185	0.0194	0.0203	0.0215	0.0228	0.0247	0.0268	0.0294	140
160	0.0164	0.0172	0.0179	0.0187	0.0196	0.0206	0.0219	0.0235	0.0254	0.0277	0.0306	160
180	0.0165	0.0173	0.0181	0.0190	0.0199	0.0210	0.0223	0.0241	0.0262	0.0286	0.0320	180
200	0.0166	0.0175	0.0183	0.0192	0.0202	0.0213	0.0228	0.0247	0.0270	0.0298	0.0338	200
220	0.0168	0.0176	0.0185	0.0194	0.0205	0.0217	0.0234	0.0255	0.0279	0.0312	0.0361	220

Prepared under Research Project No. 271-RP, sponsored by TC 8.3, and by Helipump Corp., Cleveland, OH. Data reference—B.H. Jennings: Ammonia Water Properties (Paper presented ASHRAE meeting, January, 1965).

Table 34 Refrigerant Temperature (t' = F) and Enthalpy (h = Btu/lb) of Lithium Bromide Solutions

Temp. (t = F)		Percent LiBr										
		0	10	20	30	40	45	50	55	60	65	70
80	t'	80.0	78.2	75.6	70.5	60.9	53.5	42.1	28.6	13.8	-0.2 [#]	-11.6 [#]
	h	48.0	39.2	31.8	25.6	21.6	21.2	23.0	28.7	38.9	52.7 [#]	67.1 [#]
100	t'	100.0	98.1	95.3	89.9	79.6	71.8	60.0	46.1	30.9	16.2 [#]	3.8 [#]
	h	68.0	56.6	47.0	38.7	33.2	32.1	33.2	38.2	47.8	61.1 [#]	75.1 [#]
120	t'	120.0	117.9	114.9	109.2	98.3	90.1	77.9	63.6	48.1	32.7	19.1 [#]
	h	87.9	73.6	61.7	51.7	44.7	43.0	43.6	48.0	56.9	69.4	83.0 [#]
140	t'	140.0	137.8	134.6	128.5	117.1	108.5	95.8	81.2	65.2	49.1	34.4 [#]
	h	107.9	91.0	77.0	65.1	56.5	54.1	54.1	57.9	66.1	78.0	91.1 [#]
160	t'	160.0	157.7	154.3	147.9	135.8	126.8	113.8	98.7	82.3	65.6	49.7 [#]
	h	127.9	108.2	92.0	78.2	68.1	65.1	64.7	67.9	75.4	86.6	99.2 [#]
180	t'	180.0	177.5	173.9	167.2	154.5	145.1	131.7	116.2	99.5	82.0	65.1 [#]
	h	147.9	125.4	107.9	91.9	80.4	76.6	75.3	77.7	84.6	95.1	107.2 [#]
200	t'	200.0	197.4	193.6	186.5	173.3	163.5	149.6	133.7	116.6	98.5	80.4 [#]
	h	168.0	143.4	123.3	105.3	92.1	87.4	85.9	87.8	94.1	104.0	115.6 [#]
220	t'	220.0	217.2	213.3	205.8	192.0	181.8	167.5	151.3	133.7	114.9	95.7
	h	188.1	160.7	138.2	119.0	104.1	99.0	96.5	97.8	103.3	112.5	123.6
240	t'	240.0*	237.1*	232.9	225.2	210.7	200.2	185.4	168.8	150.9	131.4	111.0
	h	208.3*	178.4*	154.0	132.6	116.0	110.3	107.1	107.7	112.5	121.1	131.6
260	t'	260.0*	256.9*	252.6*	244.5*	229.4	218.5	203.3	186.3	168.0	147.9	126.4
	h	228.6*	195.7*	169.1*	146.2*	128.1	121.6	117.6	117.6	121.6	129.5	139.5
280	t'	280.0*	276.8*	272.3*	263.8*	248.2*	236.8*	221.2	203.9	185.1	164.3	141.7
	h	249.1*	213.8*	185.1*	159.7*	140.0*	132.8*	128.1	127.5	130.6	137.9	147.6
300	t'	300.0*	296.7*	291.9*	283.1*	266.9*	255.2*	239.2*	221.4	202.3	180.8	157.0
	h	269.6*	231.6*	200.7*	173.5*	152.1*	144.1*	138.9*	137.3	139.8	146.5	155.5
320	t'	320.0*	316.5*	311.6*	302.5*	285.6*	273.5*	257.1*	238.9*	219.4	197.2	172.4
	h	290.3*	249.7*	216.3*	187.2*	164.2*	155.3*	149.5*	147.1*	148.8	154.9	163.4
340	t'	340.0*	336.4*	331.3*	321.8*	304.4*	291.9*	275.0*	256.4*	236.5*	213.7	187.7
	h	311.1*	267.9*	232.1*	201.0*	176.1*	166.6*	160.1*	157.0*	158.0*	163.5	171.0
360	t'	360.0*	356.2*	350.9*	341.1*	323.1*	310.2*	292.9*	274.0*	253.7*	230.1	203.0
	h	332.2*	286.1*	248.0*	214.9*	188.2*	178.0*	170.6*	166.8*	167.0*	171.9	178.3

*Extensions of data above 235 F are well above the original data and should be used with care.

[#]Super saturated solution.

*Extensions of data above 235 F are well above the original data and should be used with care.

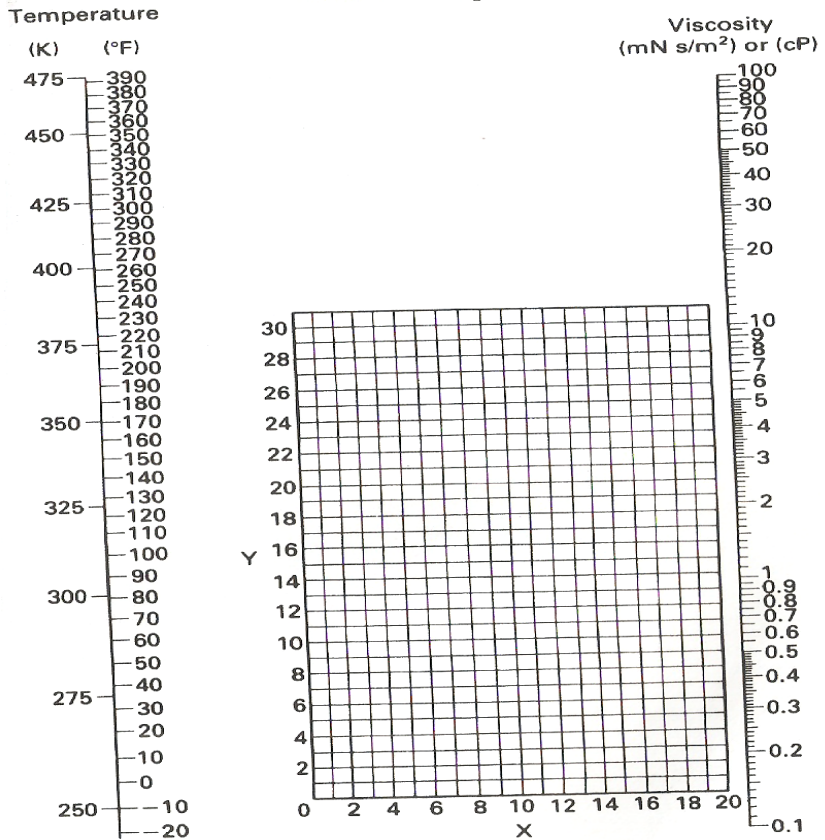
[#]Super saturated solution.

Viscosities and Densities of Liquids

Liquid	Density at 293 K (kg/m ³)		No.	Liquid	Density at 293 K (kg/m ³)		
	X	Y			X	Y	
Acetaldehyde	15.2	4.8	783 (291 K)	57 Freon-113 (CCl ₂ F-CClF ₂)	12.5	11.4	1576
Acetic acid, 100 per cent	12.1	14.2	1049	58 Glycerol, 100 per cent	2.0	30.0	1261
Acetic acid, 70 per cent	9.5	17.0	1069	59 Glycerol, 50 per cent	6.9	19.6	1126
Acetic anhydride	12.7	12.8	1083	60 Heptane	14.1	8.4	684
Acetone, 100 per cent	14.5	7.2	792	61 Hexane	14.7	7.0	659
Acetone, 35 per cent	7.9	15.0	948	62 Hydrochloric acid, 31.5 per cent	13.0	16.6	1157
Allyl alcohol	10.2	14.3	854	63 Isobutyl alcohol	7.1	18.0	779 (299 K)
Ammonia, 100 per cent	12.6	2.0	817 (194 K)	64 Isobutyric acid	12.2	14.4	949
Ammonia, 26 per cent	10.1	13.9	904	65 Isopropyl alcohol	8.2	16.0	789
Amyl acetate	11.8	12.5	879	66 Kerosene	10.2	16.9	780-820
Amyl alcohol	7.5	18.4	817	67 Linseed oil, raw	7.5	27.2	934 ± 4 (288 K)
Aniline	8.1	18.7	1022	68 Mercury	18.4	16.4	13546
Anisole	12.3	13.5	990	69 Methanol, 100 per cent	12.4	10.5	792
Arsenic trichloride	13.9	14.5	2163	70 Methanol, 90 per cent	12.3	11.8	820
Benzene	12.5	10.9	880	71 Methanol, 40 per cent	7.8	15.5	935
Brine, CaCl ₂ , 25 per cent	6.6	15.9	1228	72 Methyl acetate	14.2	8.2	924
Brine, NaCl, 25 per cent	10.2	16.6	1186 (298 K)	73 Methyl chloride	15.0	3.8	952 (273 K)
Bromine	14.2	13.2	3119	74 Methyl ethyl ketone	13.9	8.6	805
Bromotoluene	20.0	15.9	1410	75 Naphthalene	7.9	18.1	1145
Butyl acetate	12.3	11.0	882	76 Nitric acid, 95 per cent	12.8	13.8	1493
Butyl alcohol	8.6	17.2	810	77 Nitric acid, 60 per cent	10.8	17.0	1367
Butyric acid	12.1	15.3	964	78 Nitrobenzene	10.6	16.2	1205 (291 K)
Carbon dioxide	11.6	0.3	1101 (236 K)	79 Nitrotoluene	11.0	17.0	1160
Carbon disulphide	16.1	7.5	1263	80 Octane	13.7	10.0	703
Carbon tetrachloride	12.7	13.1	1595	81 Octyl alcohol	6.6	21.1	827
Chlorobenzene	12.3	12.4	1107	82 Pentachloroethane	10.9	17.3	1671 (298 K)
Chloroform	14.4	10.2	1489	83 Pentane	14.9	5.2	630 (291 K)
Chlorosulphonic acid	11.2	18.1	1787 (298 K)	84 Phenol	6.9	20.8	1071 (298 K)
Chlorotoluene, ortho	13.0	13.3	1082	85 Phosphorus tribromide	13.8	16.7	2852 (288 K)
Chlorotoluene, meta	13.3	12.5	1072	86 Phosphorus trichloride	16.2	10.9	1574
Chlorotoluene, para	13.3	12.5	1070	87 Propionic acid	12.8	13.8	992
Cresol, meta	2.5	20.8	1034	88 Propyl alcohol	9.1	16.5	804
Cyclohexanol	2.9	24.3	962	89 Propyl bromide	14.5	9.6	1353
Dibromoethane	12.7	15.8	2495	90 Propyl chloride	14.4	7.5	890
Dichloroethane	13.2	12.2	1256	91 Propyl iodide	14.1	11.6	1749
Dichloromethane	14.6	8.9	1336	92 Sodium	16.4	13.9	970
Diethyl oxalate	11.0	16.4	1079	93 Sodium hydroxide, 50%	3.2	25.8	1525
Dimethyl oxalate	12.3	15.8	1148 (327 K)	94 Stannic chloride	13.5	12.8	2226
Diphenyl	12.0	18.3	992 (346 K)	95 Sulphur dioxide	15.2	7.1	1434 (273 K)
Dipropyl oxalate	10.3	17.7	1038 (273 K)	96 Sulphuric acid, 110 per cent	7.2	27.4	1980
Ethyl acetate	13.7	9.1	901	97 Sulphuric acid, 98 per cent	7.0	24.8	1836
Ethyl alcohol, 100 per cent	10.5	13.8	789	98 Sulphuric acid, 60 per cent	10.2	21.3	1498
Ethyl alcohol, 95 per cent	9.8	14.3	804	99 Sulphuryl chloride	15.2	12.4	1667
Ethyl alcohol, 40 per cent	6.5	16.6	935	100 Tetrachloroethane	11.9	15.7	1600
Ethyl benzene	13.2	11.5	867	101 Tetrachloroethylene	14.2	12.7	1624 (288 K)
Ethyl bromide	14.5	8.1	1431	102 Titanium tetrachloride	14.4	12.3	1726
Ethyl chloride	14.8	6.0	917 (279 K)	103 Toluene	13.7	10.4	866
Ethyl ether	14.5	5.3	708 (298 K)	104 Trichloroethylene	14.8	10.5	1466
Ethyl formate	14.2	8.4	923	105 Turpentine	11.5	14.9	861-867
Ethyl iodide	14.7	10.3	1933	106 Vinyl acetate	14.0	8.8	932
Ethylene glycol	6.0	23.6	1113	107 Water	10.2	13.0	998
Formic acid	10.7	15.8	1220	108 Xylene, ortho	13.5	12.1	881
Freon-11 (CCl ₃ F)	14.4	9.0	1494 (290 K)	109 Xylene, meta	13.9	10.6	867
Freon-12 (CCl ₂ F ₂)	16.8	5.6	1486 (293 K)	110 Xylene, para	13.9	10.9	861
Freon-21 (CHCl ₂ F)	15.7	7.5	1426 (273 K)				
Freon-22 (CHClF ₂)	17.2	4.7	3870 (273 K)				

By permission from Perry's Chemical Engineers' Handbook, by Perry, R. H. and Green, D. W. (eds), 6th edn. Copyright 34, McGraw-Hill.

Viscosities of liquids



Latent Heats of Vaporization

Table 2. Latent heats of vaporisation*

Example: For water at 373 K, $\theta_c - \theta \approx (647 - 373) = 274$ K, and the latent heat of vaporisation is 2257 kJ/kg

No.	Compound	Range		θ_c	Range	θ_c	No.	Compound	Range		θ_c	Range	θ_c	
		$\theta_c - \theta$	θ_c						$\theta_c - \theta$	θ_c				$\theta_c - \theta$
		(°F)	(°F)	(K)	(K)	(K)			(°F)	(°F)	(K)	(K)	(K)	
8	Acetic acid	180-405	610	100-225	594	2	Freon-12 (C ₂ Cl ₂ F ₂)	72-360	232	40-200	384	29	Acetic acid, 100 per cent	273-353
2	Acetone	216-378	455	120-210	508	5	Freon-21 (CHCl ₂ F)	126-450	354	70-250	451	32	Acetone	293-323
9	Ammonia	90-360	271	50-200	406	6	Freon-22 (CHClF ₂)	90-306	205	50-170	369	52	Ammonia	203-323
3	Benzene	18-720	852	10-00	562	1	Freon-113 (CCl ₂ F-CClF ₂)	162-450	417	90-250	487	37	Amyl alcohol	223-298
6	Butane	162-360	307	90-200	426	10	Heptane	36-540	512	20-300	540	26	Amyl acetate	273-373
1	Carbon dioxide	18-180	88	10-100	304	11	Hexane	90-450	455	50-225	508	30	Aniline	273-403
4	Carbon disulphide	252-495	523	140-275	546	15	Isobutane	144-360	273	80-200	407	23	Benzene	283-353
2	Carbon tetrachloride	34-450	541	30-250	556	27	Methanol	72-450	464	40-250	513	27	Benzyl alcohol	253-303
7	Chloroform	252-495	505	140-275	536	19	Nitrous oxide	45-270	97	25-150	309	10	Benzyl chloride	243-303
8	Dichloromethane	270-450	421	150-250	489	9	Octane	54-540	565	30-300	569	49	Brine, 25 per cent CaCl ₂	233-293
3	Diphenyl	315-720	981	175-400	800	12	Pentane	36-360	387	20-200	470	51	Brine, 25 per cent NaCl	233-293
5	Ethane	45-270	90	25-150	305	23	Propane	72-360	205	40-200	369	44	Butyl alcohol	273-373
6	Ethyl alcohol	36-252	469	20-140	516	24	Propyl alcohol	36-360	507	20-200	537	2	Carbon disulphide	173-208
8	Ethyl alcohol	252-540	469	140-300	516	14	Sulphur dioxide	162-288	314	90-160	430	3	Carbon tetrachloride	283-333
7	Ethyl chloride	180-450	369	100-250	460	30	Water	180-900	705	100-500	647	8	Chlorobenzene	273-373
3	Ethyl ether	18-720	381	10-00	467							4	Chloroform	273-323
2	Freon-11 (CCl ₃ F)	126-450	389	70-250	471							21	Decane	193-298

*By permission from *Heat Transmission*, by W. H. McAdams, Copyright 1942, McGraw-Hill.

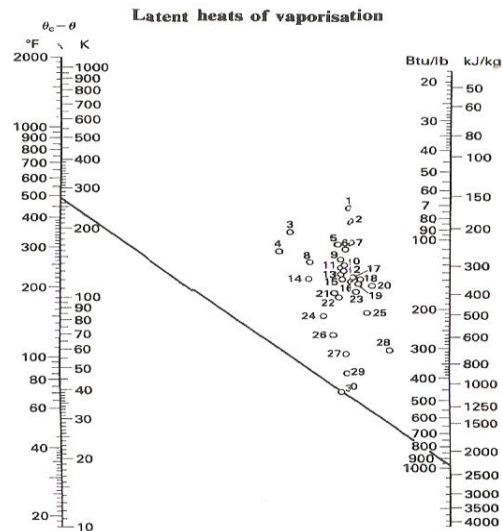
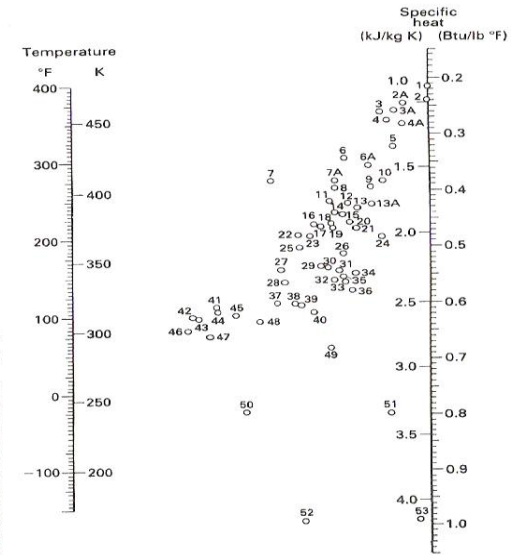


Table 3. Specific heats of liquids*

No.	Liquid	Range (K)
29	Acetic acid, 100 per cent	273-353
32	Acetone	293-323
52	Ammonia	203-323
37	Amyl alcohol	223-298
26	Amyl acetate	273-373
30	Aniline	273-403
23	Benzene	283-353
27	Benzyl alcohol	253-303
10	Benzyl chloride	243-303
49	Brine, 25 per cent CaCl ₂	233-293
51	Brine, 25 per cent NaCl	233-293
44	Butyl alcohol	273-373
2	Carbon disulphide	173-208
3	Carbon tetrachloride	283-333
8	Chlorobenzene	273-373
4	Chloroform	273-323
21	Decane	193-298
6A	Dichloroethane	243-333
5	Dichloromethane	233-323
15	Diphenyl	353-393
22	Diphenylmethane	303-373
16	Diphenyl oxide	273-473
16	Dowtherm A	273-473
24	Ethyl acetate	223-298
42	Ethyl alcohol, 100 per cent	303-353
46	Ethyl alcohol, 95 per cent	293-353
50	Ethyl alcohol, 50 per cent	293-353
25	Ethyl benzene	273-373
1	Ethyl bromide	278-298
13	Ethyl chloride	243-313
36	Ethyl ether	173-298
7	Ethyl iodide	273-373
39	Ethylene glycol	233-473
2A	Freon-11 (CCl ₃ F)	253-343
6	Freon-12 (C ₂ Cl ₂ F ₂)	233-288
4A	Freon-21 (CHCl ₂ F)	253-343
7A	Freon-22 (CHClF ₂)	253-333
3A	Freon-113 (CCl ₂ F-CClF ₂)	253-343
38	Glycerol	233-293
28	Heptane	273-333
35	Hexane	193-293
48	Hydrochloric acid, 30 per cent	293-373
41	Isomyl alcohol	283-373
43	Isobutyl alcohol	273-373
47	Isopropyl alcohol	253-323
31	Isopropyl ether	193-293
40	Methyl alcohol	233-293
13A	Methyl chloride	193-293
14	Naphthalene	363-473
12	Nitrobenzene	273-373
34	Nonane	223-298
33	Octane	223-298
3	Percchloroethylene	243-413
45	Propyl alcohol	253-373
20	Pyridine	223-298
9	Sulphuric acid, 98 per cent	283-318
11	Sulphur dioxide	253-373
23	Toluene	273-333
53	Water	283-473
19	Xylene (ortho)	273-373
18	Xylene (meta)	273-373
17	Xylene (para)	273-373

*By permission from *Heat Transmission*, by W. H. McAdams, copyright 1942, McGraw-Hill.

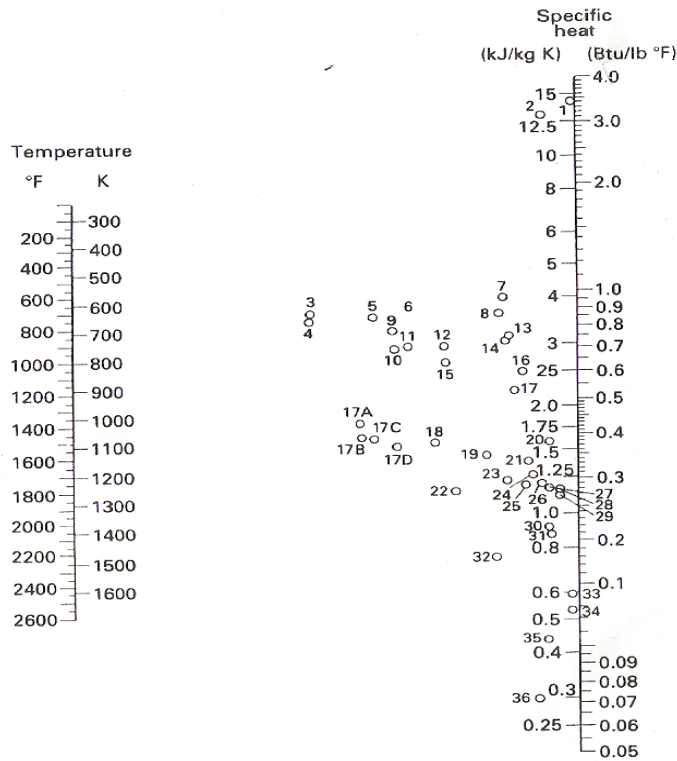
Specific heats of liquids



Specific Heats at Constant Pressure of Gases and Vapors at (at 101.kN/m²)

Gas	Range (K)	No.	Gas	Range (K)
Acetylene	273-473	1	Hydrogen	273-873
Acetylene	473-673	2	Hydrogen	873-1673
Acetylene	673-1673	35	Hydrogen bromide	273-1673
Air	273-1673	30	Hydrogen chloride	273-1673
Ammonia	273-873	20	Hydrogen fluoride	273-1673
Ammonia	873-1673	36	Hydrogen iodide	273-1673
Carbon dioxide	273-673	19	Hydrogen sulphide	273-973
Carbon dioxide	673-1673	21	Hydrogen sulphide	973-1673
Carbon monoxide	273-1673	5	Methane	273-573
Chlorine	273-473	6	Methane	573-973
Chlorine	473-1673	7	Methane	973-1673
Ethane	273-473	25	Nitric oxide	273-973
Ethane	473-873	28	Nitric oxide	973-1673
Ethane	873-1673	26	Nitrogen	273-1673
Ethylene	273-473	23	Oxygen	273-773
Ethylene	473-873	29	Oxygen	773-1673
Ethylene	873-1673	33	Sulphur	573-1673
Freon-11 (CCl ₃ F)	273-423	22	Sulphur dioxide	273-673
Freon-21 (CHCl ₂ F)	273-423	31	Sulphur dioxide	673-1673
Freon-22 (CHClF ₂)	273-423	17	Water	273-1673
Freon-113 (CCl ₂ F-CClF ₂)	273-423			

permission from Heat Transmission, by W. H. McAdams, copyright, 1942, McGraw-Hill.



Temperature (θ) (K)	Viscosity (μ) (mN s/m ²)	Temperature (θ) (K)	Viscosity (μ) (mN s/m ²)	Temperature (θ) (K)	Viscosity (μ) (mN s/m ²)
273	1.7921	306	0.7523	340	0.4233
274	1.7313	307	0.7371	341	0.4174
275	1.6728	308	0.7225	342	0.4117
276	1.6191	309	0.7085	343	0.4061
277	1.5674	310	0.6947	344	0.4006
278	1.5188	311	0.6814	345	0.3952
279	1.4728	312	0.6685	346	0.3900
280	1.4284	313	0.6560	347	0.3849
281	1.3860	314	0.6439	348	0.3799
282	1.3462	315	0.6321	349	0.3750
283	1.3077	316	0.6207	350	0.3702
284	1.2713	317	0.6097	351	0.3655
285	1.2363	318	0.5988	352	0.3610
286	1.2028	319	0.5883	353	0.3565
287	1.1709	320	0.5782	354	0.3521
288	1.1404	321	0.5683	355	0.3478
289	1.1111	322	0.5588	356	0.3436
290	1.0828	323	0.5494	357	0.3395
291	1.0559	324	0.5404	358	0.3355
292	1.0299	325	0.5315	359	0.3315
293	1.0050	326	0.5229	360	0.3276
293.2	1.0000	327	0.5146	361	0.3239
294	0.9810	328	0.5064	362	0.3202
295	0.9579	329	0.4985	363	0.3165
296	0.9358	330	0.4907	364	0.3130
297	0.9142	331	0.4832	365	0.3095
298	0.8937	332	0.4759	366	0.3060
299	0.8737	333	0.4688	367	0.3027
300	0.8545	334	0.4618	368	0.2994
301	0.8360	335	0.4550	369	0.2962
302	0.8180	336	0.4483	370	0.2930
303	0.8007	337	0.4418	371	0.2899
304	0.7840	338	0.4355	372	0.2868
305	0.7679	339	0.4293	373	0.2838

*Calculated by the formula:

$$1/\mu = 21.482 \left[(\theta - 281.435) + \sqrt{(8078.4 + (\theta - 281.435)^2)} \right] - 1200 \text{ (}\mu \text{ in N s/m}^2\text{)}$$

(By permission from Fluidity and Plasticity, by E.C. Bingham. Copyright 1922, McGraw-Hill Book Company Inc.)

Thermal Conductivities of Gases and Liquids

The extreme temperature values given constitute the experimental range. For extrapolation to other temperatures, it is suggested that the data given be plotted as $\log k$ vs. $\log T$, or that use be made of the assumption that the ratio $C_p \mu / k$ is practically independent of temperature (and of pressure, within moderate limits).

Substance	k (W/m K)	(K)	k (Btu/h ft °F)	Substance	k (W/m K)	(K)	k (Btu/h ft °F)
acetone	0.0098	273	0.0057	Chlorine	0.0074	273	0.0043
	0.0128	319	0.0074	Chloroform	0.0066	273	0.0038
	0.0171	373	0.0099		0.0080	319	0.0046
	0.0254	457	0.0147		0.0100	373	0.0058
acetylene	0.0118	198	0.0068	Cyclohexane	0.0133	457	0.0077
	0.0187	273	0.0108		0.0164	375	0.0095
	0.0242	323	0.0140	Dichlorodifluoromethane	0.0083	273	0.0048
	0.0298	373	0.0172		0.0111	323	0.0064
air	0.0164	173	0.0095		0.0139	373	0.0080
	0.0242	273	0.0140		0.0168	423	0.0097
	0.0317	373	0.0183	Ethane	0.0114	203	0.0066
	0.0391	473	0.0226		0.0149	239	0.0086
ammonia	0.0459	573	0.0265		0.0183	273	0.0106
	0.0164	213	0.0095	Ethyl acetate	0.0303	373	0.0175
	0.0222	273	0.0128		0.0125	319	0.0072
	0.0272	323	0.0157		0.0166	373	0.0096
	0.0320	373	0.0185	alcohol	0.0244	457	0.0141
benzene	0.0090	273	0.0052		0.0154	293	0.0089
	0.0126	319	0.0073	chloride	0.0215	373	0.0124
	0.0178	373	0.0103		0.0095	273	0.0055
	0.0263	457	0.0152		0.0164	373	0.0095
	0.0305	485	0.0176		0.0234	457	0.0135
butane (n-)	0.0135	273	0.0078		0.0263	485	0.0152
	0.0234	373	0.0135	ether	0.0133	273	0.0077
(iso-)	0.0138	273	0.0080		0.0171	319	0.0099
	0.0241	373	0.0139		0.0227	373	0.0131
carbon dioxide	0.0118	223	0.0068		0.0327	457	0.0189
	0.0147	273	0.0085	Ethylene	0.0362	485	0.0209
	0.0230	373	0.0133		0.0111	202	0.0064
	0.0313	473	0.0181		0.0175	273	0.0101
	0.0396	573	0.0228		0.0267	323	0.0131
disulphide	0.0069	273	0.0040		0.0279	373	0.0161
	0.0073	280	0.0042	Heptane (n-)	0.0194	473	0.0112
monoxide	0.0071	84	0.0041		0.0178	373	0.0103
	0.0080	94	0.0046	Hexane (n-)	0.0125	273	0.0072
	0.0234	213	0.0135		0.0138	293	0.0080
tetrachloride	0.0071	319	0.0041	Hexene	0.0106	273	0.0061
	0.0090	373	0.0052		0.0109	373	0.0189
	0.0112	457	0.0065		0.0225	457	0.0130
hydrogen	0.0113	173	0.0065		0.0256	485	0.0148
	0.0144	223	0.0083	Methylene chloride	0.0067	273	0.0039
	0.0173	273	0.0100		0.0085	319	0.0049
	0.0199	323	0.0115		0.0109	373	0.0063
	0.0223	373	0.0129		0.0164	485	0.0095
	0.0308	573	0.0178				

Substance	k (W/m K)	(K)	k (Btu/h ft °F)	Substance	k (W/m K)	(K)	k (Btu/h ft °F)
Hydrogen and carbon dioxide		273		Nitric oxide	0.0178	203	0.0103
0 per cent H ₂	0.0144		0.0083		0.0239	273	0.0138
20 per cent	0.0286		0.0165	Nitrogen	0.0164	173	0.0095
40 per cent	0.0467		0.0270		0.0242	273	0.0140
60 per cent	0.0709		0.0410		0.0277	323	0.0160
80 per cent	0.1070		0.0620		0.0312	373	0.0180
100 per cent	0.173		0.10	Nitrous oxide	0.0116	201	0.0067
Hydrogen and nitrogen		273			0.0157	273	0.0087
0 per cent H ₂	0.0230		0.0133		0.0222	373	0.0128
20 per cent	0.0367		0.0212	Oxygen	0.0164	173	0.0095
40 per cent	0.0542		0.0313		0.0206	223	0.0119
60 per cent	0.0758		0.0438		0.0246	273	0.0142
80 per cent	0.1098		0.0635		0.0284	323	0.0164
Hydrogen and nitrous oxide		273			0.0321	373	0.0185
0 per cent H ₂	0.0159		0.0092	Pentane (n-)	0.0128	273	0.0074
20 per cent	0.0294		0.0170		0.0144	293	0.0083
40 per cent	0.0467		0.0270	(iso-)	0.0125	273	0.0072
60 per cent	0.0709		0.0410		0.0220	373	0.0127
80 per cent	0.112		0.0650	Propane	0.0151	273	0.0087
Hydrogen sulphide	0.0132	273	0.0076		0.0261	373	0.0151
Mercury	0.0341	473	0.0197	Sulphur dioxide	0.0087	273	0.0050
Methane	0.0173	173	0.0100		0.0119	373	0.0069
	0.0251	223	0.0145	Water vapour	0.0208	319	0.0120
	0.0302	273	0.0175		0.0237	373	0.0137
	0.0372	323	0.0215	acetate	0.0324	473	0.0187
Methyl alcohol	0.0144	273	0.0083		0.0429	573	0.0248
	0.0222	373	0.0128	chloride	0.0545	673	0.0315
	0.0102	273	0.0059		0.0763	773	0.0441
	0.0118	293	0.0068				
	0.0092	273	0.0053				
	0.0125	319	0.0072				
	0.0163	373	0.0094				

*By permission from *Heat Transmission*, by W. H. McAdams, copyright 1942, McGraw-Hill.

